A Genetic Study of Dystroglycan in the *Drosophila melanogaster* Eye

Nadia Yolaine Melian

Biology, McGill University, Montréal

June 2009

A thesis submitted to McGill University in partial fulfillment of the requirements of the degree of Doctor of Philosophy

Abstract

Dystroglycan (DG) is a cell surface receptor that interacts both with the extracellular matrix (ECM) and the intracellular cytoskeleton. DG serves as the core protein of the dystrophin associated complex (DGC) linked to muscular dystrophies (MDs). A subset of MDs called Dystroglycanopathies, are associated with mutations which reduce DG's ability to interact with the ECM. In addition to muscle degeneration, Dystroglycanopathies have central nervous system defects including eye anomalies, lissencephaly and mental retardation. DG is conserved in *D. melanogaster*, where its deficiency in muscle leads to muscle degeneration, demonstrating that *D. melanogaster* serves as a model for MDs. Deficiency in DG during *D. melanogaster* eye development was studied to gain insights into the function of DG in the nervous system. Once the expression and localisation of DG was established, the eye development of two series of *Dg* mutant alleles was characterised using: immunofluorescence, histology, scanning electron microscopy and cell death assays. During photoreceptor (R cell) specification, DG concentrates to the apical surface and this location is maintained through early pupal development. The first *Dg* allele series tested, exemplified by Dg^{248}, also contains a deletion in the mitochondrial ribosomal protein L34 (*mRpL34*). However, due to the mitochondrial dysfunction, Dg^{248} may serve as a model for the function of DG during metabolic stress. The severe

disruption of eye development observed in eyes mosaic for *Dg*^{248} is significantly rescued by the transgenic expression of *mRpL34*. *Dg*^{248} eyes develop progressive loss of R cell morphology beginning during early pupa. *Dg*^{248} R cell pupal development is associated with the migration of R cell nuclei into their axons. Cell death levels are high during early *Dg*^{248} eye development and inhibition of this cell death, using the baculovirus caspase inhibitor p35, is detrimental to *Dg*^{248} eye development, suggesting a defect in compensatory proliferation. The second series of alleles, EMS *Dg*^{0*} affecting only *Dg*, develop retina that appear largely normal. The retina of EMS *Dg*^{0*} however, are 2/3 the length of normal retina. Endogenous reduction of DG using RNA interference during eye development leads to a rough adult eye with disrupted retina. Together, these data suggest that DG is necessary for neuronal differentiation.

Résumé

La dystroglycan (DG) est une réceptrice cellulaire qui interagit à la fois avec la matrice extracellulaire (MEC) et le squelette intracellulaire. La DG est le noyau du complexe associé à la dystrophine, lié à la dystrophie musculaire (DM). Un groupe de DMs, nommé les Dystroglycanopathies, est associé aux mutations qui réduisent la capacité de la DG à interagir avec la MEC. Les Dystroglycanopathies ont, en plus de la dégénération musculaire, des défauts du system nerveux central (SNC) qui inclut des anomalies des yeux, la lissencephaly et des déficiences mentales. Conserver dans la *D. melanogaster*, la déficience de DG dans les muscles produit une dégénération indiquant que la *D. melanogaster* peut être un model pour les DMs. Une déficience de DG pendant le développement de l'œil de la *D. melanogaster* a été produite pour gagner des connaissances de la fonction sur la DG dans le SNC. Une foi que l'expression et la localisation de la DG ont été établies, le développement de l'œil de deux séries d'allèles du *Dg* fut déterminée en utilisant plusieurs outils incluant l'immunofluorescence, l'histologie, la microscopie électronique à balayage et des analyses de morts cellulaires. Pendant la spécification des photorécepteurs (R), la DG est concentrée à leur surface apicale et cette localisation est maintenue pendant le début du développement de la pupe. Le premier allèle de *Dg* testé, Dg^{248}, contient aussi une délétion du gène de la protéine ribosomale de la

mitochondrie L34 (*mRpL34*). La disruption sévère de l'oeil mosaic Dg^{248} est sauvée de façon significative par un transgene du *mRpL34*. Cependant, due à la dysfonction de la mitochondrie, Dg^{248} peux servir comme model du rôle du DG pendant le stress métabolique. Les yeux Dg^{248} ont une perte de morphologie progressive pendant le développement de la pupe. Le développement des cellules R Dg^{248} est associé avec la migration de leur noyau dans leur axone. La mort cellulaire est élevée tôt pendant le développement et l'inhibition de cette mort, par l'inhibiteur de caspase du baculovirus la p35, est nocive au développement de l'œil, suggérant une déficience en la prolifération compensatoire. La seconde série d'allèle, EMS Dg^{0*} qui perturbent seulement le *Dg*, développe une rétine qui apparaît normale. Cependant la rétine des EMS Dg^{0*} sont le deux tiers plus court qu'une rétine normale. La réduction du DG avec la ARN interférente pendant le développement de l'œil produit un œil adulte rigoureux, et une rétine perturber. Ensemble les donnés suggèrent que la DG fonctionne pendant la différentiation neuronale.

Contributions of co-authors

Chapter Two **Dystroglycan during Eye Development** by Nadia Y. Melian, Mario Pantoja, Hakima Moukhles, Hannele Ruohola-Baker and Sal Carbonetto

Dr. Hakima Moukhles performed the histology and imaging of the *Dg*^{248} chimeric mice eyes in figure 1 D and E.

Mario Pantoja performed the imaging and analysis of the rhabdomere length in figure 10 D and E. Mario also provided the materials and methods necessary for the rhabdomere length analysis.

Chapter Four **Evidence That Dystroglycan Is Associated with Dynamin and Regulates Endocytosis** by Yougen Zhan, Mathieu R. Tremblay, Nadia Melian, and Salvatore Carbonetto

This is a published manuscript containing the work of the first author Yougen Zhan. My contribution was limited to the co-localisation of dystroglycan and dynamin in the mouse adult retina, figure 4C. I also wrote the Materials and Methods.

Contributions to Original Knowledge

Chapter Two **Dystroglycan during Eye Development** by Nadia Y. Melian, Mario Pantoja, Hakima Moukhles, Hannele Ruohola-Baker and Sal Carbonetto

In this chapter we show for the first time that the DG isoform, predicted to be glycosylated, is expressed throughout early eye development. Expressed generally prior to differentiation, once cells become specified, it is the R cells which express this DG isoform in the developing drosophila eye. We are the first to perform single cell mosaic analysis of Dg^{248}. We show that the morphology of mosaic eyes composed of the dystroglycan allele Dg^{248} is significantly rescued by the gene for the mitochondrial ribosomal protein L34. We are also the first to characterise the eyes of EMS Dg^{0*} mutant lines showing that they have normal retinal patterning but develop thinner retinas.

Chapter Three **Characterization of Dystroglycan's role in the Developing Eye during Metabolic Stress** by Nadia Melian and Sal Carbonetto

We are the first to characterise the cell death in the mosaic eyes of the Dg^{248} dystroglycan allele. We demonstrate that apoptotic cell death occurs early in development and that early inhibition of this apoptotic cell death is detrimental to the development of Dg^{248} mosaics eyes, which may reflect a deficiency in compensatory proliferation. We are the first to detect nuclear migration defects

in *Dg*^{248} R cells. We are also the first to determine the state of polarity of *Dg*^{248} photoreceptor cells showing that it is normal during development.

A manuscript is in preparation for submission to PNAS by Yougen Zhan, Nadia Y. Melian, Mario Pantoja, Hannele Ruohola-Baker, Charles W Bourque, Yong Rao and Salvatore Carbonetto. It will contain: figures 2, 3, 8 (one panel) and 10 from chapter two; and figure 1 from chapter 3.

Chapter Four **Evidence That Dystroglycan Is Associated with Dynamin and Regulates Endocytosis** by Yougen Zhan, Mathieu R. Tremblay, Nadia Melian, and Salvatore Carobonetto

Within this work I show the novel co-localisation of dystroglycan with dynamin in the outer plexiform layer of the adult mouse retina.

Acknowledgements

First and foremost I thank my supervisor Dr. Salvatore Carbonetto for the multiple projects which have provided me a solid foundation in biological research. My committee members Drs. Jackie Vogel, Paul Holland and Yong Rao provided me with guidance and council. I thank the members of Dr. Carbonetto's laboratory, both past and present, for scientific discussion including: Hakima Moukhles, Yen May Ong, Huashan Peng, Waris Shah, Mathieu Tremblay, Raphaël Vézina-Audette and Yougen Zhan. Thank you to Dr. Don van Meyel for his generous teaching and advice. Thank you to the members of both Dr. van Meyel's and Dr. Rao's laboratory for scientific discussion and invaluable help. Thank you to the members of the Centre for research in Neuroscience and the Biology Department, for scientific discussions during the retreats, seminars and journal clubs. Thank you to Dr. Hannele Ruohola-Baker and Mario Pantoja for their scientific collaboration. Many thanks to Dr. Robert Ray for fly lines. Thank you to Dr. Judith Lacoste for technical advice on confocal microscopy. Thank you to Line Mongeon for the Scanning Electron Microscopy work. Special thanks to Margaret Attiwell for her humour when teaching me epon sectioning. Thank you to Daniel Houle for his technical knowledge of mice husbandry. Lastly, I would like to thank my family and my

partner Neils Christensen, who provided me with unconditional support during this endeavour.

Table of Contents

List of Figures

List of Abbreviations

% p.d.	Percent pupal development
AJ	Adherens junction
AMPK	AMP kinase
bp	Base pairs
CNS	Central Nervous System
DIAP	Drosophila inhibitors of apoptosis proteins
DIC	Differential interference contrast
DiI	octadecyl (C_{18}) indocarbocyanine
Dg/DG	Dystroglycan gene/protein
DGC	Dystrophin glycoprotein complex
dsRNA	Double stranded RNA
Dys/DYS	Dystrophin
EMS	ethyl methane sulfonate
Ey	Eyeless
f-actin	Filamentous actin
FLP	Flipase
FRT	Flippase Recognition Target
GFP	Green fluorescence Protein
GMR	Glass multimer reporter
H&E	Hematoxylin and eosin
Kb	Kilo base pairs
MARCM	Mosaic analysis with repressible marker
MD	Muscular Dystrophy
MF	Morphogenetic Furrow
mES cell	Mouse embryonic stem cell
mRNA	messenger RNA
PCD	Programmed cell death
R cell	Photoreceptor cell
RHG	Reaper, hid, grim

RNA	Ribonucleic acid
RNAi	Interference RNA
SEM	Scanning electron microscopy or micrograph
siRNA	Short interfering RNA
TUNEL	Terminal deoxynucleotidyl transferase dUTP nick end labelling
UAS	Upstream activating sequence
WT	Wild type
ZA	Zonula Adherens

Chapter One - Introduction and Literature Review

Introduction

During vertebrate development, the retina develops from the optic cup, an evagination of the developing forebrain, and is therefore a part of the central nervous system (CNS). Simplicity, accessibility and its non-vital requirement have made the retina a model for the developing CNS. The developing vertebrate retina provides a method to study a range of CNS specific pathways including neuronal degeneration and differentiation (Chen & Cepko 2009).

The invertebrate retina also provides a model for CNS development. Though the architecture of the vertebrate and the invertebrate eye are dramatically different, similar regulatory networks and pathways direct eye development and function in both phyla. (Chow & Lang 2001). The vertebrate transcription factor *Pax6* and its *Drosophila* homologues *eyeless* (*ey*) and *twin of eyeless* (*toy*) specify eye development (Hanson & Van Heyningen 1995). Later in development, retinal differentiation in both vertebrates and *Drosophila* follows a wave of hedgehog signalling (Neumann & Nuesslein-Volhard 2000). During this wave of differentiation the transcription factors *Drosophila atonal*, and the vertebrate *Atonal homologue 5* both act to specify the first retinal neuronal cell type (Hsiung & Moses 2002). It is predicted that up to 60% - 70% of human diseases have *Drosophila* counter parts (Reiter et al 2001). It is also estimated that two thirds of the lethal genes in *Drosophila* are required for the assembly

and neuronal connectivity of the eye (Thaker & Kankel 1992). *Drosophila* developmental genetics therefore provides a versatile system (Thomas & Wassarman 1999) which can bring new insights into vertebrate eye development.

The *Drosophila* Compound Eye

The *Drosophila* adult eye is composed of approximately 800 unit eyes or ommatidia (Ready et al 1976). Each ommatidium contains eight photoreceptor (R) cells, four cone cells, and two primary pigment cells. The ommatidium is further surrounded by a hexagonal lattice of 12 interommatidial cells shared between the ommatidium which include bristle, secondary and tertiary pigment cells. Together the ommatidia and their interommatidial cells form an eye with a precise hexagonal facet array.

Externally each facet, seen by scanning electron microscopy (SEM), is a single ommatidium (fig.1 C). Internally the hexagonal array of ommatidia can be seen (fig.1 D). At the centre of each ommatidium are eight R cells. R cells 1 to 6 span the length of the retina. R cells 7 and 8 span only half the width of the eye, with R7 at the most distal end of the retina and R8 at the proximal end of the retina. Each R cell has a rhabdomere, the photon sensing organelle, produced by multiple infolding of the cell membrane into stacks of microvilli spanning the

length of the R cell. The rhabdomeres of R cells 1 to 6 are arranged in an asymmetrical trapezoid pattern, with their cell bodies radially placed (fig.1 D). The rhabdomeres of cells 7 and 8 are borne on stalks extending inward from their cell bodies and occupy a central position. Arrangement of the other cells composing the eye is also highly ordered. Within an eye the ommatidia, and the R cells within them, are highly ordered relative to each other. Each eye is divided by a horizontal equator and within each half all ommatidia are arranged in the same orientation. Each half is the mirror image of the other engendering planar polarity. Detecting perturbations to this precise array is one of the strengths of the use of the eye in *Drosophila* genetics.

Drosophila Eye Development

The adult *Drosophila* eye is the product of precise developmental events that begin in the embryo and proceed through the larval, pupal and adult stages (Wolff & Ready 1991a). The primordia of the *Drosophila* adult eye structure arises in the epidermal invaginations called imaginal discs (Cagan & Ready 1989). The eye is derived from the eye-antennal imaginal disc which arises from about 20 cells of the embryonic blastoderm. Imaginal discs grow into a flattened hollow sac composed of two separate layers of distinct cell types enveloped by a basement membrane (Martin et al 1999). One cell layer is organised into a thick

columnar epithelium, the disc proper. The cells from the disc proper go on to contribute to the cells of the adult eye. The other cell layer is a thinner monolayer of squamous cells called the peripodial membrane (fig.1 A). The peripodial membrane does not differentiate to form imaginal structures. The peripodial membrane does however, provide instructive cues to the patterning of the disc proper (Gibson & Schubiger 2000).

Differentiation is a process that extends over a period of five days (Cagan & Ready 1989). Cell specification and differentiation begins in the middle of the third larval instar stage, after the passage of the dorsal-ventral morphogenetic furrow (MF) across the eye disc proper. The MF travels across from the posterior to the anterior end of the eye disc. Anterior to the MF the progenitor cells undergo division to generate an epithelial field for the differentiation events that commence with the furrow. Posterior to the furrow, cell type specification occurs in the neuroepithelium. Amongst the cell types, R cells are recruited and commit to a neuronal cell fate (fig.1 A). The MF reaches the anterior end by the early pupal stage. The eye disc is then everted with the peripodial membrane of the eye anlagen contracting and providing a motive force to evert the eye disc (Milner 1983). The apical surface of the disc proper forms the external surface of the adult eye. The peripodial membrane degenerates during this stage. The

eye disc R cell differentiation ends when, at the end of the pupal stage, the R cells have formed rhabdomeres and are fully elongated.

Pattern formation in the eye is intimately coupled with polarised growth. The cells of the retina display apical-basal polarity similar to all epithelia. During the third instar stage the group of eight specified R cells are joined to their neighbours by a distinct adherens junction (AJ), the zonula adherens (ZA), at the apical surface (Tepass & Harris 2007). The ZA mediates adhesion between neighbouring cells by linking the actin cytoskeleton of one cell to that of the next cell via the transmembrane cadherin adhesion molecules and their associated catenin adaptor complex (Pacquelet & Rorth 2005). During early pupa development the R cell apical membranes detach from the apical surface and are turned inward 90° towards each other. The apical membranes, along with the surrounding ZA which separates the apical and basolateral membranes, expand perpendicularly to the plane of the epithelium (beginning around 30% p.d.), eventually reaching the basal surface of the retina (ending around 50% p.d.). During this time the retina and the R cells within it do not change in size. Once the ZA reaches the basal surface then both the R cell and its ZA elongate five fold along the optical axis (Longley & Ready 1995) attaining a length of 90-100μm. Maintenance of apico-basal cell polarity and adherens junction in R cells requires Crumbs a transmembrane apical determinant in epithelial cells (Richard

et al 2006, van de Pavert et al 2004). The apical R cell membranes, initially in direct contact with each other, separate at about 55% p.d. (fig.1 B). This detachment forms an interrhabdomeral space giving the R cell cluster a barrel shape. Following detachment, the R cell apical membrane differentiates into a rhabdomere. The rhabdomere membrane is connected to the ZA through a stalk membrane. AJs further anchor the distal and proximal tips of the rhabdomeres.

Cell Death

Cell death is ubiquitous and necessary for the development of an organism. The mechanisms used by cells to die, lie on a continuum between necrosis and apoptosis (Leist & Jaattela 2001, Lockshin & Zakeri 2002). The differences between the extremes lies in the energy required and the response elicited within the organism. Necrosis is characterised by organelle swelling and is an unregulated process not requiring energy. Release of cellular contents into the extracellular space during necrosis elicits an inflammatory response by the organism causing tissue damage to surrounding non-dying tissue (Syntichaki & Tavernarakis 2002). Programmed cell death (PCD), as exemplified by apoptosis, is a genetically regulated, energy requiring process characterised by the presence of nucleaosomal degradation, compaction of chromatin, phosphotidlyserine externalisation, cell shrinkage and cellular blebbing into

apoptotic bodies (Strasser et al 2000). During apoptosis a cell essentially cleaves itself into smaller vesicle packets ready for internalisation by neighbouring cells (e.g. *C. elegans)* (Reddien et al 2001) or by phagocytes (e.g. mammals) (Franc 2002) thereby preventing any inflammatory response.

Many extracellular and intracellular signals may trigger cell death including interaction with the extracellular matrix (ECM) and metabolic stress. The ECM has been shown to be a source of both anti and pro-cell death signals (Mongiat et al 2007, Romani et al 2009). This is because the ECM is, in addition to being a structural scaffold, also a reservoir of many other secreted molecules including growth factors and cytokines. Attachment of cells to the ECM is essential to support cell survival, growth, and proliferation and the lack of these interactions can trigger a form of apoptotic cell death called anoikis (Miner & Yurchenco 2004). Integrin mediated cell-ECM (Reginato et al 2003) contact has been shown to protect against anoikis, but it is one of many opposing signals (Puthalakath et al 2001) which a cell must integrate (Joo et al 2008). The intracellular metabolic status of a cell is critical for its functioning and survival. Perturbation of a cell's ability to generate energy due to anoxia or glucose deprivation, may initiate programmed cell death. Metabolic stress has been shown to induce gene transcription to negatively affect mitochondrial morphology and function (Kim & Youn 2009) leading to apoptosis. Neurons are cells which

are particularly sensitive to metabolic stress due to their high energy demands and their lack of energy reserves(Minke & Agam 2003, Schmidt et al 2008).

Programmed cell death pathways in *Drosophila*

The components of the apoptotic pathway are conserved between mammals and *Drosophila* (Richardson & Kumar 2002), with less redundancy in *Drosophila*. The cysteine protease family of caspases are the main executioners of the apoptotic process. In *Drosophila* there are seven caspase genes. Critical for apoptosis is Dronc (Dorstyn et al 1999), a caspase-9-like initiator caspase. Dcp-1 and DrIce, are caspase-3-like effector caspases (Xu et al 2006). In the absence of apoptotic signals *Drosophila* inhibitors of apoptosis proteins (DIAP) bind to caspases and inhibit their activity. In cells, Dronc is constitutively active but inhibited by DIAPs (Meier et al 2000). The pro-apoptotic group of proteins including reaper, hid and grim (RHG) bind to DIAPs essentially inhibiting the inhibitors to initiate the caspase cascade (Grether et al 1995). Once freed, Dronc binds the adaptor protein Ark to form the apoptosome (Adams & Cory 2002, Srivastava et al 2007). The apoptosome cleaves and activates effector caspases initiating a cascade of caspase activity which leads to the controlled degradation of the cell. The point of apoptosis control in *Drosophila* is controlling the activity of the initiator caspase Dronc. Since Dronc is constitutively inhibited by DIAPs,

cell death signals therefore contribute to regulating the RHG group of proteins to dictate the output caspase activity (Ryoo et al 2002).

Apoptosis does have beneficial effects. During development it is a necessary mechanism helping to shape morphology (Bursch 2004). Apoptosis may also trigger repair. Accidental cell death in response to stress and damage can induce additional divisions of the surrounding surviving cells, a mechanism termed apoptosis-induced compensatory proliferation (Fan & Bergmann 2008a). A process recognised over thirty years ago in *Drosophila* (Haynie 1977), it has also been found to occur in mammals (Valentin-Vega et al 2008). In proliferating *Drosophila* eye and wing tissue Dronc coordinates cell death and compensatory proliferation through the induction of the mitogens decapentaplegic and wingless by the Jun N-terminal Kinase pathway and p53 transcription factor (Ryoo et al 2004, Wells et al 2006). In differentiated *Drosophila* eye effector caspases active the hedgehog signalling pathway to induce compensatory proliferation (Fan & Bergmann 2008b).

Program cell death during *Drosophila* Eye Development

Cell death is a normal part of the developmental process. Apoptosis is inhibited early by eyeless during early eye development to promote eye development (Kronhamn et al 2002). Apoptosis is also inhibited in the anterior

region of the third instar disc with the exception of a small band just anterior to the MF (Bonini et al 1993, Wolff & Ready 1991b). The third instar has a second larger band of cell death in the posterior region. In the pupal eye imaginal disc, cell death occurs around 24% and 30% p.d. to remove supernumerary interommatidial cells to establish the precise hexagonal lattice in the *Drosophila* eye (Cagan & Ready 1989, Monserrate & Baker Brachmann 2006, Wolff & Ready 1991b). The last wave of cell death occurs between 60-70% p.d., to remove the perimeter ommatidal clusters (Wolff & Ready 1991b).

Throughout all of development the eye disc is connected to the brain (Campos et al 1995). However, the developing *Drosophila* eye does not receive pro-survival cues from the brain. While retinal development and differentiation can proceed in the absence of connections with the brain, R-cell survival after eclosion requires interactions with the underlying optic ganglia (Campos et al 1992).

Dystroglycan and its functions in vertebrates

DG is a cell surface adhesion receptor (Schwarzbauer 1999) expressed in a number of different cell types including epithelial cells, glia, muscle, immune and neurons (Durbeej et al 1998). Dystroglycan is the product of a single gene, *Dag1*, which is post-translationally cleaved into two into the peripheral α-DG and

the transmembrane β-DG protein (Ibraghimov-Beskrovnaya et al 1992). The α and β-DG subunits interact non-covalently to form a complex. Extracellularly, DG interacts with the extracellular matrix (ECM) through its binding of laminin (Gee et al 1993), agrin (Gee et al 1994), pikachurin (Sato et al 2008) and perlecan (Talts et al 1999). Intracellularly, DG is linked to the cytoskeleton via its interaction with dystrophin (Jung et al 1995) or its homologue utrophin (James et al 1996). Other intracellular binding partners include Grb2 (Yang et al 1995) and dynamin (Zhan et al 2005). DG was initially thought to function as simply a structural component maintaining cell attachment to the ECM and coordinating it with the cytoskeleton (Ervasti & Campbell 1993). It has become clear, through its involvement in a variety of cellular processes such as neuromuscular junction formation (Jacobson et al 2001, Peng et al 1999, Tremblay & Carbonetto 2006) and epithelia development (Durbeej et al 1995), that DG must also contribute either directly or indirectly to signalling pathways. Together, the binding partners suggest that DG may be acting as an ECM sensor, signalling environmental changes to the cell.

Muscular dystrophies (MD) are genetic diseases often linked with the dysfunction of the dystrophin associated glycoprotein complex (DGC) (Sciandra et al 2003); in which DG forms the structural core. DG is expressed in a wide number of cell types including astrocytes (Blank et al 1997), neurons (Zaccaria et

al 2001), epithelial cells (Durbeej & Campbell 1999) and muscle cells (Durbeej et al 1998). The pathology of many MDs may therefore not be the degeneration of skeletal muscle, but can also include central nervous system abnormalities (Cohn 2005). For example, the Muscle-eye-brain disease (Dincer et al 2003), Walker-Warburg Syndrome (Beltran-Valero De Bernabe et al 2002) and Fukuyama MD (Ohtsuka-Tsurumi et al 2004), have along with a muscular pathology, central nervous system abnormalities including eye malformations and abnormal brain morphology. The glycosylation of α -DG dictates its binding partners (Pall et al 1996). In these diseases, called Dystroglycanopathies, DG is hypoglycosylated, functionally inhibiting its interaction with the ECM (Grewal & Hewitt 2003) (Huizing et al 2004).

Within the mature mammalian and avian retina DG can be localised extrasynaptically to the ribbon synapse of R cells in the outer plexiform layer and to the endfeet of Muller cells at the inner limiting membrane (Blank et al 1997, Jastrow et al 2006, Montanaro et al 1995). Pikachurin has been found to be a DG ligand at the ribbon synapse. Pikachurin null mice have improper apposition of bipolar cell dendrites to the R cell synapse suggesting DG is required for proper synaptic structure (Sato et al 2008). DG also localises to blood vessels of the retina (Moukhles et al 2000). In the Xenopus laevis, DG is proposed to be involved in retinal layering and ocular development (Lunardi et al 2006). DG has

also been shown to have a role in neuroepithelial proliferation and differentiation in the avian developing retina (Schroder et al 2007).

Dystroglycan and cell Death

As noted above, basement membranes have essential roles in maintaining cell survival by providing cues about the presence of structural support or simply as being traps for growth factors allowing them to interact with cell surface receptors(Erickson & Couchman 2000). DG has been shown not to be necessary for basement membrane formation(Li et al 2002); it could therefore be promoting cell survival by acting as sensor to detect the presence of the BM. Experiments have shown that an absence of DG compromises cell survival. Complete *Dag1* knock-out mice are embryonic lethal at E6.5 (Williamson et al 1997). The conditional knock out of *Dag1* in the epiblast layer of the murine embryo generates pups who survive only a few weeks (Satz et al 2008)}, showing a requirement of DG in the morphogenesis of the brain and the eye, and ultimately survival. Chimaeric animals with muscles composed largely of *Dag1* null cells have muscular dystrophy (Côté et al 1999), demonstrating signs of necrosis in skeletal muscle. A muscle cell line transformed with anti-sense *Dag1* shows increased levels of cell death (Montanaro et al 1999). Disruption of the laminin binding to α-DG also increased cell death in muscle cells through

perturbation of the PI3/AKT signalling pathway (Langenbach & Rando 2002a). Finally, the ectoderm layer of *Dag1* null embryoid bodies (EB) demonstrated enhanced cell death (Li et al 2002). All these experiments suggest that physical or functional removal of DG leads to cell death indicating the importance of DG as a signalling centre.

Drosophila Dystroglycan

A *Dg* ortholog has been found in *Drosophila* (Greener & Roberts 2000) and initial studies suggest that the invertebrate DG has similar functions as its mammalian counterpart. As the DG null chimaeric mice demonstrate a progressive muscular dystrophy (Côté et al 1999), so does the reduction of DG in *Drosophila* melanogaster muscles (Shcherbata et al 2007). This demonstrates that DG's role in muscular dystrophies can be studied using the *Drosophila* model system.

The *Drosophila* DG protein, deduced by conceptual translation, has the same domain structure as its vertebrate ortholog; the N-terminal portion of α-DG, the mucin-like region which is O-glycosylated and required for interaction with the ECM, the C-terminal domain of α-DG, a transmembrane domain and finally the β-DG, however it is has not been shown to be cleaved. The conservation of the glycosyltransferases required for DG glycosylation in *Drosophila* O-

mannosyltransferase-1 and 2, suggest that *Drosophila* DG is glycosylated (Haines et al 2007, Ichimiya et al 2004). *Drosophila* DG also conserves the amino acid sequence of the c terminal dystrophin (DYS) binding site (Deng et al 2003), and it has been demonstrated that *Drosophila* DG and DYS can physically interact. (Yatsenko et al 2007).

In contrast to vertebrate *Dag1*, *Drosophila Dg* is subject to differential splicing of its mRNA. Sequencing of embryonic cDNA libraries led to the identification of 3 different splice forms which produce three predicted isoforms (fig.2): DG-A lacks exon 8, DG-B lacks domains encoded by both exon 8 and 9, DG-C lack the domain encoded by exon 9. Exon 8 is predicted to encode the mucin-like region of DG (Deng et al 2003). In the embryo it has been shown that differential splicing is developmentally regulated and tissue specific. DG is expressed within the embryonic nervous system. The DG-C form is found on neurons, whereas the DG-B is found on glia (Schneider & Baumgartner 2008).

As in vertebrates, DG is expressed in multiple cell types including oocyte follicular epithelial cells (Deng et al 2003) and muscle cells (Medioni et al 2008, Shcherbata et al 2007). Tissue specific gene expression in adult *Drosophila*, reveals that *Dg* mRNA is highly enriched in the CNS (Chintapalli et al 2007). The adult brain expresses *Dg* mRNA 12.20 times higher relative to the whole body. The thoraccicoabdominal ganglion (ventral nerve cord) also has an enrichment of

Dg mRNA 11.70 times higher relative to the whole body. This suggests DG has a functional role in the Drosophila CNS.

The first series of *Dg* alleles reported, available at the start of this study, were deletions of *Dg*'s first non-coding exon, including the alleles Dg^{248} and Dg^{323}, which were reported to be lethal (Deng et al 2003) (figure 2). These mutations were generated by imprecise excision of the P element *EP(2)2241* that is inserted into the first non-coding exon of *Dg*. Though the Dg^{2241} stock is lethal, out-crossing yields homozygous viable lines (Christoforou et al 2008). Complementation tests of the *Dg* deletion series, to the then known 5' neighbouring genes CG8418 and Rho1, showed the deletion was specific to *Dg*. The *Dg* deletion series were reported to have a loss of oocyte cell polarity which could be rescued by the expression of transgenic *Dg-RC* (Yatsenko et al 2007). The rescue further supported the idea that the deletion was specific for *Dg*. The second series of four *Dg* alleles were more recently generated by chemical mutagenesis using ethyl methane sulfonate (EMS), Dg^{0*} (Christoforou et al 2008). All four alleles introduce premature stop codons into the sequence. The series includes two nonsense mutations Dg^{043} and Dg^{086} and two deletions Dg^{038} and Dg^{055} (figure 2). The EMS Dg^{0*} alleles believed to be null for DG, are viable. Genetic interaction studies of *Dg* alleles demonstrate that it interacts with the notch signalling pathway providing evidence that DGC is not only required for the

canonical structural role but also as a signalling centre (Christoforou et al 2008, Kucherenko et al 2008) .

Recent findings demonstrate that the *Dg* deletions series not only deletes *Dg*'s first non-coding exon but also deletes portions of the promoter of the 5' neighbouring gene, the mitochondrial ribosomal protein L34 (*mRpL34)* (figure 2). At the time of the initial studies using the *Dg* deletion lines, the gene was not annotated, and the complementation and rescue experiments did not suggest the deletion of another gene. The *Drosophila mRpL34* gene was predicted, by bioinformatics, from its homology to the human *mRpL34* gene (Marygold, S. personal communication to Flybase Id FBrf0191530). Nuclear encoded mRps are structural components of the mitochondrial ribosome necessary for the translation of mitochondrial DNA (Miller et al 2004). Mutations within *Drosophila* ribosomal protein genes are part of a group of mutations called Minute mutations, whose phenotypes are a direct result of suboptimal proteins synthesis (Marygold et al 2005). Expression of a genomic transgene of *mRpL34* in the *Dg* deletion series demonstrated rescue of the loss of polarity in follicular epithelial cells (Mirouse et al 2009). Expression of transgenic *Dg-RC* could also rescue the loss of polarity. Both *Dg* and *mRpL34* could rescue the loss of polarity in the *Dg* deletion series follicular cells. The deletion of *mRpL34* was predicted to place metabolic stress on the cells, due to the dysfunction of mitochondrial ribosomes.

To test this hypothesis the same group, placed the EMS *Dg*^{0*} oocytes under metabolic stress through glucose restriction. This resulted in a loss of polarity in the follicular epithelia which led them to suggest that DG is required to maintain epithelial cell polarity during cellular metabolic stress. Further experiments suggest that the mechanism of this stress related polarity maintenance is predicted to involve binding to its ligand perlecan and proper localisation of mysosin II, within the cell for activation by the stress pathway AMP kinase (AMPK).

In a more recent report a temperature sensitive mutant, *atu*, was found to be a *Dg* hypomorph (Takeuchi et al 2009). They also generated a deletion of *Dg* in its first non-coding exon demonstrating an 85% reduction in DG expression. These *Dg* mutants, which seek out and survive at lower temperatures, have higher metabolic rates. There findings also suggest a decrease in DG leads to increased internal concentration of calcium ions resulting in the activation of a mitochondrial dehydrogenase, thereby increasing mitochondrial oxidative metabolism. Regulation of metabolism during conditions of metabolic stress is particularly important in the CNS, where neurons have a high metabolic rate and are sensitive to changes in the supply of glucose. These recent findings open up a new field of research for DG where it may play critical roles in regulating metabolic rates and/or responses to metabolic stress. Since DG is expressed in

neurons it may have a more specific role in neuroprotection from metabolic stress.

Rationale and Objectives

Dystroglycanopathies are MDs with CNS anomalies which include lissencephaly, mental retardation and ocular anomalies (Martin 2005). DG is expressed in the CNS, including neurons and glia. Deficiencies in the vertebrate *Dag1* gene have shown that it is required in the development of the CNS (Moore et al 2002, Satz et al 2008). DG is conserved in *Drosophila* (Greener & Roberts 2000), and the DG mRNA enrichment in the CNS of *Drosophila* indicates its expression and function in these tissues (Chintapalli et al 2007).

The aim of this study will be to determine the role of DG in the development of the *Drosophila* eye, a versatile model of the developing CNS. This may be tested by determining DG localisation within the developing *Drosophila* eye and then determining the developmental impact of reduced DG levels on eye development. The use of RNA interference (Dietzl et al 2007) may test the impact of reducing endogenous DG levels during eye development. Two series of *Dg* alleles may be tested to determine the impact of genetic reduction of DG, the *Dg* deletion (Deng et al 2003) and the EMS Dg^{0*} alleles (Christoforou et al 2008) (Chapter 2).

Recent findings suggest DG may have a role in protecting cells during metabolic stress (Mirouse et al 2009). This study also aims to characterise the role of DG in the developing *Drosophila* eye under metabolic stress, by

characterising the development of the *Dg* deletion allele Dg^{248}. Whether DG contributes to protecting cells by inhibiting apoptotic cell death or maintaining cell polarity will be tested (Chapter 3).

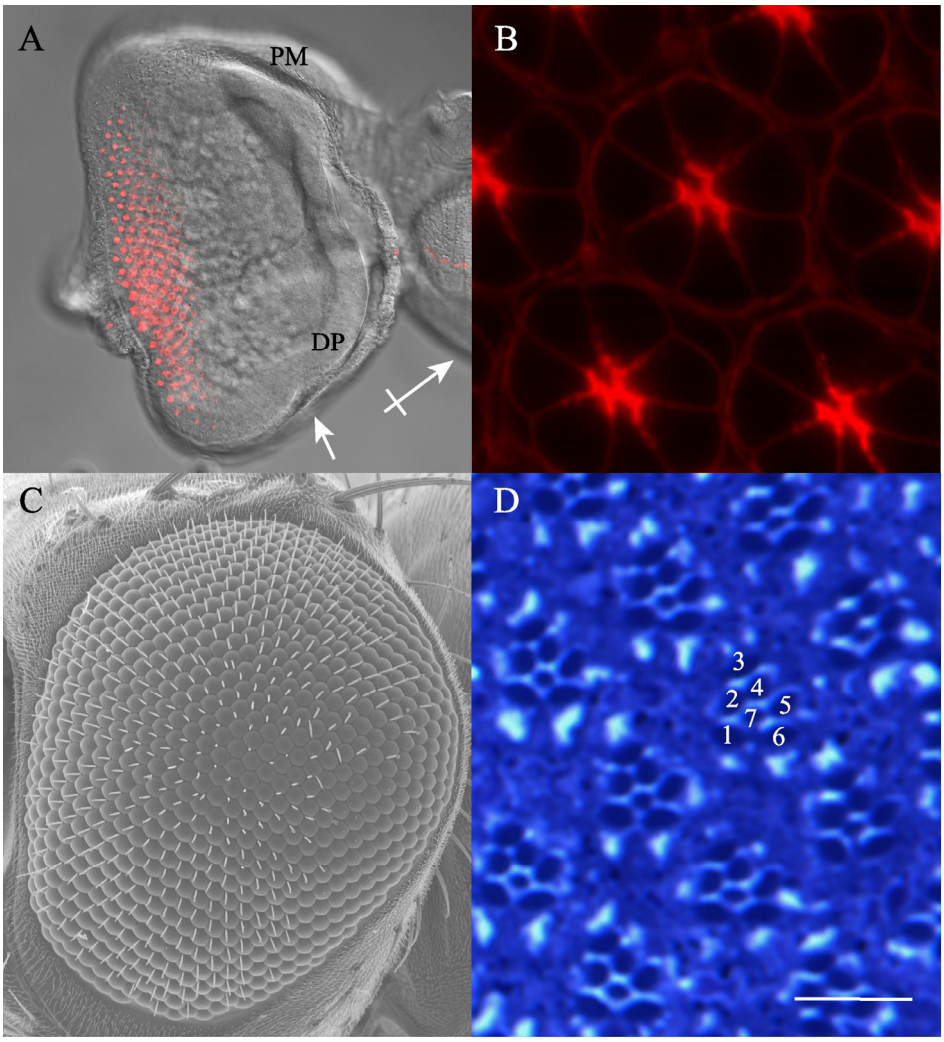
A
PM
DP
B
C
D
3
2
4
7
5
1
6

Figure 1. Development of the *Drosophila* Eye.

A) Third Larval Instar. A differential interference contrast image merged with a single fluorescent confocal plane of a third instar eye disc stained with the R cell membrane marker (red). The orientation of the tissue with respect to the body axis is indicated by the crossed arrow which points anteriorly. The central eye disc is flanked by the antennal disc anteriorly and the most posterior projection is the optic stalk. The eye imaginal disc is a sac with the disc proper (DP) and the peripodial membrane (PM) separated by a lumen. The arrow points to the dorsal ventral morphogenetic furrow, the wave of differentiation that travels across the disc. Posterior to the disc cells become specified and initiate differentiation. Differentiating R cells are identified by chaoptin. B) Mid pupa. A confocal planar section through a 52% p.d. eye disc stained with phalloidin to highlight f-actin. Seven R cells are seen per ommatidia. The eighth R cell has migrated to its lower plane which is out of focus. R cells, at this stage are still interacting through zonula adherens at the level of the apical domains, highlighted by high concentration of f-actin labelling. C) Adult external eye. The SEM of an adult eye shows the ≈800 facets composing the eye. The facets are ordered into a hexagonal pattern. D) Adult internal eye. A planar section through the retina shows the hexagonal patterning of ommatidia. At the core of each ommatidium are the R cells. Seven R cells are seen in this plane. The rhabdomeres are

arranged in an asymmetric trapezoid pattern (numbers are placed on each R cell rhabdomere). The scale bar is: 72 μm in A, 30 μm in B, 150 μm in C and 9 μm in D.

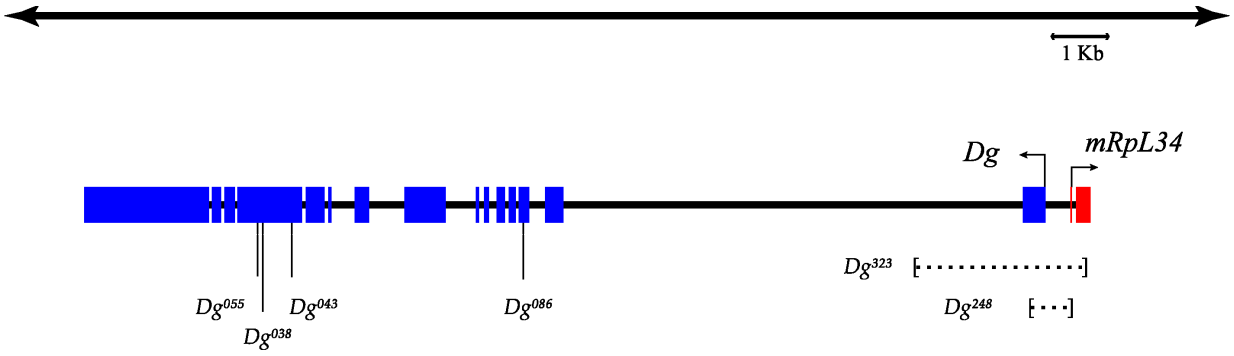
1 Kb
Dg
mRpL34
Dg055
Dg038
Dg043
Dg086
Dg323
Dg248

Figure 2. The genomic map of *Dg* and *mRpL34*

The intron (black line) and exon (coloured blocks) structure of the *Dg* (blue) and *mRpL34* (red) loci with a representation of *Dg* alleles. The EMS Dg^{0*} series of alleles introduce premature stop codons into the sequence (indicated) through deletions in Dg^{055} and Dg^{038}, as well as point mutations in Dg^{043} and Dg^{086}. The deletion series of *Dg* alleles in addition to deleting all or part of *Dg*'s first non-coding exon deletes portions of the *mRpL34* gene; Dg^{323} deletes both the *mRpL34* promoter and part of the coding sequence and Dg^{248} (used in this study) deletes the *mRpL34* promoter region. The deleted region is shown as a dashed line.

Chapter Two - Dystroglycan during Eye Development

by Nadia Y. Melian, Mario Pantoja, Hakima Moukhles, Hannele Ruohola-Baker and Sal Carbonetto

Introduction

Dystroglycanopathies are muscular dystrophies where DG's inability to interact with the ECM leads to CNS defects (Martin 2005). These defects include ocular malformations suggesting that DG has a role in eye development. The genetic tools available for studying the role of DG during eye development included chimeric mice and the *Drosophila* developing eye. Though DG was known to be expressed in the vertebrate R cell synapse the role of DG during eye development was not known at the time of these studies due to the embryonic lethality of *Dag1* knockout mice. The *Dag1* chimeric mouse was therefore used to determine if DG had a developmental role in eye formation.

The *Drosophila* DG homolog was recently identified (Greener & Roberts 2000). Endogenous knockdown of DG in *Drosophila* muscle leads to progressive muscle degeneration (Shcherbata et al 2007). This is similar to the muscular dystrophy observed in the *Dag1* chimeric mice (Côté et al 1999). *Drosophila* could therefore be a valuable tool to study the function of DG during eye development. DG is expressed during *Drosophila* embryonic development including in the embryonic nervous system (Schneider & Baumgartner 2008), and further characterisation of DG localisation during eye development would be a valuable clue to its functions. *Drosophila* allows the use of RNA interference (Dietzl et al 2007) to down-regulate endogenous protein levels in a precise

spatio-temporal fashion. Different *Dg* alleles (Christoforou et al 2008, Deng et al 2003) allows study of eye development with a genetic reduction of DG. Together these tools allow us to determine the consequences of decreased DG levels on eye development providing evidence of the mechanisms in which DG functions in the eye. Using mosaic analysis during development also allows the cell autonomy of DG to be established. Together, these experiments may provide evidence for the mechanisms in which DG participates during eye development.

Materials and Methods

Analysis of eyes in DG deficient chimeric mice:

As described previously (Côté et al 1999), mice mosaic for wild type and DG-null cells were generated by injecting blastocysts with mouse embryonic stem (mES) cells that were null in both DG alleles. DG-wt mES cells were also injected to generate control mosaics. Injections were performed by a transgenic facility run by Dr. A. Peterson at the Royal Victoria Hospital, McGill University. This yielded animals with different degrees of mosaicism. The percent contribution of the DG null or wt cells to an organ was quantified by assaying the ratio between the different electrophoretic variants of glucose phosphate isomerase (GPI) of the parent mouse strains (Charles & Lee 1980). The double *Dag1* knockout and wild type R1 mES cells were of a 129 strain background (Nagy et al 1993) whereas the recipient blastocysts were from the C57Bl/6J strain. The agouti coat color of the resulting animals was used as a marker for high mES contribution to the animal. The agouti animals were produced after six series of injections of DG-wt mES and eighteen series of DG-null mES injections. Statistical analysis of the mosaic populations was performed using the statistical software SPSS v.11.

To analyse the effect of *Dg* deficiency on mosaic eye development, chimeric eyes were dissected to determine both DG-null mES cell contribution to

the tissue and the cytoarchitecture of the eye. Mice were anaesthetized with xylazine (2mg/ml, Bayer) and Ketamine hydrochloride (15mg/ml Ayerst). Eyes were dissected and flash frozen in the cryopreserver O.C.T. (Sakura) using liquid nitrogen cooled 2-methylbutane. Mice eyes were sectioned using a Leica CM3050S cryostat. Some sections were used to make a representative protein extract of the DG deficient eye for a GPI assay to determine the contribution of DG deficient cells to the eye using the methods described (Peterson et al 1978). Other sections were post fixed using 4% paraformaldehyde and stained with hematoxylin and eosin (H&E) to reveal cytoarchitecture of the DG deficient retina.

Drosophila Strains

D. melanogaster were raised on cornmeal-yeast-agar medium at 25˚C. The *Dg* alleles have been previously described. The *w; FRT42D* Dg^{248}*/cyo* (Deng et al 2003) (a gift from Hannele Ruohola-Baker) was ready for clonal analysis. The wild type: yw; FRT42D line (Bloomington stock center) was used to generate wt mosaics. The EMS Dg^{0*} mutants Dg^{038}/cyo, Dg^{043}*/cyo*, Dg^{055}/cyo, Dg^{086}/cyo (Christoforou et al 2008) (gifts from Robert Ray) were used directly as the stocks became homozygous. Homozygous wt or Dg^{248} clones were generated by using ey-FLP/FRT (Xu & Rubin 1993) system. The *y w, GMR-LacZ*

ey-FLP; FRT42D lw⁺/Bc was used to generate large patches and the *y w, GMR-LacZ ey-FLP; FRT42D GMR-myr-GFP* was used to generate small patches (Bloomington Stock Center). To generate eyes composed entirely of mutant cells, the mosaic system (Stowers & Schwarz 1999) w; *FRT42D GMR-Hid Cl2/cyo; ey-gal4, UAS-FLP* (Bloomington Stock Center) was modified to *y w, GMR-LacZ ey-FLP; FRT42D GMR-Hid Cl2/Bc.* The *mRpL34* transgene *P[w⁺, mRpL34⁺]42.1/TM6B, Hu, Tb* (Mirouse et al 2009)(a gift from Robert Ray), *w; FRT42D Dg^{248}/cyo* and yw;*FRT42D* were used to construct *w; FRT42DDg^{248}/Bc; P[w⁺, mRpL34⁺]52.1/Tb* and *w; FRT42D; P[w⁺, mRpL34⁺]52.1/Tb,* to be used for clonal analysis. *c155-gal4* and *elav-gal4* (Bloomington stock centre) and *UAS-Dg-RC* (Deng et al 2003) (a gift from Hannele Ruohola-Baker) were used to generate mosaics expressing DG-C in R cells. The lines *c155-gal4; FRT42D Dg^{248}/Bc; UAS-Dg-RC/Tb* and *c155-gal4; FRT42D; UAS-Dg-RC/Tb* were constructed and used for mosaic analysis. The lines *eyFLP; FRT42D lw+/Bc*; *UAS-Dg-RC* and *yw; FRT42D; elav-gal4* and *yw;FRT42D Dg^{248}/Bc; elav-gal4* were constructed for mosaic analysis. The line tub-gal4 (Bloomington stock Center) was used to construct *w; FRT42D Dg^{248}/Bc; tub-gal4/Tb and w; FRT42D; tub-gal4/Tb.* For MARCM analysis the line *hsFLP, UAS-mCD8GFP; FRT42D tubulin-Gal80/Bc* (Bloomington Stock Center) was crossed with *w; FRT42D Dg^{248}/Bc; tub-gal4/Tb or w; FRT42D; tub-gal4/Tb* and placed into a new food vial

daily. When the larvae of a vial reached early third instar they were heat shocked in a 38˚C water bath for one hour. This induced the expression of FLP to generate single cell clones. RNAi analysis was performed using the following lines. The DysRNAi line *UAS-Tg4Dys N-term* (Deng et al 2003) (a gift from Hannele Ruohola-Baker). The lines *UAS-dsDg30A* (Deng et al 2003) and *UAS-dsDg12* (a gift from Marie-Laure Parmentier) were used to construct *UAS-dsDg12/Bc;UASdsDg30A* (DgRNAi), which target the C-terminal of the mRNA common to all three known *Dg* mRNA splice variants. The lines *UAS-Dcr2* (X chromosome) (a gift from Georg Dietzl and Barry Dickson)(Dietzl et al 2007) and *GMR-gal4* (Freeman, Bloomington Stock Centre) were used to construct *UAS-Dcr2; GMR-gal4/Bc* (Driver). The driver was crossed to DgRNAi, DysRNAi or the control w^{118} (Bloomington Stock Center). Pupa staging was performed under the assumption that 1% pupal development (p.d.) corresponds to 1h at 25˚C.

Staining and Imaging

Immunofluorescence of eye discs was performed by following standard procedures (Walther & Pichaud 2006). Primary antibodies were used as follows: rabbit anti-DG^{ex8} (1/50) (Deng et al 2003) (a gift from Martina Schneider), rabbit anti-DGcyto (Carbonetto in-house reagent), mouse anti-chaoptin (1/250 Developmental Studies Hybridoma Bank [DSHB]) and chick anti-GFP (1/100

Invitrogen). Tissue was also stained by octadecyl (C_{18}) indocarbocyanine (DiI) (1/200, Invitrogen), or Phalloidin (1/2000, Sigma-Aldrich). Epifluorescent imaging was performed using a Zeiss axioskop plus. Confocal imaging of whole mount tissue was performed using a Zeiss LSM510 Meta Confocal microscope. 3D reconstructions and reslicing were performed using the software Volocity from Improvision/PerkinElmer. Image projections were performed using Aim Image Browser (Zeiss). Images were cropped using Photoshop CS2 (Adobe). Confocal microscopy acquisition and volocity image analyses were performed at the CIAN core facility (Biology Dept., McGill University, Montréal).

To image adult fly heads, flies were placed at -80˚C for 10 minutes, then placed under a dissecting scope (Zeiss Stemi 2000) and images were taken using a Nikon Eclipse E600 digital camera. Images were cropped using Photoshop CS2 (Adobe).

Histology of adult eyes was prepared as modified from Gaengel and Mlodzik (Gaengel & Mlodzik 2008). Briefly, fly heads were decapitated and half an eye sliced off. Heads were placed in 2% gluteraldehyde in 0.1M PB, on ice for 30 min. Heads were then post fixed by adding an equal volume of 2% OsO_4 in 0.1 PB, for 1 hour on ice. The solution was then changed to 2% OsO_4 in 0.1 PB, for 2 hours on ice. After osmication, specimens were dehydrated in increasing dilutions of ethanol on ice. Samples were cleared with propylene

oxide at room temperature. Samples were incubated in a 1:1 solution of epon and propylene oxide followed by 100% epon, each overnight at 4˚C. Samples were embedded and baked overnight. Planar semi-thin 0.9 μm sections were cut using an ultratome and stained with 0.5% toluidine blue. Light phase images were visualised on a Nikon eclipse E600 microscope and images captured using software from Metamorph.

Scanning Electron Microscopy

Whole flies were dehydrated in increasing concentrations of ethanol in water (25, 50, 75, 100% ethanol) each one hour at room temperature. Flies were then incubated in increasing concentrations of amyl acetate in ethanol (25, 50, 75, 100% amyl acetate) each thirty minutes at room temperature. Following critical point drying, flies were coated with gold/palladium. Scanning electron microscopy (SEM) was performed at the McGill Facility for Electronic Microscopy Research on a Hitachi S-3000N Variable Pressure-SEM.

Rhabdomere length analysis

Histological sections of fly heads were prepared from paraffin wax embedded material. The following protocol is modified from Shcherbata et al. 2007 (Shcherbata et al 2007). Briefly, flies were placed in Heisenberg fly collars

(Model #10731, 4M Instrument & Tool LLC, New York) and fixed in Carnoy's solution (6:3:1 ethanol (EtOH):chloroform:glacial acetic acid) overnight at 4 °; then further dehydrated in 100% EtOH (2x10 min) at room temperature (RT) and, finally, infiltrated with paraffin (Poly/Fin, Triangle Biomedical Sciences, Inc) using the following procedure. Samples were placed in methyl benzoate for 30 min at 65°, then transferred to a methyl benzoate:paraffin solution (1:1) and further incubated at 65° for 30 min, and finally placed in paraffin alone at 65° for an additional 30 min. Afterwards samples were placed in casts, and then filled with melted paraffin (65°). Once cooled and solidified, the collars were removed and frontal sections of the fly heads were cut with a rotary microtome (Leica 820 Histocut) at an 8 micron (um) thickness. Paraffin was removed with xylene (2x4 min) and the sections were rehydrated (100% EtOH 2x4 min, 95% EtOH 1x3 min, 70% EtOH 1x2 min, H_2O 1x1 min) then stained with hematoxylin and eosin using standard protocols (H&E staining). Sections were covered with DPX Mountant (Fluka), cover-slipped and analyzed using confocal microscopy (Leica). Utilizing the fluorescence of the H&E stains, red channel images were viewed and analyzed. Sections corresponding to the midpoint of the fly head (from front to back) were used to obtain rhabdomere lengths. Rhabdomeres at the midpoint of the adult fly brain abutting the eye (the lamina) were measured using Leica software. Six to 14 fly heads were analyzed in a single sample preparation; and

provided that both eyes were intact this corresponded to up to 12 to 28 measurements per preparation.

Results

DG deficiency in mice results in severe eye defects.

Chimeric mice deficient for DG were generated as previously described (Côté et al 1999) and the contribution of DG-null cells in the eye was determined by assaying electrophoretic variants of glucose phosphoisomerase (Peterson et al 1978). Chimeric adult eyes deficient in DG generally showed corneal opacities (fig.1B). Some mice with closed eyelids (fig.1C) developed microphthalmia (fig1.E) or anophthalmia. DG deficient retinas generally had conserved retinal lamination (fig.1E) but retinal folds were also found. Within the retinal layers there were fewer cells. In particular, the outer nuclear layer where R cells are present is much thinner and the stained R cells are fewer and disorganized (Fig. 7E). Fusion of the lens to the retina was also found (fig.1E, arrow).

Malformations may arise spontaneously in strains of inbred mice (Smith et al 1994). To determine whether the frequency of eye abnormalities in DG-null chimeras was significant, the DG-wt and DG-null chimeric populations were compared. Eye malformations, including opacity and microphthalmia, occurred with a frequency of 0.17 in DG-null chimeras, but had no occurrence in DG-wt chimeras. The difference in frequency of eye defects between the two populations of n= 30 DG-null chimeras and n=22 DG-wt animals is statistically different: $t_{(29)} = 2.11$, $p= 0.043$ by independent sample t-test. If only analyzing

the frequency of eye malformations within the dissected population of only the DG-null chimeras (n=34), by comparing agouti coat high mouse embryonic stem (mES) cell contributors versus black coat low mES cell contributors, the frequency of eye malformations increases to 0.29 with a significant difference of $t_{(33)} = 3.71$, $p = 0.001$ by independent sample t-test.

Dystroglycan isoform C concentrates on the apical surface of developing R cells.

To determine whether DG isoforms are expressed during eye development, an antibody specific to the isoform predicted to be glycosylated was used to detect DG-C expression at different developmental stages. Mosaic clones were induced using the Eyeless (ey) driven FLP/FRT mitotic recombination (Theodosiou & Xu 1998). A mosaic system, using post MF driven membrane bound GFP to label wt and unflipped heterozygote cells, was used to generate patches of the DG deficient allele, *Dg*^{248}. Third instar discs were stained for DG (fig.2 A and C:magenta) and GFP (fig.2 B and C:green). Areas lacking GFP also lacked DG (fig.2 C) confirming the specificity of the antibody in third instar eye discs. The single field examined (A-F) is localised in the posterior region of the third instar disc. This area has been exposed to the wave of specification of the MF (fig.2 A and D arrow) traveling anteriorly across the eye disc (fig.2 A and D crossed arrow). To determine whether DG-C localizes to the

newly specified R cells, the eye disc was also stained for chaoptin, an R cell specific membrane marker (fig.2 D and F:magenta) which expresses after the MF has passed. DG-C (fig.2 E and F:green) co-localizes with chaoptin (fig.2 F). The pattern of chaoptin's apical staining reflects the ordered array of ommatidia within the disc. DG-C shows this pattern immediately posterior to the MF, prior to chaoptin expression indicating that concentration of DG-C to the apical surface is an early event in R cell specification. To determine if, in the third instar eye disc, DG-C expression is restricted to R cells, a wild type disc was stained for DG-C (fig.2 H) and DiI (fig.2 G) to label all membranes of the disc tissue. The basal view of the 3D reconstruction of the whole mount third instar eye disc reveals that DG-C also concentrates at the basal surface in the anterior region of the disc (fig.2 G-J) both prior to and at the MF (asterisks in fig.2 G-J). A sagittal view through the same disc shows DG-C localised to projections spanning between the peripodial membrane and the disc proper at the MF (fig.2 J). The sagittal view also shows the basal concentration of DG-C in the anterior regions as well as the apical concentration in the posterior specified R cells. Together this localisation data indicate that, in the third instar, DG-C may be contributing to multiple developmental events. It is clearly expressed early in developing R cells and it also potentially has roles in the proliferative anterior region and on the coordinating peripodial projections.

Early pupal *Dg*^{248} mosaic eye discs were examined to determine whether DG-C expression and localization persisted during development (fig.3 A-D). *Dg*^{248} mosaic eye discs were examined at 40% p.d. for expression of DG-C (fig.3 C and D magenta) and GFP (fig.3 B and D green). The R cell marker chaoptin outlined R cells (fig.3 A). The membrane bound GFP also outlined wild-type R cells (fig.3 B and D green) that localize DG-C to their apical surfaces (fig.3 D). A lower concentration of DG-C is also found at the lateral surfaces of R cells

Decreasing endogenous levels of DG or DYS during eye development leads to retinal disruption and facet roughening in the adult eye.

When using a genetic deficiency, at the onset of development redundant molecular systems may compensate for a loss of DG. To gain functional information about DG specifically during a specified period of eye development RNA interference (RNAi) was used to degrade the endogenous *Dg* mRNA levels thereby leading to the reduction of DG protein levels. DG was specifically targeted by expressing an UAS-double stranded *Dg* RNA at the onset of cell specification using the GMR-gal4 driver (Moses & Rubin 1991). This driver expressed GAL4 in all cells types posterior to the MF beginning at the third instar and continuing during pupal development. DG down-regulation thereby begins at the time during development when it becomes concentrated to the apical tip of

the R cells and this is decreased in *Drosophila* expressing *Dg* RNAi using the GMR driver (fig.4 E and F).

Targeting of *Dg* mRNA starting at the MF leads to a smaller rough adult eye phenotype (fig.4 B) with mispatterned facets (fig.4B'). The GMR driver alone (fig.4 A and A') and the *dsDgRNAi* alone (fig. 4 D and D') eyes develop normal external eye facets. Though the *dsDgRNAi* alone control develops a normal retina (fig. 4 D''), the GMR-gal4 driver alone does lead to some disruption of the retina (fig. 4 A''). Previous work indicates that accumulation of GAL4 can induce apoptosis in neurons in a dosage dependent fashion (Rezaval et al 2007). The retinal driver alone tissue however, still maintains ommatidia which are patterned in a hexagonal fashion (fig.4 A'' outline), each ommatidium having developed R cells (fig.4 A'' arrow). When *dsDgRNAi* is expressed at the time of R cell specification onward, retinal tissue (in all the animals examined) is disrupted (fig.4 B''), beyond that seen in the control lines (fig. 4 A''). Ommatidial patterning is lost and the R cells that do develop have altered morphologies with enlarged rhabdomeres (fig.4 B'' arrow).

Dystrophin is an intracellular binding partner shown to physically interact with DG in *Drosophila* (Kucherenko et al 2008). DYS is expressed in the developing eye disc where it may be a binding partner for DG (van der Plas et al 2007). When the DG cytosolic binding partner DYS mRNA is targeted for

degradation, during eye development, the resulting adult eye facets are slightly roughened (fig.4 C), though the facets maintain hexagonal patterning (fig.4 C'). The retina of eyes expressing *dsDysRNA* (fig.4 C'') are however disrupted more severely with a loss of ommatidial patterning and the presence of vacuoles. R cells are present in retina down regulating *Dys*, but they have an altered morphology with enlarged rhabdomeres. Together these data suggest that DG and DYS may function together to maintain normal eye development.

Dg^{248} has a cell autonomous effect during eye development.

Understanding cell autonomy may help localise the mode of action of Dg^{248} in R cells. Mosaic analysis with repressible cell marker (MARCM) single cell clones and small patch mosaic clones were examined. MARCM allowed the generation of single mutant cells, which were identified by the expression of membrane bound GFP driven by a ubiquitous tub-GAL4 driver. Co-labelling with chaoptin, the R cell marker, allowed the identification of single Dg^{248} R cells. The small patch mosaic system uses ey-FLP to generate mutant in all cell types of the retina followed by the use of GMR-GFP to label the wt or unflipped cells. The GMR driver labels the majority of the cells with the exception of cone cells. A total of 25 adult R cells, each a single cell MARCM clone homozygous for Dg^{248} were found to develop normally (fig. 5). However Dg^{248} small patch mosaics,

show only cell autonomous disruptions beginning during early pupal development (fig.6). During early pupation wild type ommatidia are composed of the eight R cells, each roughly occupying an equal fraction of the ommatidial volume, and attached to other R cells at their lateral and apical surfaces. The R cells of ommatidia composed solely of Dg^{248} R cells (fig.6 asterisk), form disorganized clusters of cells not always interacting with their neighbours for the whole proximal-distal length of their apical surfaces. However, the morphology of the wt R cells within Dg^{248} ommatidia remains normal (fig.6 arrowhead). Conversely, an ommatidium containing a single Dg^{248} R cell surrounded by wild type R cells maintains a normal morphology (fig.6 arrow). In all instances the effects seen were cell autonomous. Together the MARCM and the small patch mosaic of Dg^{248} suggests a cell autonomous role for Dg^{248} in the morphology of the R cells that may be rescued if surrounded by a threshold number of wt photoreceptors.

mRpL34 significantly rescues development of the disrupted Dg^{248} eye.

Previous studies of DG in *Drosophila* were performed using the deletion alleles Dg^{248} and Dg^{323}. Large clones of Dg^{248} in mosaic eyes had been shown to lead to an apparent degeneration of retinal tissue (Zhan et al in prep). Recent work (Mirouse et al 2009) has demonstrated that the Dg^{248} deletion allele not only deletes a *Dg* regulatory domain but also the regulatory region of the

mitochondrial ribosomal protein L34 (*mRpL34*) gene. mRpL34 is a structural protein of the mitochondrial ribosome. In follicular cells of the oocyte *mRpL34* is able to rescue the loss of polarity of Dg^{248} mosaic clones (Mirouse et al 2009). To determine if *mRpL34* could do the same to the Dg^{248} eye phenotype, Dg^{248} mosaics expressing a genomic *mRpL34* transgene in the background were generated (Dg^{248}mosaic + *mRpL34*).

Problems in Dg^{248} eye development are first seen during early pupal stages as previously mentioned (fig.6), where Dg^{248} R cells form abnormal morphologies in ommatidia. To determine the impact of *mRpL34* on Dg^{248} R cell pupal development small patch mosaics were generated. Wt mosaic ommatidia (fig.7 arrow in series A), develop normal R cell morphologies (fig.7 A''') with DG-C localised to their apical surfaces (fig.7 A). In Dg^{248} mosaic ommatidia (fig.7 arrow in series B) R cells develop abnormal morphologies (fig.7 C''') and do not express DG-C (fig.7 B). Dg^{248} *mosaic* ommatidia expressing *mRpL34* in the background (fig.7 arrow in series C) develop R cells with the normal R cell morphology (fig.7 C'''), but they still lack the expression of DG-C (fig.7 C) at their apical surfaces. This data indicates that *mRpL34* significantly rescues the early pupal morphology of Dg^{248} R cells.

To determine if *mRpL34* rescues the adult stages of Dg^{248} mosaic eye development a mosaic system generating an eye composed solely of one

genotype (Stowers & Schwarz 1999) was used to compare eye development of *Dg*^{248} mosaics in the presence or absence of *mRpL34*. A wt mosaic formed a normal eye (fig.8 A-A''). The expression of the genomic *mRpL34* transgene, in the background of a wt mosaic, did not affect eye development (fig.8 B-B''). *Dg*^{248} mosaics generated highly disrupted eyes (fig.8 C-C'). Examination of the facets by SEM revealed areas of facet flattening (C, arrow) and disruption of the hexagonal patterning of facets (fig.4 C'). The internal ommatidial patterning was also disrupted (fig.8 C''). Within the disrupted retina, R cells and their rhabdomeres were present (fig.8 C'', arrow), but with aberrant morphology. The number of R cells per ommatidium was not constant and lower than the expected 7 R cells normally found in a single planar section (fig.8 A''). Expression of the genomic *mRpL34* transgene significantly rescued the morphology of *Dg*^{248} mosaics (fig.8 D-D''). The facet morphology and patterning returned to normal (fig.8 D'') as did the ommatidial patterning (fig.8 D''). Together these data indicate that the *mRpL34* transgene can significantly rescue both early and late *Dg*^{248} pupal development to generate a normally patterned *Dg*^{248} adult eye.

The expression of *Dg-RC* in R cells does not significantly rescue *Dg*^{248} mosaic eye morphology.

Since the *Dg*^{248} deletion affects both DG and mRpL34 expression, and *mRpL34* rescues significantly *Dg*^{248} mosaic eye development (fig. 9), then expression of DG may have similar results. This has been shown to be true for follicular epithelial cells of the oocyte where the *mRpL3*4 transgene and *Dg-RC* can independently rescue loss of polarity in *Dg*^{248} epithelial cells (Mirouse et al 2009). Unlike the genomic *mRpL34* transgene which may be expressed in all cells of the developing eye, we could only use the spatio-temporal Gal4/UAS system to target expression of *Dg-RC* in a restricted pattern. Since DG-C was shown to be expressed in R cells (fig.2 and 3), drivers specific to R cells (*elav-gal4* and *C155-gal4*) were used to target expression of *UAS-Dg-RC* specifically in R-cells from the onset of specification at third instar on ward in development (fig.9 N). The expression of *Dg-RC* using both drivers (C155, fig.9 D and elav fig.5 L) did not significantly rescue the facet anomalies observed on large clones of *Dg*^{248} (fig. 5 arrow in panels C, D and I-L). This may be due to detrimental over-expression of DG-C or that DG-C may be required in a different spatio-temporal pattern.

EMS *Dg*^{0*} alleles do not perturb retinal organisation but do regulate retinal thickness.

To determine whether DG plays a regulatory role in eye development the recent EMS series of Dg^{0*} mutations (Christoforou et al 2008), which only perturb *Dg*, were examined. Since these lines are homozygous viable, adult eyes were examined. The SEM of a wild type eye (fig.10 A) shows the normal array of ommatidia. The histology of a cross-section (fig. 10 A') through the internal eye shows the typical pattern of ommatidia. Dg^{043} (fig.10 B, B') and Dg^{086} (fig.10 C, C') were also examined to determine the effect of DG deficiency on eye development. The internal patterning of ommatidia patterning is normal in these DG deficient retinas (fig.10 B', C' and D'). They maintain planar polarity (fig.10 C' line and data not shown) demonstrating that a deficiency of DG does not perturb the overall development and cell patterning of the eye. The SEM of EMS Dg^{0*} mutants show subtle variances from the wild type form. The SEM of Dg^{043} eyes are mispatterned (fig.10 B arrow) in a small area of the eye. This mispatterning was probably not caught in the histology since only a fraction of the adult Dg^{043} (frequency of 0.2), showed mispatterning. The SEM of Dg^{086} (fig. 10 C) showed a normal patterning of ommatidia, but the overall shape of the eye was more spherical and smaller, relative to the wild type.

Localisation of DG at the actin rich apical surface of early pupal R cells may allow it to have a regulatory function on the cytoskeleton. During late pupation R cells elongate requiring modification of the underlying cytoskeleton.

DG may contribute to the regulation of R cell elongation. The retinal thickness of the EMS *Dg^{0*}*, was quantified (fig.10 E and F). Wild type retina (fig.10 E), stained with H&E to highlight photoreceptor rhabdomeres, have average rhabdomere lengths of 96.99 μm; n=11, whereas EMS *Dg^{0*}* mutants have retinas 2/3 the thickness of wild type with an average rhabdomere length of 63.17 μm, n=14 (fig.10 F). Together these data indicate that DG does not regulate the overall development and cell patterning of the eye, but appears to determine adult R cell length.

The EMS *Dg^{0*}* mutant lines are believed to be null alleles (Christoforou et al 2008). To verify that DG-C was not expressed during eye development, third instar eye disc were stained using an antibody specific for the exon 8 epitope present in the DG-C isoform {Deng, 2003 #795}(fig.11). As shown (fig. 2), R cells concentrate DG-C to their apical surfaces. Using chaoptin the R cell marker, to identify the apical tip of R cells (fig.11), the DG-C apical localisation in wt (fig.11 A), *Dg^{043}* (fig.11 B) and *Dg^{086}* (fig 11.C) were compared. As expected, wt eye discs localise DG-C (fig.11 A' and magenta A'') to the apical tip of R cells (fig.8 A' and green A'') and the merge (fig.11 A'') shows the distinct hexagonal pattern of ommatidia. The *Dg^{043}* disc shows residual levels of the DG-C exon 8 epitope (fig.11 B' arrow and magenta B'') on the apical surface of R cells (fig.11 B and green B''). The *Dg^{086}* disc showed no detectable levels of DG-C exon 8

epitope (fig.11 C' arrow and magenta C'') on the apical surface of R cells (fig.11 C and green C''). In *Dg*^{043} truncated isoforms of DG-C are may detected since the nonsense mutation occurs 3' to exon 8. The localisation of the exon 8 epitope on *Dg*^{043} R cells suggests that residual DG isoforms may still be expressed in the EMS *Dg*^{0*} mutant lines.

The chimeric data suggest a requirement for DG during eye development. Throughout *Drosophila* eye development DG-RC is expressed, becoming concentrated at R cell apical surfaces. The *Dg* deletion series also deletes *mRpL34* which significantly rescues their disrupted eye morphology. Analysis of the EMS *Dg*^{0*} series which perturbs only the *Dg* gene, suggest the function of DG during *Drosophila* development is to regulate R cell differentiation.

Figures

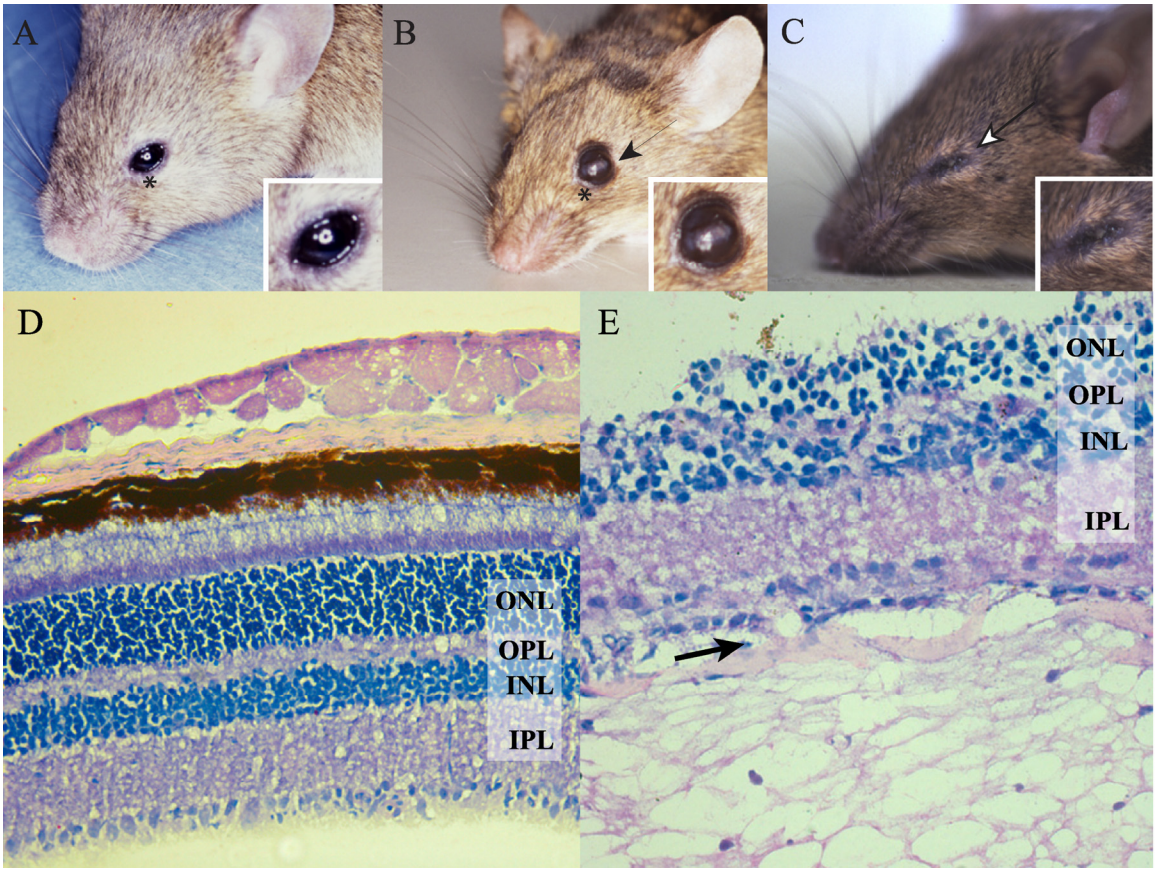

Figure 1. Chimeric mice deficient for DG have eye abnormalities.

A) Wild type adult eye. B and C) DG deficient chimeric adult eyes. Insets are higher magnifications of respective eye and the asterisks (A and B) are reflections due to the use of a flash. DG deficiency results in corneal opacities (B; arrow). Some DG deficient mosaic animals had closed eyelids (arrow, C) with either anophthalmia or microphthalmia (not shown). D) The haematoxylin and eosin staining of a wild type retina shows normal lamination; the outer nuclear layer (ONL), outer plexiform layer (OPL) and the inner nuclear layer (INL). E) The haematoxylin and eosin staining of a DG deficient retina (60% DG null cells) has more or less normal retinal layering but each nuclear layer has a fewer number of cells and the lens is fused to the retina (arrow).

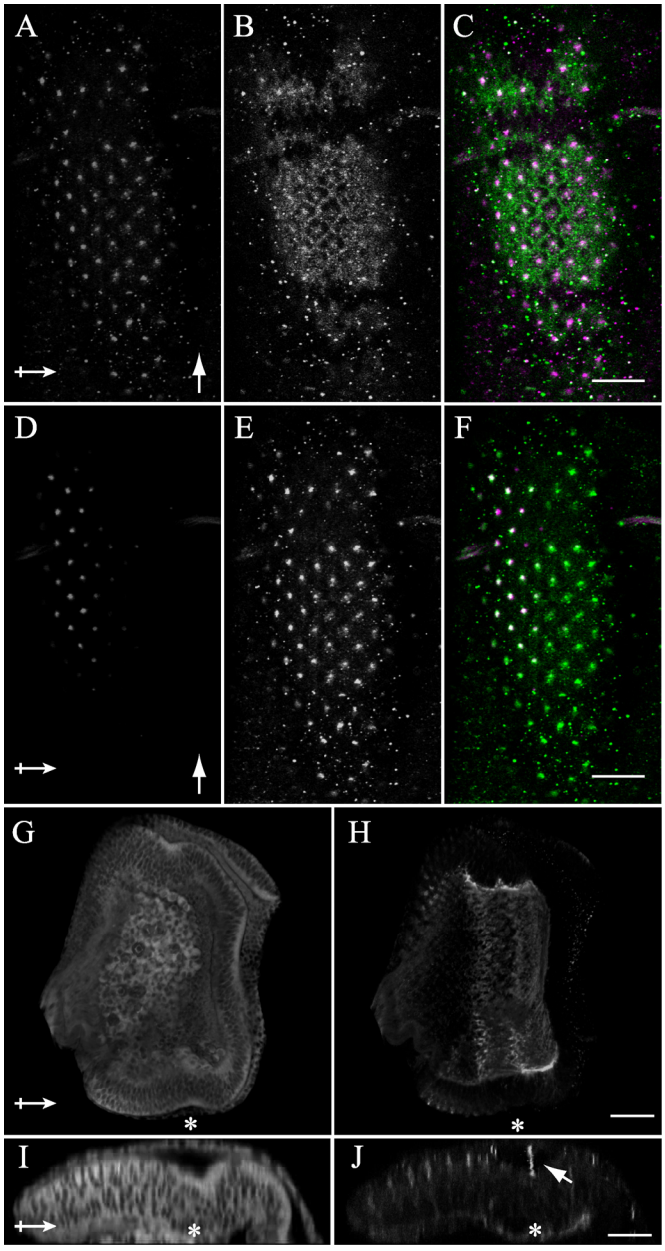
A
B
C
D
E
F
G
H
I
J

Figure 2. DG-C is expressed in multiple regions during third instar eye development.

DG-C is expressed during the third instar stage (A-J). The apical surface of the third instar posterior eye disc was used to determine the specificity of the antibody to DG-C (A and C magenta) using *Dg*^{248} small mosaic patch. GFP negative regions indicate *Dg*^{248} patches (B and C green) in a whole mount third instar disc. Areas lacking GFP also lack DG-C (C is merge of A and B). In the posterior region of the third instar disc, DG-C is concentrated at the apical surface of R cells. In the same field as in A-C, the R cells were localised by their chaoptin expression (D and F magenta) which is expressed at a later stage after the MF passage. The DG-C expression of wild type cells (E and F) co-localizes with the R cells (F is a merge of D and E) at this later stage of specification. A confocal stack of a whole mount wild type third instar disc stained with octadecyl (C_{18}) indocarbocyanine (DiI) (G) to highlight membranes was reconstructed, using the Volocity software, into 3D (G and H) with the view onto the basal surface of the disc. The expression of DG-C (H) also localizes to the basal surface of the third instar disc in the anterior region of the disc and at the morphogenetic furrow. Digital reorientation, using the Volocity software, through the same DiI stained disc to generate a sagittal section reveals that DG-C (J) is also found at the MF spanning the peripodial space between the disc proper and

the peripodial membrane (J, arrow). The sagittal section also confirms the concentration of DG-C to the apical surface of R cells in the posterior region and to the basal surface in the anterior region. A-F, the scale bar is 20μm, G-J the scale bar is 25μm and the arrow (A-F) and the asterisks (G-J) indicates the position of the morphogenetic furrow and the direction of the tissue is indicated by the crossed arrow pointing toward the anterior.

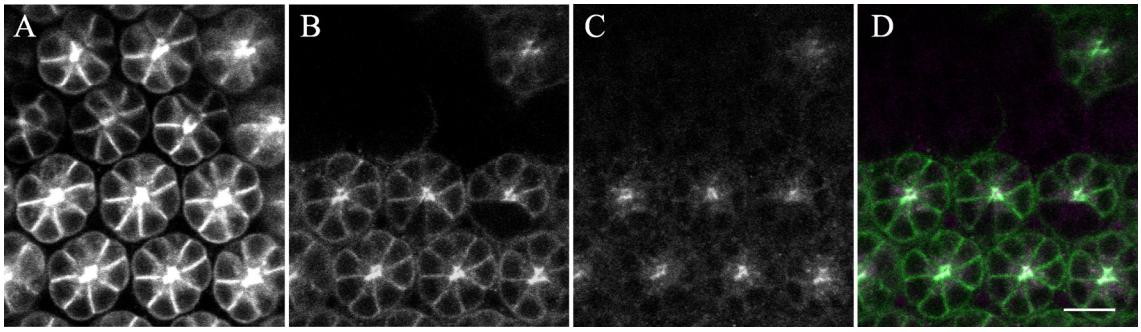
A
B
C
D

Figure 3. DG-C is expressed by R cells during early pupal eye development.

DG-C was localised during early eye disc development. A single confocal plane through a whole mount 40% p.d. *Dg*^{248} small patch mosaic pupal eye disc shows that DG-C (C and D magenta) localises to the apical surface of R cells. Areas lacking GFP (B and D green) are *Dg*^{248} patches. *Dg*^{248} patches also lacked expression of DG-C indicating the specificity of the antibody at this developmental stage. GFP positive wild type R cells, highlighted by the membrane bound GFP, localise DG-C to their apical surfaces. There are also lower concentrations of DG-C on the lateral R cell surfaces. The R cell marker chaoptin (A) highlights all the R cells within the field. Scale bar in D is 10μm.

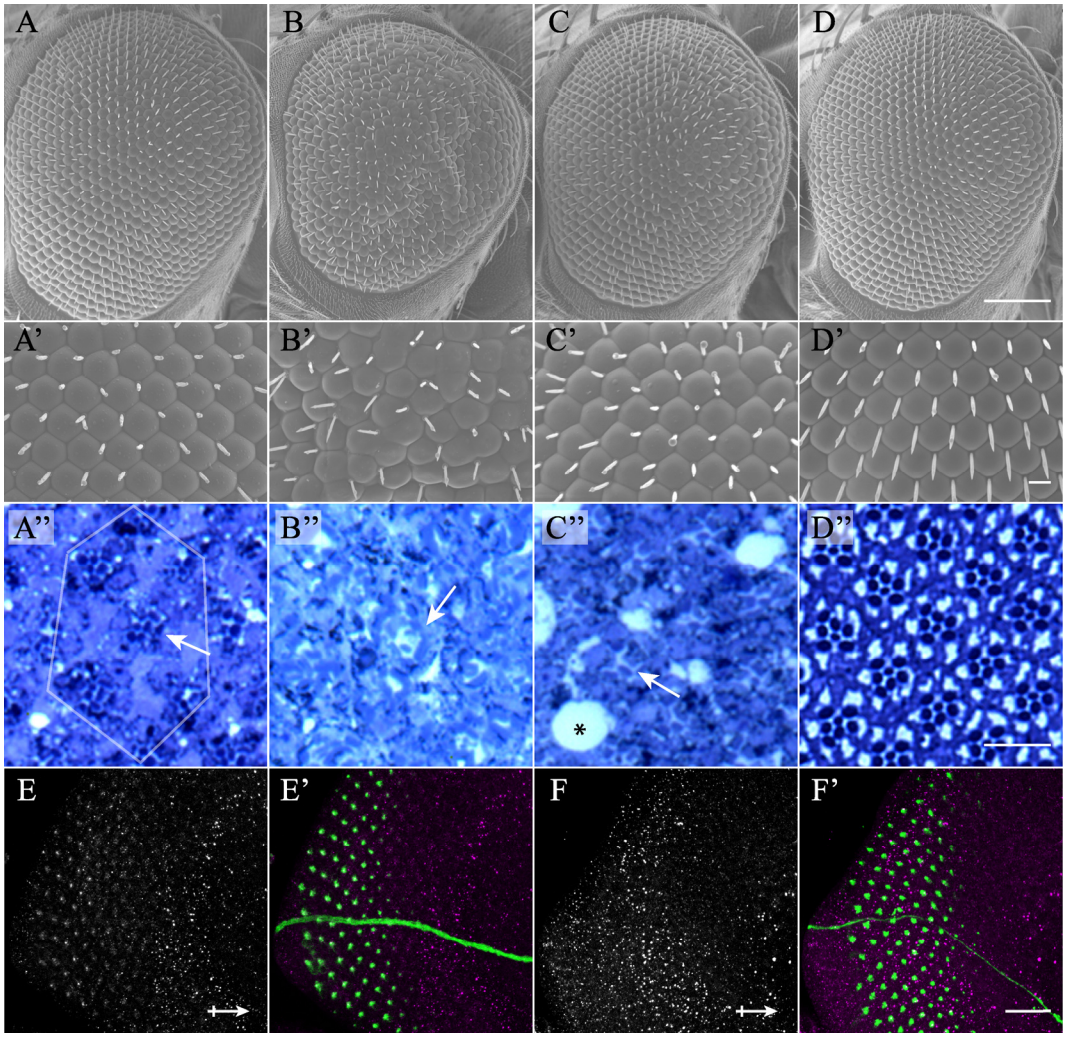
A
B
C
D
A'
B'
C'
D'
A''
B''
C''
D''
*
E
E'
F
F'

Figure 4. Knockdown of endogenous DG and DYS leads to disrupted rough adult eyes.

RNAi was used to knockdown endogenous protein levels of DG and DYS using the GMR-driver specific for cells posterior to the morphogenetic furrow from the third instar onward. SEM of the GMR-gal4 driver alone (A and A') and the *Dg* RNAi alone (D and D') show the normal facet patterning. Panels A' to D' are higher magnifications of A-D. Knockdown of endogenous levels of DG leads to smaller, rough eyes (B) with mispatterned and fused facets (B'). Knockdown of endogenous DYS levels does not disrupt the facet patterning (C') but does cause low levels of eye roughening (C) since the facet pattern is not as precise as in the controls. The normal ommatidial patterning is seen in the retina of DgRNAi alone (D''). The GMR driver alone retina show some disruption of the retina (A''), but the hexagonal ommatidial patterning (A'' outline) is still present with R cells (A'' arrow) at their centre. When DG is knocked down the retina is disrupted further and R cells have abnormally shaped rhabdomeres (B'' arrow). Knockdown of DYS causes greater retinal disruption with enlarged R cell rhabdomeres (C'' arrow) and presence of vacuoles throughout the retina (C'' asterisk). Immunoflurescent detection of DG in third instar eye discs confirmed the knockdown of DG expression. Confocal projections (4μm) through the apical surface of third instar eye discs (E – F'). A GMR driver alone eye disc expressing

wt levels of DG-C (E and E' magenta) on the apical tip of R-cells as detected by chaoptin (E' green). The DG-C (F and F' magenta) localisation in a disc where DgRNAi is driven by GMR driver is decreased at the apical tip of R cells visualised by chaoptin (F' green). The direction of the tissue is indicated by the crossed arrow pointing toward the anterior (E-F). Scale bars are: A-D, 100 μm; A'-D', 10 μm, A''-D'', 10 μm and E-F' 25 μm.

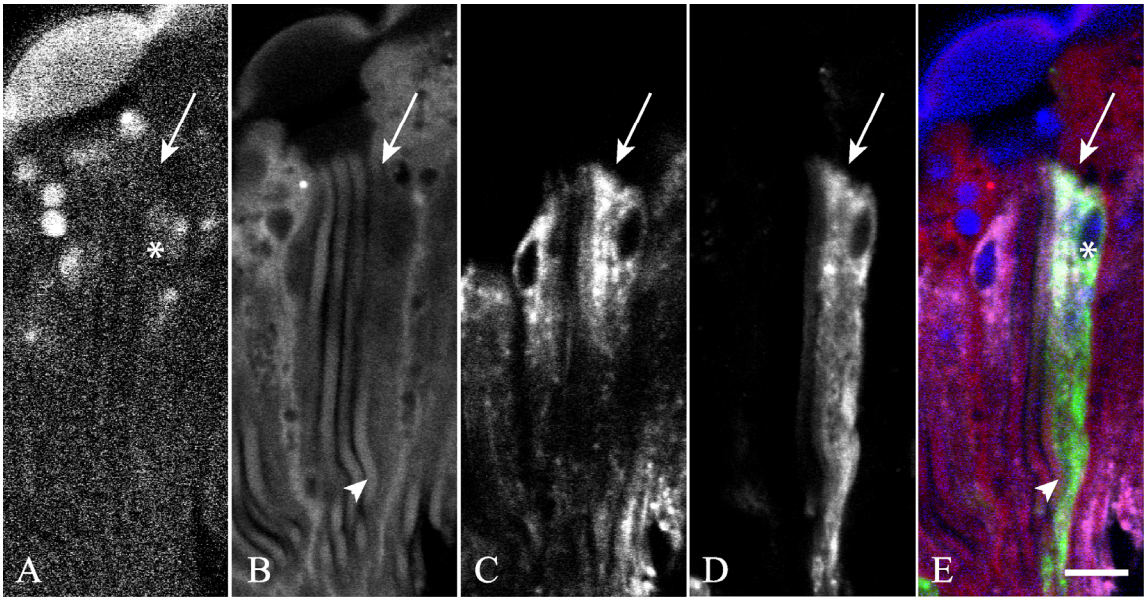
A
B
C
D
E

Figure 5. MARCM analysis indicates that *Dg*^{248} is not required cell autonomously in R cells.

A single mutant R cell (arrow in all panels) in an otherwise wt ommatidium is shown in an adult retina in which clones were induced by heat shock during third instar. A) Hoechst staining identifies nuclei (asterisk A and E); B, phalloidin detects f-actin, highlighting the landmark R-cell rhabdomeres (arrowhead); C, chaoptin identifies the R cells and D, the GFP positively identifies the single *Dg*^{248} homozygous R cell. The *Dg*^{248} R cell have an apparently normal morphology (n = 23 cells). Scale bar is 9 microns.

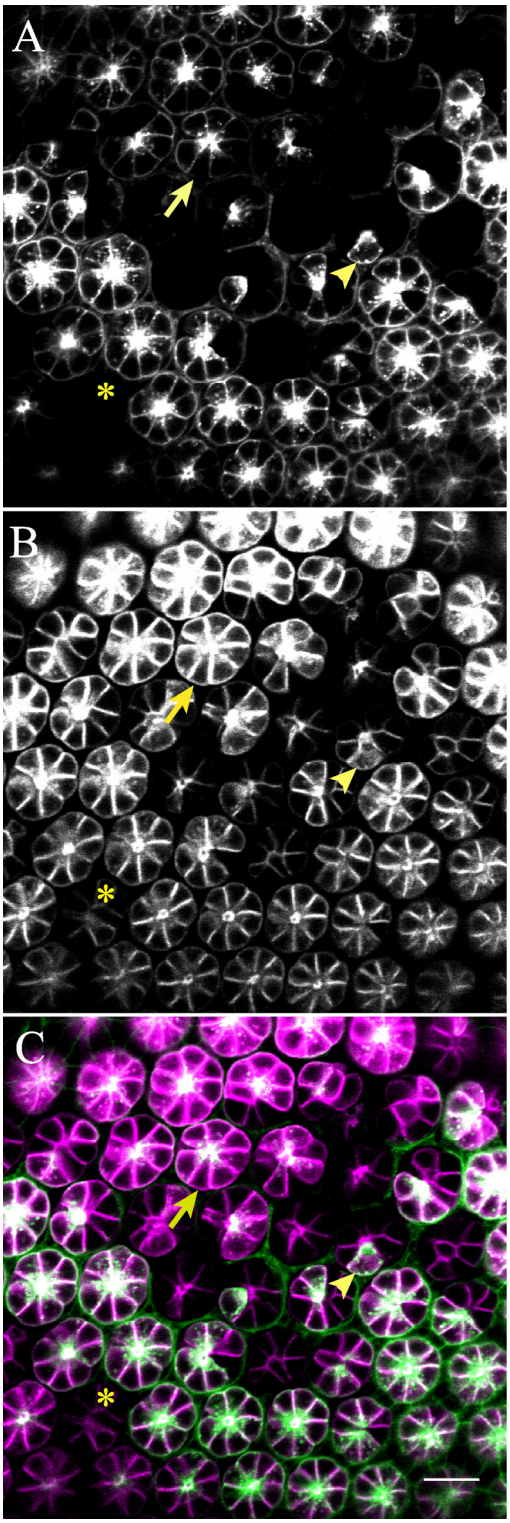
A
B
C

Figure 6. *Dg*^{248} small patch mosaics suggest a cell autonomous role for *Dg*^{248} in R cells.

Confocal z-stacks through retina were examined and the morphology of the mutant and wild type clones assessed. An example of a single confocal plane of focus of a 35% p.d. retina is shown with chaoptin (B, and C magenta) identifying the R cells and GFP (A, C) identifies the genotype of cells, where a lack of GFP identifies mosaic patches. When an ommatidium is composed solely of *Dg*^{248} R cells there is a loss of morphology where they fail to form the normal pie shape where each R cell contributes to an equal portion of the ommatidial volume (asterisk). When a single wt R cell is present in a *Dg*^{248} ommatidium it maintains its shape (arrowhead). When a *Dg*^{248} R cell is present within a wt ommatidium its morphology remains normal (arrow). Scale bar is 9 μm.

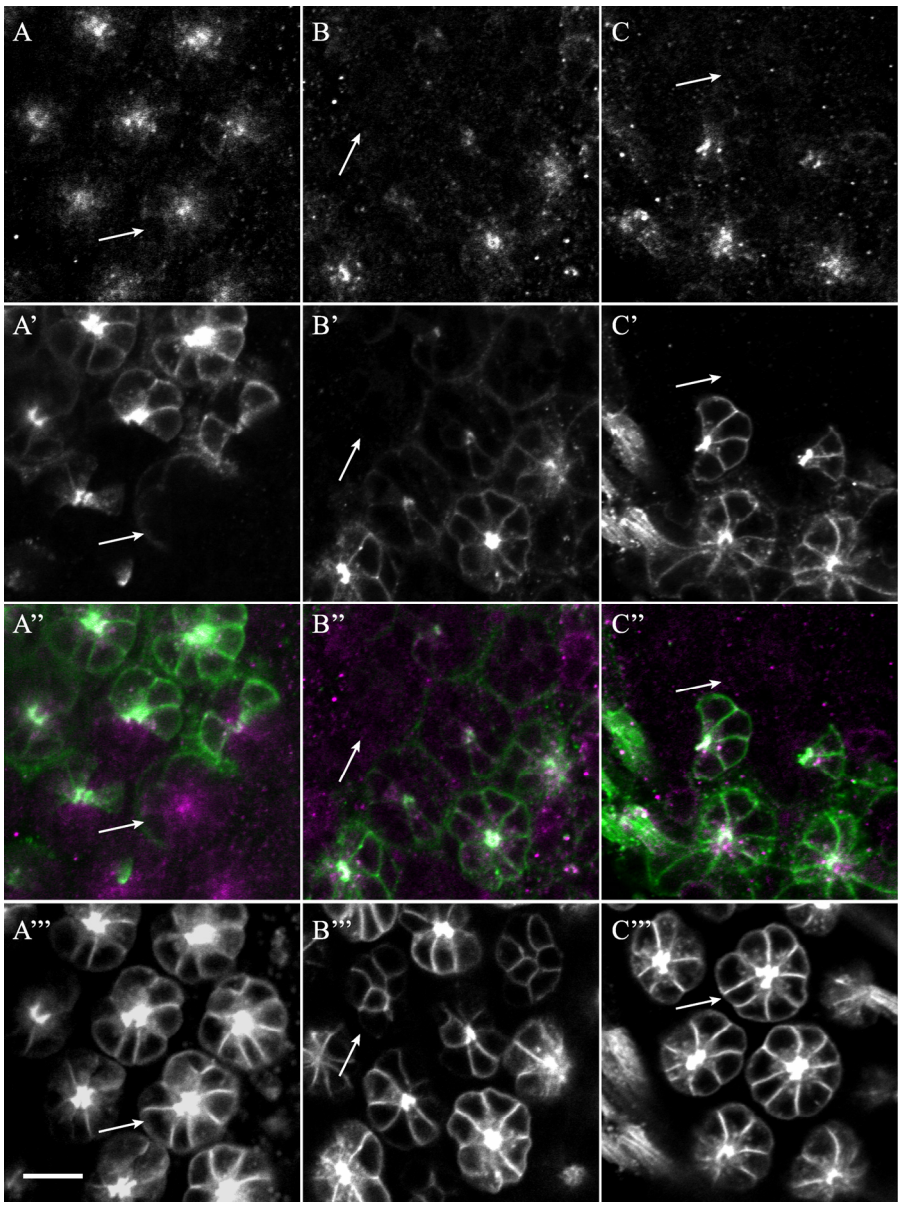
A
B
C
A'
B'
C'
A''
B''
C''
A'''
B'''
C'''

Figure 7. *mRpL34* significantly rescues the morphology of pupal *Dg*^{248} R cells

Small patch mosaic 35% p.d. pupal eye discs of different genotypes were examined for their expression of DG at the apical surface of R cells and the resulting R cell morphology. A) Wt small patch mosaic. B) *Dg*^{248} small patch mosaic. C) *Dg*^{248} small patch mosaic expressing *mRpL34* genomic transgene in the background. Expression of DG-C (A-C and A''-C'': magenta). Expression of GFP identifies the genotype of cells, where a lack of GFP identifies mosaic patches (A'-C' and A''-C'': green). The membrane marker chaoptin outlines R cells (A''' C'''). The arrow in each eye disc points to an ommatidium where all R cells are mosaic, as shown by a lack of GFP. Series A) In wild type mosaic ommatidia; R cells have a normal morphology (A''') and express and localise DG-C (A) to their apical surfaces. Series B) In *Dg*^{248} mosaic ommatidia; R cells do not have the normal R cell morphology (B''') and do not express DG-C (B). Series C) In *Dg*^{248} ommatidia expressing the *mRpL34* genomic transgene; R cells have a normal morphology (C''') but do not express and localise DG-C (C) to their apical membranes. Scale bar is 9μm.

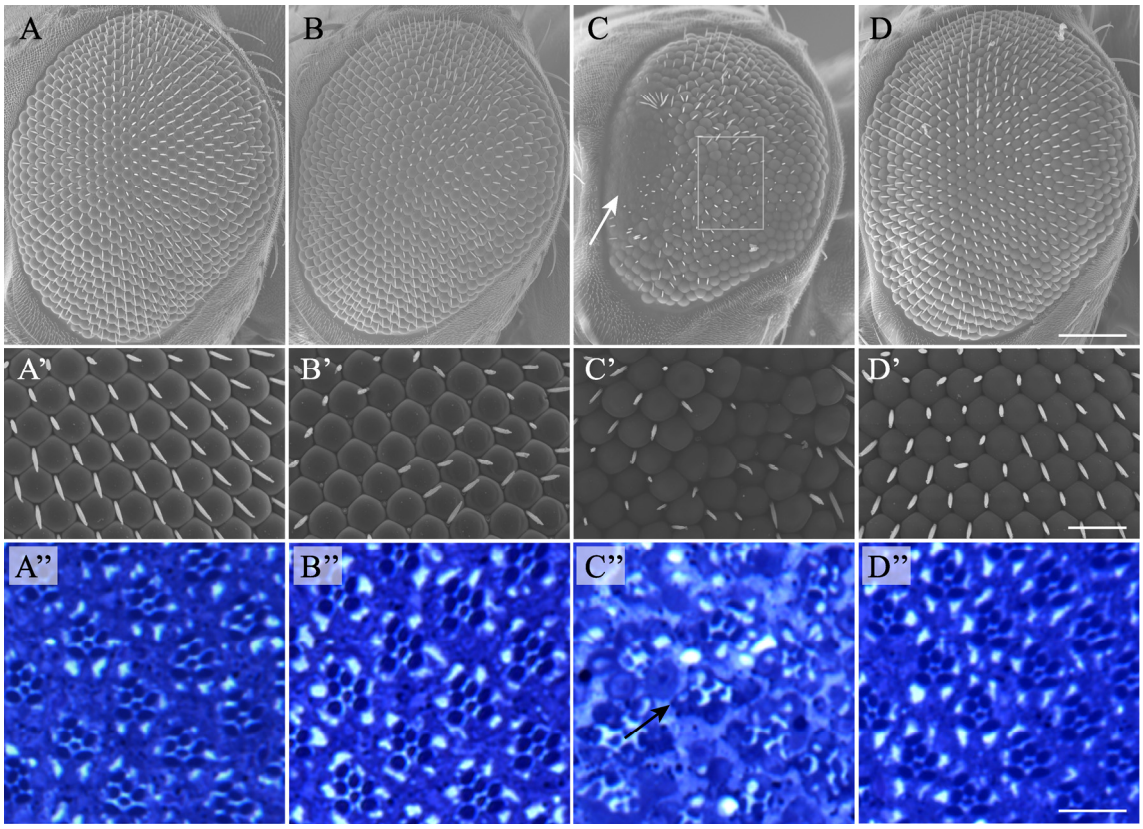
A
B
C
D
A'
B'
C'
D'
A''
B''
C''
D''

Figure 8. *mRpL34* significantly rescues the disrupted *Dg^{248}* adult eye

Female adult eyes (2 days old) were generated using a mosaic system that produces eyes composed of a single genotype to compare wt mosaics (A), wt mosaics expressing the genomic *mRpL34* transgene (B), *Dg^{248}* mosaics (C) and *Dg^{248}* mosaics expressing the genomic *mRpL34* transgene. Scanning electron micrograph (SEM) (A-D and A'-D' higher magnification) and semi-thin sections (A''-D'') were used to evaluate resultant eye morphology. The wt mosaic develops the normal pattern of facets (A, A') and has a normal ommatidial pattern (A''). Expression of the genomic *mRpL34* transgene does not perturb normal eye development (B-B''). A *Dg^{248}* mosaic shows a highly disrupted eye. Areas of the eye have flattened facets (C arrow) and facet patterning is disrupted (C' is a magnification of the area outlined in C). Internal ommatidial patterning is also disrupted. R cells are present and have formed rhabdomeres (C'' arrow). Expression of the *mRpL34* significantly rescues the *Dg^{248}* mosaic eye as measured by the outer facet patterning (D and D') and the internal ommatidial patterning (D''). Scale bars are: A-D, 100 μm; A'-D', 25 μm and A''-D'', 10 μm.

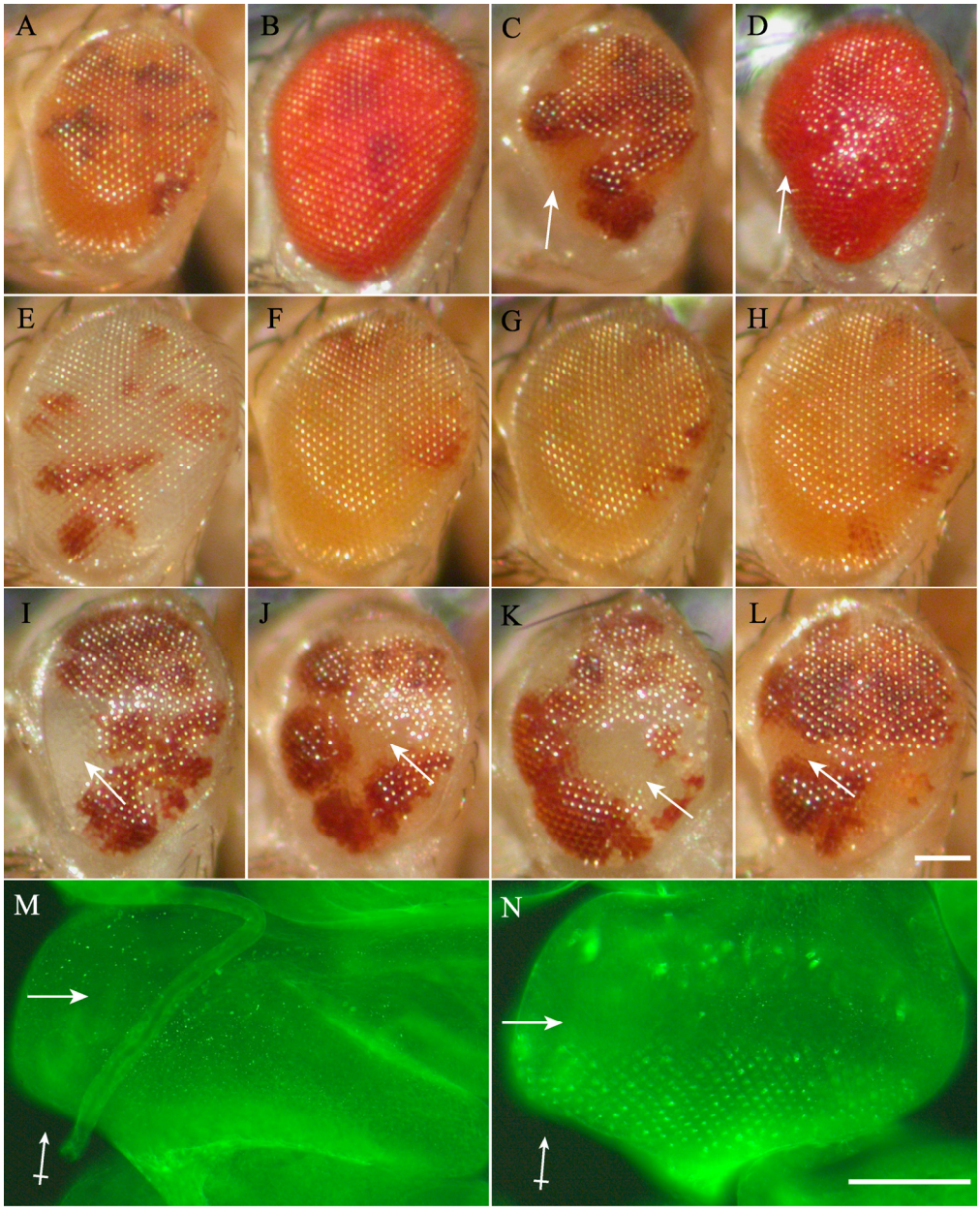
A
B
C
D
E
F
G
H
I
J
K
L
M
N

Figure 9. The expression of *Dg-RC* in R cells does not significantly rescue the disrupted Dg^{248} adult eye.

Female adult eyes (2 days old) with large patch mosaics were examined for their resulting morphology. Areas of the eye which are dark red are cells which have not undergone mitotic recombination and are wt for *Dg*, the rest of the paler tissue has undergone mitotic recombination and is the Dg^{248} tissue of interest. Expression of *Dg-RC* during R cell development is performed using the Gal4/UAS system using R cell specific drivers *C155* (A-D) or *elav* (E-N). Wt mosaics eyes expressing only *UAS-Dg-RC* alone (A) or *C155-gal4* and *UAS-Dg-RC* (B) develop normally. Dg^{248} mosaics expressing *UAS-Dg-RC* alone (C) develop abnormal eyes (flattened facet, arrow) which are not significantly rescued when *C155-gal4* and *UAS-Dg-RC* (D) are present. The second R cell specific driver, *elav-gal4*, gave similar results. Wt mosaic are normal whether alone (E), or expressing *UAS-Dg-RC* alone (F), *elav-gal* 4 alone (G) or expressing DG-C in R cell when *elav-gal4* and *UAS-Dg-RC* are both present. The development of aberrant eyes is not significantly altered in Dg^{248} mosaics (I) (I-L, flattened facet, arrow) when expressing *UAS-Dg-RC* alone (J), *elav-gal4* alone (K) or expressing DG-C in R cell when elav-gal4 and *UAS-Dg-RC* are both present (L). Scale bar is 100 μm. Third instar eye discs were stained for DG using an antibody to the DG cytosolic tail using a dilution only able to detect over-

expressed protein levels. Epifluroescent imaging of the control *Dg*^{248}mosaic disc expressing *UAS-Dg-RC* alone (M) shows no specific staining in R cells located posterior to the MF (arrow in M and N). The direction of the tissue is indicated by the crossed arrow pointing toward the anterior. Epifluroescent imaging of the *Dg*^{248} mosaic disc with both *elav-gal4* and *UAS-Dg-RC* (N) shows specific expression of DG in R cells found posterior to the MF. Scale bar is 50 μm .

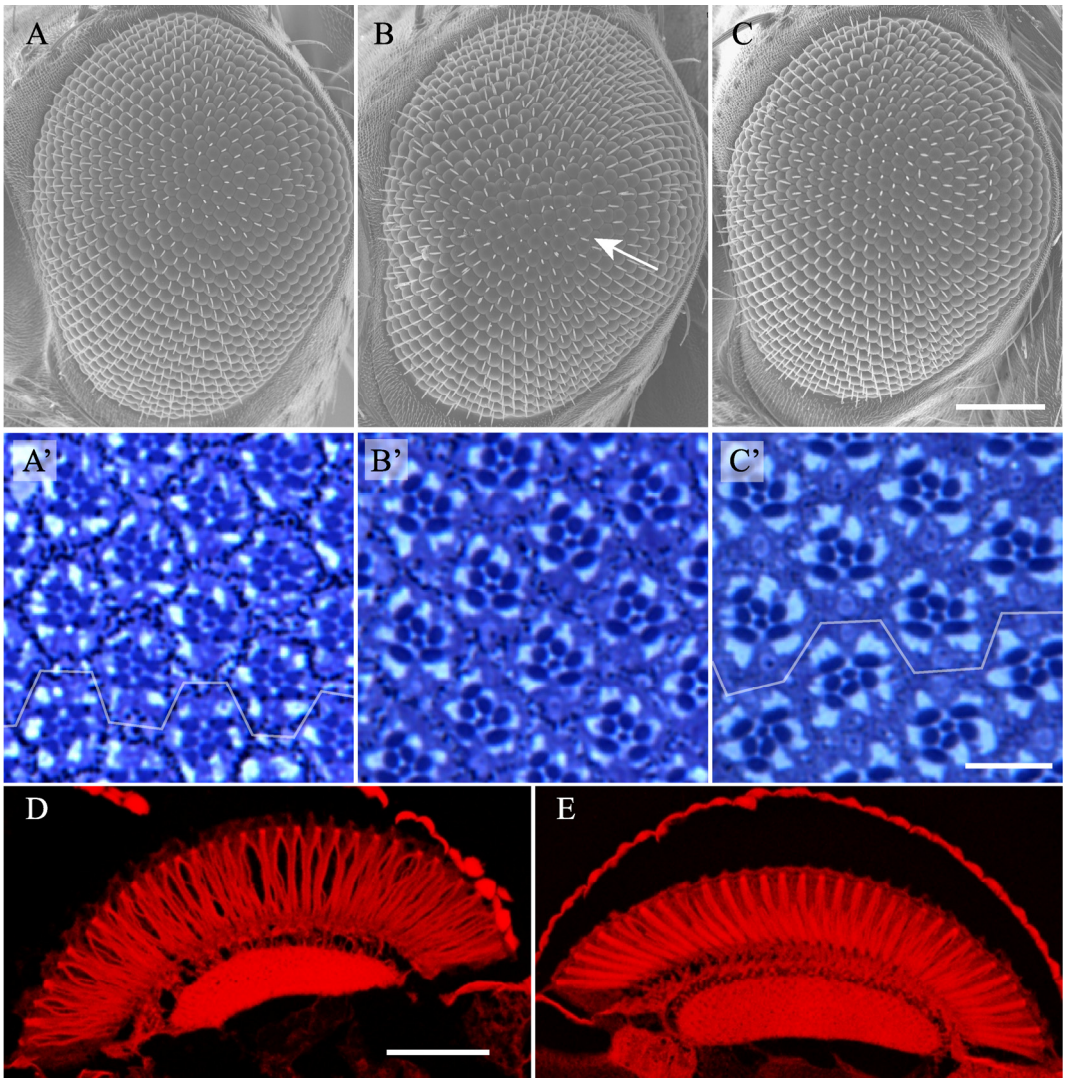
A
B
C
A'
B'
C'
D
E

Figure 10. The EMS *Dg^{0*}* mutants develop thinner adult retina.

Scanning electron micrograph of female adult eyes (A-C; two days old) and the corresponding histology (A'-C'), of different lines of EMS *Dg^{0*}* alleles. A wild type eye shows the ordered array of ommatidia, both on the surface (A) and within the retina (A'). On the surface, a *Dg^{043}* eye (B) has a small region (arrow) of mis-patterned ommatidia. Within the *Dg^{043}* retina (B') the patterning of the retina is normal. The surface of a *Dg^{086}* eye (C), as well as the within the retina (C'), shows a normal pattern of ommatidia. The *Dg^{086}* eye shape is more spherical relative to wild type. The haematoxylin and eosin fluorescence highlights the rhabdomeres of wild type (E) and *Dg^{055}/Dg^{043}* R cells (F) in frontal retinal sections of adult eyes. The retinal length of *Dg^{055}/Dg^{043}* is shorter (average length = 63.17 μm, n=14) than wild type retina (average length = 96.99 μm, n=11). The scale bars are 100 μm (A-D); 10 μm (A'-D') and 75 μm (E and F). The line, in A' and C', outlines the retinal equator.

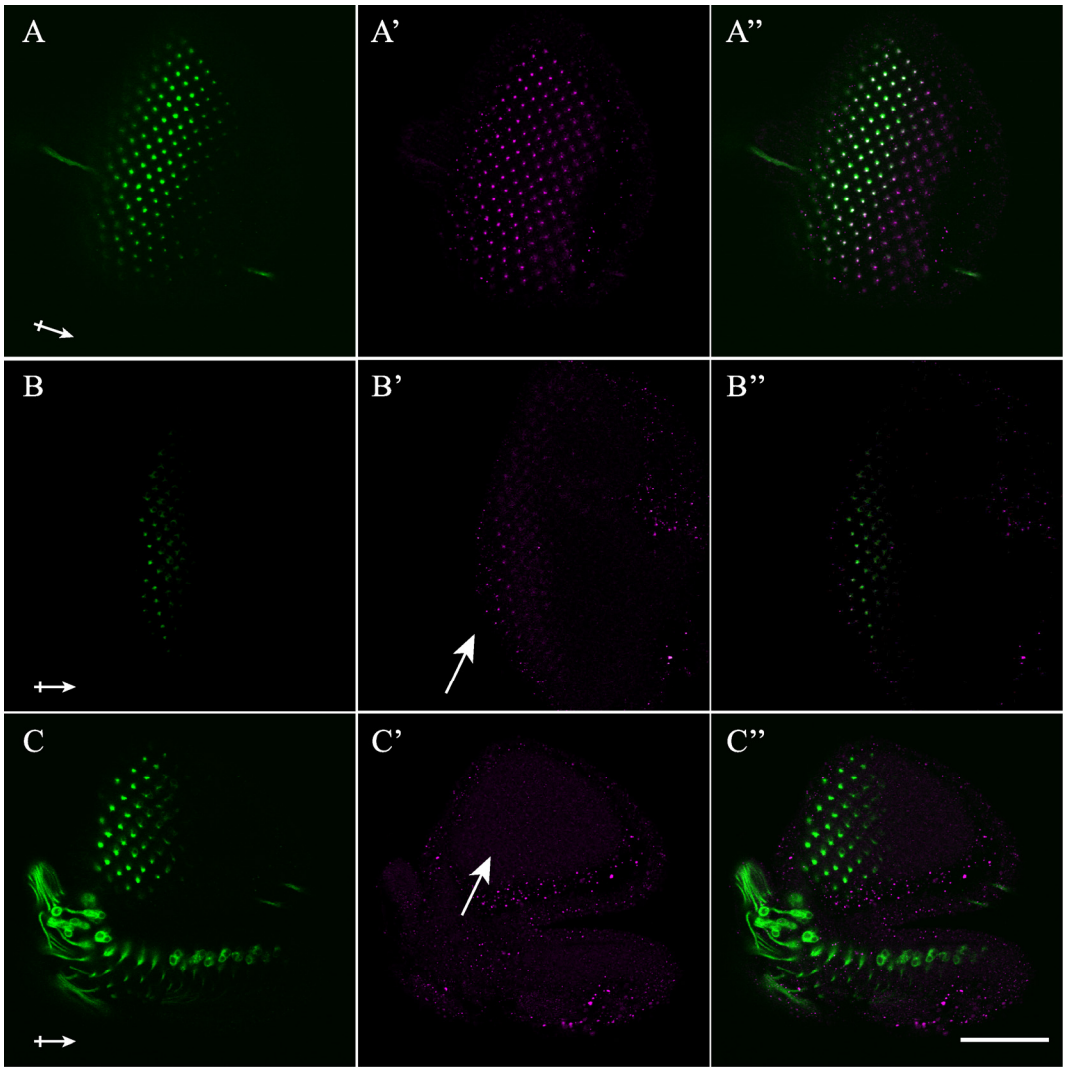
A
A'
A''
B
B'
B''
C
C'
C''

Figure 11. *Dg*^{043} developing eye discs express residual levels of DG-C.

EMS *Dg*^{0*} mutant third instar eye discs were stained for chaoptin (A-C) and DG-C (A'-C'). The merges of the fields (A''-C'') reveals any co-localisation. Confocal planar sections, through the apical surface of whole mount eye discs were used to optimise the co-localisation of chaoptin and DG-C. The wt eye disc shows the typical apical pattern of chaoptin (A and A'') which co-localises with DG-C (A and A''). A *Dg*^{043} eye disc shows a low concentration of DG-C (B' arrow and magenta in B'') specific to R cells (B and green in B''). A *Dg*^{086} eye disc does not express DG-C (C' arrow and magenta in C'') at the apical surface of its R cells (C and green in C''). The direction of the tissue is indicated by the crossed arrow pointing toward the anterior.

Discussion

The chimeric mice deficient in DG develop microphthalmia, a small eye within the orbit, or anophthalmia, absence of an eye. In human populations these defects occur with a combined prevalence of 30 per 100 000 births (Verma & Fitzpatrick 2007). These congenital ocular anomalies are associated with both genetic and environmental factors. Genetic factors include mutations within transcription factor genes that control eye specification, such as *Pax6*, and other transcription factors that control development of ventral retina and optic fissure, such as *Pax2* or mutations with in the Wnt signalling pathway (Liu & Nathans 2008). DG may play a similar regulatory role in eye development. Importantly, the loss of DG function in the *Dag1* null chimeric eyes is similar to eye malformations present in Dystroglycanopathies. The phenotypes observed in *Dag1* null chimeric eyes; the corneal clouding, microphthalmia and thinner, but largely intact retinal layering, are also seen in the eyes of mice with epiblast-specific loss of DG (Satz et al 2008). This finding further supports a signalling role for DG during eye development.

DG is expressed in the developing *Drosophila* eye. When and where a protein is expressed and localised can provide clues as to its functions. In the third instar eye disc DG-C is located in three distinct places where very different cellular processes are occurring.

Firstly, the localisation of DG-C in the anterior region of the third instar eye disc could indicate that it plays a role in cell proliferation. The generation of a smaller Dg^{086} eyes may indicate that DG is required to establish the correct number of cells. Through extracellular cues, DG signalling has a proposed role in modulation of the cell cycle (Higginson et al 2008). Indeed in the anterior region, DG concentrates to the basal surface, where the basement membrane that ensheaths the eye disc is found (Martin et al 1999).

Secondly, DG-C is found at the MF both on the basal surface of disc proper and on processes spanning the lumen of the eye disc. Peripodial translumenal extensions expressing DG-C were observed directly above the MF suggesting a furrow specific function. Future experiments will be necessary to determine whether these translumenal extensions expressing DG-C arise from the peripodial cells or the disc proper. The peripodial membrane provides instructive cues for the patterning of the disc proper (Cho et al 2000, Gibson & Schubiger 2000). Translumenal extensions are thought to be a mechanism by which the peripodial membrane and the disc proper communicate. Knock down of endogenous *Dg* mRNA, using *dsDgRNAi*, specifically in imaginal disc peripodial membranes is late pupa lethal with exteriorly normal eyes. If DG provides developmental cues at the MF through peripodial translumenal extensions, and since EMS *Dg0** mutants have shorter retina, it would be

interesting to determine the length of the retina in these peripodial membrane specific DG knocked down eyes.

Thirdly and lastly, DG-C is expressed by R cells where it is concentrated to their apical surfaces. DG-C localisation to the apical surface is an early event after the onset of R cell specification. This apical location is maintained during early pupal development. The expression of DG-C in R cell supports the finding in the embryo where DG-C is specifically expressed in neurons (Schneider & Baumgartner 2008). The apical surface is the area which develops the rhabdomere, the actin rich sensory region of the R cell. Apical localisation of DG would provide the R cell with the capacity to anchor the actin cytoskeleton and the possibility to contribute to its regulation.

The apical DG localisation in invertebrates is significantly different from that in vertebrate R cells. In vertebrate R cells DG is localised not to the light sensing outer segment, but to the synaptic terminals of photoreceptors (Koulen et al 1998). This maybe due to the fact that mammalian outer segments are composed of modified cilia having a microtubule base. This study does not exclude DG localisation to the invertebrate R cell synapse, since it was not determined. This suggests DG may have been recruited to invertebrate R cells apical membranes for its ability to stabilise and modulate the underlying actin cytoskeleton.

RNAi mediated knockdown of DG and DYS generated a small, rough adult eye phenotype. Rough eye mutants are a well known phenotypic class of mutants. Disruptions in multiple cellular processes during development have been shown to generate rough eyes. Prevention of cell death, as seen in *roughest* and *echinous* mutants (Wolff & Ready 1991b), leads to a surplus of interommatidial cells. Mutation in *rugose*, an A kinase anchor protein gene, leads to cone cell death (Wech & Nagel 2005). The *marbles* mutant affects apical nuclear migration (Fischer-Vize & Mosley 1994). Mutation in *Rap/Fzr* interferes with ubiquitin-ligase-mediated protein degradation (Kaplow et al 2007). Comparison to other rough eye phenotypes may suggest genetic pathways in which the DGC may participate. A common factor in the pathways leading to a rough external eye is cell death. The disruption in DG and DYS RNAi retina suggests the DGC may regulate cell death as suggested in previous studies (Langenbach & Rando 2002b, Li et al 2002).

If disruption of endogenous DG could lead to such disrupted development, it was hypothesised that a genetic deficiency would have a similar effect. Studies began using the deletion series of *Dg* alleles. At the time of their generation these alleles had been shown to disrupt only *Dg* and not it's then known neighbouring genes of *CG8414* and *Rho1* (Deng et al 2003). These alleles were embryonic lethal, suggesting a vital role for DG during development.

Disruption in the oocyte could be rescued by expression of DG-C (Yatsenko et al 2007). It was hypothesised that DG could play a role in eye development and it could be rescued by expression of DG-C. Due to the lethality of this series, mosaic analysis using the eyFLP system was used to study the role of DG during eye development. Indeed *Dg*^{248} mosaic eyes did develop severely disrupted adult eyes; with aberrant R cell morphology, loss of retinal patterning and flattened facets. This finding supported the *DgRNAi* rough eye phenotype. The effect of *Dg*^{248} on R cell development was cell autonomous. Small clones of *Dg*^{248} R cells have a perturbed morphology which does not extend to neighbouring cells. However, adult single mutant *Dg*^{248} R cells become specified and show an apparently normal morphology. A lack of disruption may be because most *Dg*^{248} single R cells undergo cell death at an earlier stage. It may also be the result of compensation by neighbouring wt cells. Small patch *Dg*^{248} mosaic analysis suggests that when a single *Dg*^{248} R cell is present in an otherwise wt ommatidium it retains its morphology. This suggests a communication between R cells and their cellular environment which may compensate the deficiency experienced in a single cell. Together the *Dg*^{248} mosaic analysis suggested a critical role for DG during R cell development.

Later, bioinformatics predicted the presence of a gene immediately neighbouring DG. The *Dg*^{248} deletion was therefore found to perturb two genes,

one known, *Dg,* and a second the predicted mitochondrial ribosomal protein L34, *mRpL34*. Even though expression of DG-C rescued the Dg^{248} follicular cell disruption, expression of *mRpL34* also could rescue (Mirouse et al 2009). The question then arose if *mRpL34* could be contributing to the disrupted Dg^{248} mosaic eye.

This study demonstrates that the *mRpL34* transgene significantly rescues the eye morphology of the Dg^{248} mosaic eye, by returning the normally patterned facets and ommatidia. Whether Dg^{248} + *mRpL34* transgene mosaic eyes develop thinner retina, like the EMS Dg^{0*} mutants, needs to be determined. To determine precisely how each gene product is contributing to the net phenotype also requires further analysis (Mani et al 2008). Three possibilities exist: 1) one gene could be contributing 100% to the phenotype [A or B]; 2) each contributes an independent portion of the phenotype [A+B] and have an additive effect; 3) or they may have a synergistic effect and the phenotype is significant only when both are deficient. The solution for Dg^{248} may only be possible when a deletion of the *mRpL34* gene is made, which may be possible through homologous recombination (Venken & Bellen 2007). Expression of a *Dg-RC* transgene in R cells did not significantly rescue the Dg^{248} mosaic eye. Though DG-C is expressed in R cells multiple factors may have contributed to the inability to rescue. DG-C's localisation is polarised within R cells with a high

concentration at the apical surface, which may be critical for its function. The expression of the transgenic DG-C may have been at too high a level perturbing and preventing its concentration to the R cell apical membrane. Also, multiple DG isoforms exist. It has yet to be determined what DG isoforms are expressed and their spatio-temporal patterns and functions within the developing eye.

The overall deficiency of *Dg* in the *Drosophila* is not as drastic as the effect seen in the mouse, i.e. no anophthalmia. Aside from the obvious evolutionary divergence another reason for this may be due to the fact that, as mentioned above, we do not yet know which DG isoforms (known or novel) may be functioning during eye development. The EMS Dg^{0*} may not prevent the production of all DG isoforms. Residual DG levels, as seen with the presence of the exon 8 epitope detection in Dg^{043}, of these unaffected isoforms may be sufficient for eye development with normal R cell patterning. Generation of a *Dg* allele with a complete deletion of the coding region will be necessary to answer this question. Possible strategies would include imprecise excision using the transposition of a Hobo element found in the first non-coding exon of DG. Hobo element excision could be used to excise DG only because excision is unidirectional and has the capacity of deleting 60 bp to 60 Kb of DNA (Huet et al 2002). Precise excision elements presently available could delete three genes, DG and two 3' neighbouring genes (Parks et al 2004). One of these genes

however, is a predicted agrin like gene *SP2353*, whose protein may be a potential DG ligand. Another reason for the discrepancy in phenotypes may be that as shown in the oocyte, *Dg* may be required under metabolic stress induced by glucose deprivation. The EMS Dg^{0*} oocyte follicular epithelial cells lose polarity only when placed under metabolic stress (Mirouse et al 2009). This function of polarity maintenance by DG during metabolic stress is thought to act downstream of the AMPK pathway. However, unlike in the oocyte, AMPK is not required for differentiation, but for the neuroprotection of mature R cells (Spasic et al 2008). If DG is required under metabolic stress conditions during development it may involve a different pathway than AMPK or DG may not be required in developing R cells, but rather in mature R cell.

Discrepancy in the eye phenotypes between adult eye facets phenotype of the RNAi mutants relative to the Dg^{248} + *mRpL34* and EMS Dg^{0*} may be due to the factors discussed above. Discrepancy may also arise since the expression of DG and DYS was inhibited starting at the time of R cell specification and not beginning at the embryonic stages of eye development. Disruption of the eye may have occurred because no other mechanisms were able to compensate rapidly enough for the loss of DG's functions at this time of development.

Understanding how a neuron changes shape requires an understanding of how the cytoskeleton is altered during development. The ability to remodel the

actin cytoskeleton has been linked to retinal elongation and rhabdomere morphogenesis. Decreased expression starting at the MF, of cofilin an actin depolymerising factor, during eye development, leads to a shorter retina and wider rhabdomeres (Pham et al 2008). Retinal shortening was found in the EMS Dg^{0*} mutants and decreased expression of DG or DYS by RNAi leads to highly disrupted R cells with disrupted rhabdomeres. DG may be important in regulating the actin cytoskeleton. In *Drosophila,* the actin-based motor protein nonmuscle myosin II is required for tissue morphogenesis (Zajac & Discher 2008). During eye development myosin II activity is required at the time of morphogenetic furrow initiation (Edwards & Kiehart 1996). The external facet disruption seen in myosin II deficient eyes is similar to the *Dg* RNAi mediated knockdown in the eye beginning at the MF. Myosin II has been shown to be downstream of DG during epithelial metabolic stress (Mirouse et al 2009), it may also be downstream during eye development.

Dg may be interacting with other developmental pathways during *Drosophila* eye development. *Dg* has been shown to interact genetically with the notch pathway in wing vein development (Christoforou et al 2008, Kucherenko et al 2008). During the third instar the notch pathway may be involved in peripodial to disc proper translumenal communication (Gibson & Schubiger 2001) where DG localisation has been detected. *Drosophila* with lower activity levels of fringe,

a notch glycosyltransferase, have smaller eyes (Papayannopoulos et al 1998). Flies with over-expressed levels of Fringe during the second instar and in the peripodial membrane also develop smaller eyes (Cho & Choi 1998, Gibson & Schubiger 2000). Disrupting activity of serrate, a ligand of notch, in the peripodial membrane also reduces the size of the adult eye (Gibson & Schubiger 2000). It may be interesting to determine whether *Dg* and members of the Notch signalling pathway interact to determine retinal size.

In mice, a lack of DG during eye development replicates the ocular anomalies found in Dystroglycanopathies. In *Drosophila* DG is expressed in early eye development and becomes localised to R cells apon the initiation of eye disc cell specification. The RNAi mediated knockdown of DG generates a severe defect in eye morphogenesis. *Dg* alleles develop eyes with normal retinal morphology and patterning, but are thinner. Together, the present data indicate that DG functions in R cell differentiation

Bridging Text

DG is expressed widely in both the vertebrate and invertebrates (Durbeej et al 1998). The studies in chapter 2 discussed the effect of alleles of DG during eye development, initially in chimeric mice and then in *Drosophila*. Chimeric *Dag1* mice developed anomalies similar to those found in patients with Dystroglycanopathies (Martin 2005), suggesting that DG has important functions within eye and retinal development. DG was also found to play a role in the differentiation of R cells during *Drosophila* eye development. The putatively glycosylated form of DG-C was found to be expressed in the developing retina where it was concentrated to the apical membrane of developing R cells. A series of deletion mutants (Deng et al 2003) was recently shown to also delete the neighbouring gene mitochondrial ribosomal protein L34 (*mRpL34*) (Mirouse et al 2009). MRPL34 is a structural protein of the mitochondrial ribosome, disruption of which can ultimately lead to mitochondrial dysfunction. It has been proposed that DG is required to maintain cell polarity during metabolic stress (Mirouse et al 2009). I showed that an *mRpL34* transgene significantly rescued the highly disrupted *Dg* deletion mosaic eye. The deletion series of Dg alleles may therefore be a model to study the role of DG during eye development under metabolic stress.

Chapter Three - Characterisation of Dystroglycan's role in the Developing Drosophila Eye during Metabolic Stress

by Nadia Y. Melian and Sal Carbonetto

Introduction

A new function of DG is emerging from recent *Drosophila* studies. The finding that the 'atu' allele, a severe hypomorphic allele of *Dg,* has a higher metabolic rate suggests DG may contribute to metabolic homeostasis (Takeuchi et al 2009). DG has also been found to be necessary in maintaining epithelial polarity during metabolic stress (Mirouse et al 2009). These findings points to roles in DG in stabilising metabolic rates and protecting cells form metabolic stress. These functions would be critical in neurons of the CNS which have high metabolic rates and experience metabolic stress. Dystroglycanopathies, the MDs where DG lacks interaction with its extracellular ligands suggests DG plays important roles in the CNS (Martin 2006). Thus DG in neurons may be a regulator of the neuronal response to metabolic stress.

The *Drosophila* eye is a model for neuronal development (Pappu & Mardon 2004). A series of *Dg* alleles contain a deletion in the first non-coding exon which also partially deletes the neighbouring gene *mRpL34* a mitochondrial ribosomal protein (Deng et al 2003, Mirouse et al 2009). Ribosomal proteins are structural proteins required in equal proportions for the generation of the ribosome (Koc et al 2001). Disruption of even one will perturb the ribosome structure and therefore its function in translation (Marygold et al 2005). In the case of mitochondrial ribosomal proteins the translation of mitochondrial genes

will be affected (Miller et al 2004, O'Brien et al 2005). The mitochondrial genome encodes proteins important for cellular respiration. By perturbing *mRpL34* the *Dg* deletion series serendipitously generated perturbation of the mitochondria's role as generator of metabolic energy (O'Brien et al 2005).

Studying the development of the *Dg* deletion allele Dg^{248} would effectively be an insight to the consequence of a lack of DG during metabolic stress. Work in the previous chapter demonstrated that R cell morphology is perturbed beginning at the early pupal stage. The resulting adult eye did not maintain retinal hexagonal patterning and has disrupted R cells and flattened facets. Understanding the mechanisms that lead to this disrupted adult Dg^{248} eye may provide information about the functions of DG during metabolic stress. Since DG has been shown to maintain epithelial polarity during metabolic stress (Mirouse et al 2009), the establishment and maintenance of R cell polarity was studied. Cellular stress including, metabolic stress, may lead to cell death (Kim & Youn 2009, Minke & Agam 2003, Schmidt et al 2008) which may account for the apparent degeneration of the Dg^{248} mosaic eye. DG has been proposed to regulate cell death (Langenbach & Rando 2002a). Whether apoptosis is initiated in the Dg^{248} eye will be tested. The role of DG in inhibition of cell death and in polarity maintenance during metabolic stress was examined.

Materials and Methods

Drosophila Strains

D. melanogaster were raised on cornmeal-yeast-agar medium at 25˚C. The *Dg* alleles have been previously described. The *w; FRT42D* Dg^{248}*/cyo* (Deng et al 2003) (a gift from H. Ruohola-Baker) is ready for mosaic analysis. The wild type *yw; FRT42D* (Bloomington stock centre) line was used to generate wt mosaics. Homozygous wt or Dg^{248} clones were generated by using ey-FLP/FRT (Xu & Rubin 1993) system. The *y w, GMR-LacZ ey-FLP; FRT42D* lw^{+}*/Bc* was used to generate large patches and the *y w, GMR-LacZ ey-FLP; FRT42D GMR-myr-GFP* was used to generate small patches (Bloomington Stock Center). To generate eyes composed entirely of mutant cells, the mosaic system by (Stowers & Schwarz 1999) was used w; *FRT42D GMR-Hid Cl2/cyo; ey-gal4, UAS-FLP* (Bloomington Stock Center). Apoptotic cell death may be inhibited by the expression of the baculovirus caspase inhibitor p35. The lines *UAS-p35* and *elav-gal4* (Bloomington stock centre) were recombined onto the same third chromosome by using eye colour to detect recombination. The presence of the *elav-gal4* on recombined chromosomes was detected by crossing it with *yw; Pin[yt]/cyo; UAS-mCD8GFP* (Bloomington) and staining for the expression of GFP in the progeny's third instar eye discs. The presence of the *UAS-p35* on the recombined chromosome was tested for its ability to repress *GMR-Hid/Bc*

(Bloomington Stock Center). Once recombination was confirmed the lines w*; FRT42D* Dg^{248}*/Bc; elav-gal4, UAS-p35/Tb* and w*; FRT42D; elav-gal4, UAS-p35/Tb* were constructed. Also constructed, were the control lines *FRT42D* Dg^{248}*/Bc; elav-gal4* and*, FRT42D* Dg^{248}*/Bc; UAS-p35* and*, FRT42D; elav-gal4* and *FRT42D; UAS-p35.* These lines were used for mosaic analysis. The line *GMR-p35* on the X chromosome (Bloomington Stock Center) was used to construct the lines *GMR-p35; FRT42D* Dg^{248}*/Bc;* and *GMR-p35; FRT42D* to be used in mosaic analysis. Pupal staging was performed under the assumption that 1% pupal development (p.d.) corresponds to 1h at 25˚C.

Staining and Imaging

Tissue dissection and immunofluorescence of eye discs was performed by following standard procedures (Walther & Pichaud 2006). Slices of 75% and 95% p.d. eyes were obtained by using a vibratome to cut 80 μm slices from fixed head samples Primary antibodies were used as follows: mouse anti-chaoptin (1/250), mouse anti-β catenin (1/100), mouse anti-β tubulin (1/100) and rat anti-elav (1/250) [all from Developmental Studies Hybridoma Bank]; Rabbit anti-GFP (1/100 Invitrogen) and rat anti-crumbs (a gift from Ulrich Tepass). Tissue was also stained with Hoechst (1/5000, Invitrogen) or phalloidin (1/2000, Invitrogen). Confocal imaging of whole mount tissue was performed using a Zeiss LSM510

Meta Confocal microscope. Stack reslicing was performed using Volocity from Improvision/PerkinElmer. Images were cropped using Photoshop CS2 (Adobe). Confocal microscopy acquisition and velocity image analyses were performed at the CIAN core facility (Biology Dept., McGill University, Montréal).

To image adult fly heads, flies were placed at -80˚C for 10 minutes, then placed under a dissecting scope (Zeiss Stemi 2000) and images were taken using a Nikon Eclipse E600 digital camera. Images were cropped using Photoshop CS2 (Adobe).

Terminal dUTP nick-end labelling (TUNEL) cell death assay was performed on third instar eye disc, 75% and 95% p.d. head slices following the manufacturer's instructions (Chemicon, ApopTagRed). The entire whole mount eye discs were imaged and recorded by confocal microscopy. The numbers and volume of apoptotic bodies per eye disc were quantified using the software Volocity from Improvision/PerkinElmer.

Results

Understanding the impact of the *Dg*^{248} allele on eye development may contribute to a greater understanding the role of *Dg* during metabolic stress. Whether apoptosis contributed to the previously described apparent degeneration of the eye was tested.

To determine the full extent of R cell morphology defects during eye development, *Dg*^{248} small clone mosaics eye disc were analysed. Rotation of planar confocal stacks through *Dg*^{248} small patch mosaics discs into transversal sections provided greater information of the R cell morphology and the sub-localisation of the nuclei within *Dg*^{248} R cells. During pupal development a portion of *Dg*^{248} R cell nuclei migrate past the retinal floor (fig.1, dashed line). In an ommatidium composed solely of *Dg*^{248} R cells, three R cell nuclei are found within the axonal projections (fig.1, arrow) as identified by the R cell membrane marker chaoptin (fig.1 A). This finding demonstrates that in *Dg*^{248} R cells nuclear localisation to the cell body is disrupted and nuclei migrate into their axon, suggesting that during metabolic stress DG may regulate the activity of the cytoskeleton.

To determine whether the disrupted adult eye generated in *Dg*^{248} eye mosaics was a result of increased apoptosis, Terminal dUTP nick-end labelling (Tunel) assays were performed on *Dg*^{248} large patch mosaics during different

stages of development. The assay detects levels of cleaved DNA, a hallmark of cell death. Tunel assays indicate that *Dg*^{248} large patch mosaic eyes show higher levels of cell death at the third instar stage of development (fig. 2). The end result of apoptosis is the regulated cleavage of a cell into smaller packets, called apoptotic bodies. These apoptotic bodies are cleared through endocytosis by neighbouring cells. Larger volumes and numbers of apoptotic bodies therefore, are markers of the levels of apoptotic cell death in a tissue. The mean total volume and number of apoptotic bodies per third instar eye disc was significantly higher for *Dg*^{248} large patch mosaic eyes than for wt mosaic eyes. The mean number and volume of apoptotic bodies in wt mosaic discs (n=14) were 57.8 and 578.5 μm^3 respectively per eye disc. The mean number and volume of apoptotic bodies in *Dg*^{248} large patch mosaic discs (n=15) were 137.9 and 2 147.01 μm^3 respectively per eye disc. The difference between the means was significantly different for both the number and the volume of the apoptotic bodies per eye disc; two-sided t-test, p= 0.007, and two-sided t-test p=0.004 respectively. The later stages of pupal development, 75% p.d and 95% p.d., of the large patch mosaics showed no cell death, in both *Dg*^{248} and wt mosaics (fig 3). Thus the apparent eye degeneration in *Dg*^{248} mosaics observed is associated with higher levels of DNA cleavage not during pupal development, but during the third instar at a time when DG-C is expressed and retinal cell specification begins.

To test which cell death pathway *Dg*^{248} could be involved in, the baculovirus anti-apoptotic protein p35 (Hay et al 1994, Jabbour 2004) which inhibits effector caspases apoptotic cell death pathway, was expressed in the *Dg*^{248} mosaics. If cell death in *Dg*^{248} could be inhibited by p35 it would indicate *Dg*^{248} initiates an apoptotic cell death pathway. The use of the GAL4/UAS system was used to inhibit apoptotic cell death at different developmental time points.

DG-C is expressed by R cells and may be functioning specifically in these cells. To inhibit cell death specifically in R cells, p35 was expressed in large patch mosaics using the elav promoter which expresses in R cells starting at the third instar larval stage onward (fig. 4). Expression of p35 in *Dg*^{248} large patch mosaic R cells did not significantly prevent the disruption of the *Dg*^{248} adult eye morphology (fig.4 F). Expression of p35 using the GMR promoter, which expresses in all cell types posterior to the MF of the third instar onwards, also did not significantly prevent the disruption of the *Dg*^{248} adult eye morphology (fig.5 D).

High levels of apoptosis were detected during third instar development of *Dg*^{248} mosaics. Expressing the caspase inhibitor at the onset of specification may be too late to affect apoptosis. Early expression of p35 was achieved using ey-Gal4, which expresses in all retinal cell types during the second instar and in

the anterior region of the third instar eye disc both in the disc proper and the peripodial membrane. When p35 is expressed early in development a worsening of the *Dg*^{248} mosaic eye morphology was observed (fig. 6 D and H). The effect varied between the sexes though in both, the major phenotype was an apparent reduction in the overall size of the eye (females 50% and males 60%). In females (fig. 6 H), a more severe reduction of the eye, either uni- or bilaterally, was observed in a subpopulation of female adults (23% of adult females). Within the male population, a more severe phenotype was observed in a subpopulation of males (12% of adult males). In males, this phenotype was the partition of the eye into two independent reduced portions (fig.6 D2). In an extreme example no eye formed (fig.6 D3). The expression of p35 early in eye development had no apparent disruptive effects on wt mosaic eye morphology (fig.6 C and G) suggesting that the expression of p35 inhibits an apoptotic pathway early on in *Dg*^{248} mosaics. Together these data suggest that apoptotic cell death in *Dg*^{248} mosaics is occurring early in eye development and that its inhibition is detrimental to further eye development.

To determine whether a lack of nuclear position, increased apoptosis and apparent degeneration was secondary to a failure of the R cells to maintain an apical/basal polarity, the polarity markers β-catenin (fig. 7) and crumbs (fig. 8) were localised in *Dg*^{248} ommatidia of 50% and 75% p.d. small patch mosaics.

β-catenin is a marker for the apical zonula adherens junctions which form between R cells of a same ommatidium. In wt 50% p.d. ommatidium β-catenin concentrates at apical cell to cell contacts between each R cell along the entire proximal-distal length of the photoreceptors (fig.7 A-C). At 75% p.d. β-catenin is still present along the whole length of the apical membrane of the R cells and is also highly concentrated at the proximal and distal adherens junctions (fig.7 I and J). *Dg*^{248} 50% p.d. ommatidia do localise β-catenin to apical points of cell to cell contact (fig.7 D-F). The punctuate shape of the zonula adherens however, is not as concentrated as in wt (fig. 7 M and N) as the localisation of β-catenin is more diffuse relative to the more punctuate wt localisation. The planar pattern of β-catenin is not like the stereotypical wt planar pattern, but does reflect the contact points being made by the *Dg*^{248} R cells. The number of cell: cell contact points in the proximal region of the *Dg*^{248} ommatidium, is lower than the equivalent plane in the wt. This may reflect a differential delay in the extension of the zonula adherens in the R cells of the ommatidium.

Crumbs, an apical membrane determinant, is normally expressed at 50% p.d. on the apical surface of R cells (fig. 8 B, F and J) and at 75%p.d. on the stalk membrane adjacent to the rhabdomere (fig.8 O and P). *Dg*^{248} 50%p.d. R cells localise crumbs to their apical surfaces (fig.8 D, H and L). The pattern of the apical surface in *Dg*^{248} ommatidium is different from wild type, but does

correspond to the pattern of the apical membrane contacts between R cells of the same ommatidium (fig.8 C, G, and K). There is a lack of crumbs accumulation along the proximal surfaces (fig.8. L), probably due to the lack of central apical R cell contact points at this level (fig.8 K). At 75% p.d. crumbs is still accumulated along the apical surface of *Dg*^{248} R cells (fig.8 S and T).

To determine if the apparent degeneration and the migrating nuclei of *Dg*^{248} R cells were due to disruption of the actin or microtubule cytoskeleton, β-tubulin and f-actin were localised in *Dg*^{248}small clone mosaics. In an ommatidium composed of six *Dg*^{248} R cells, β-tubulin can be detected and localises to the apical region (fig 9 A-C). The actin cytoskeleton is highly concentrated at the apical surface of R cells in the light-sensing organelle called the rhabdomere. Phalloidin was used to stain for f-actin. As expected the 50% photoreceptors localise f-actin apically where they have elongated their rhabdomeres along their entire length (fig. 10 B, F and J). *Dg*^{248} 50% p.d. R cells however only have high concentrations of actin in the distal apical contact points (fig. 10 D, H and L). As seen with crumbs, the proximal ommatidial planes lack central apical R cell contact points. By 75% however, the *Dg*^{248} R cells have elongated their rhabdomeres along their entire length (fig. 10N).

Quantitatively, all *Dg*^{248} R cells expressed crumbs, β-catenin, β-tubulin and actin on their apical surfaces or cellular compartments respectively.

Together these data indicate that by the end of differentiation, polarisation has occurred and the cytoskeleton is not disrupted in *Dg*^{248} R cells. This means that the apparent degeneration does not result from a lack of polarity maintenance.

Figures

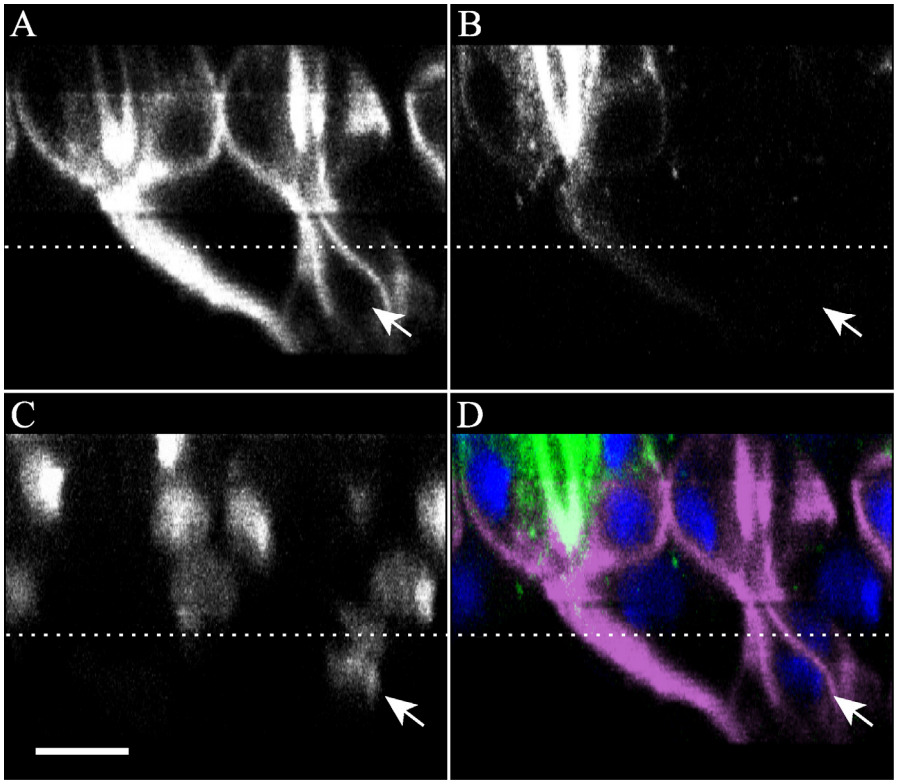

Figure 1. During early pupal development *Dg*^{248} R cell nuclei migrate from their cell body into their axons.

A planar confocal stack through a whole mount 40% p.d. *Dg*^{248} small patch mosaic disc was observed in its transversal plane using the software Volocity. A) Chaoptin labels the plasma membrane of R cells. B) Lack of GFP identifies an ommatidium composed of eight *Dg*^{248} R cells. C) DAPI staining of nuclei. D) A merge of A, B and C. The dashed line indicates the location of the retinal floor and the arrow indicates that some nuclei have migrated past the retinal floor into the axons. Nuclei not contained within R cells belong to the surrounding interommatidial cells. Scale bar is 10 μm.

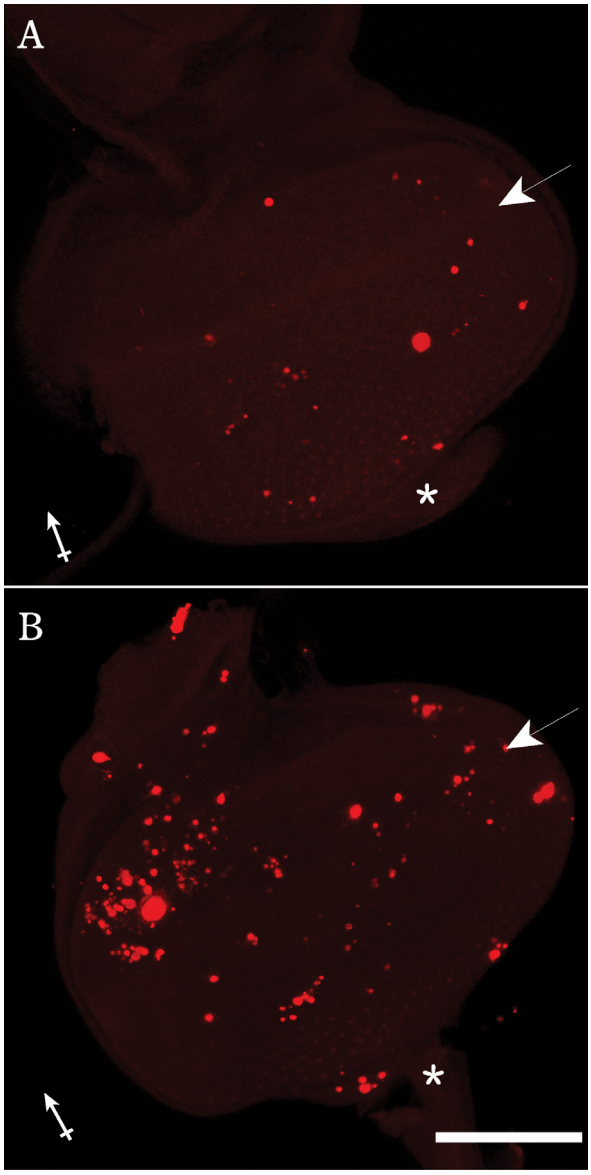
A
B

Figure 2. Increased cell death occurs in third instar eye discs of *Dg*^{248} large patch mosaics.

TUNEL cell death assay was performed on third instar whole mount large patch mosaic eye discs. A) A planar projection of a wt large mosaic eye disc confocal stack. B) A planar projection of a *Dg*^{248} large patch mosaic eye disc confocal stack. DG deficient third instar eye discs appear to have higher levels of cell death. The morphogenetic furrow is indicated by an arrow and the optic stalk is indicated by an asterisks. The direction of the tissue is indicated by the crossed arrow pointing toward the anterior. Note fluorescent bleed through of R cell co-labelling in the posterior region seen as faint puncta. Scale bar = 64 microns.

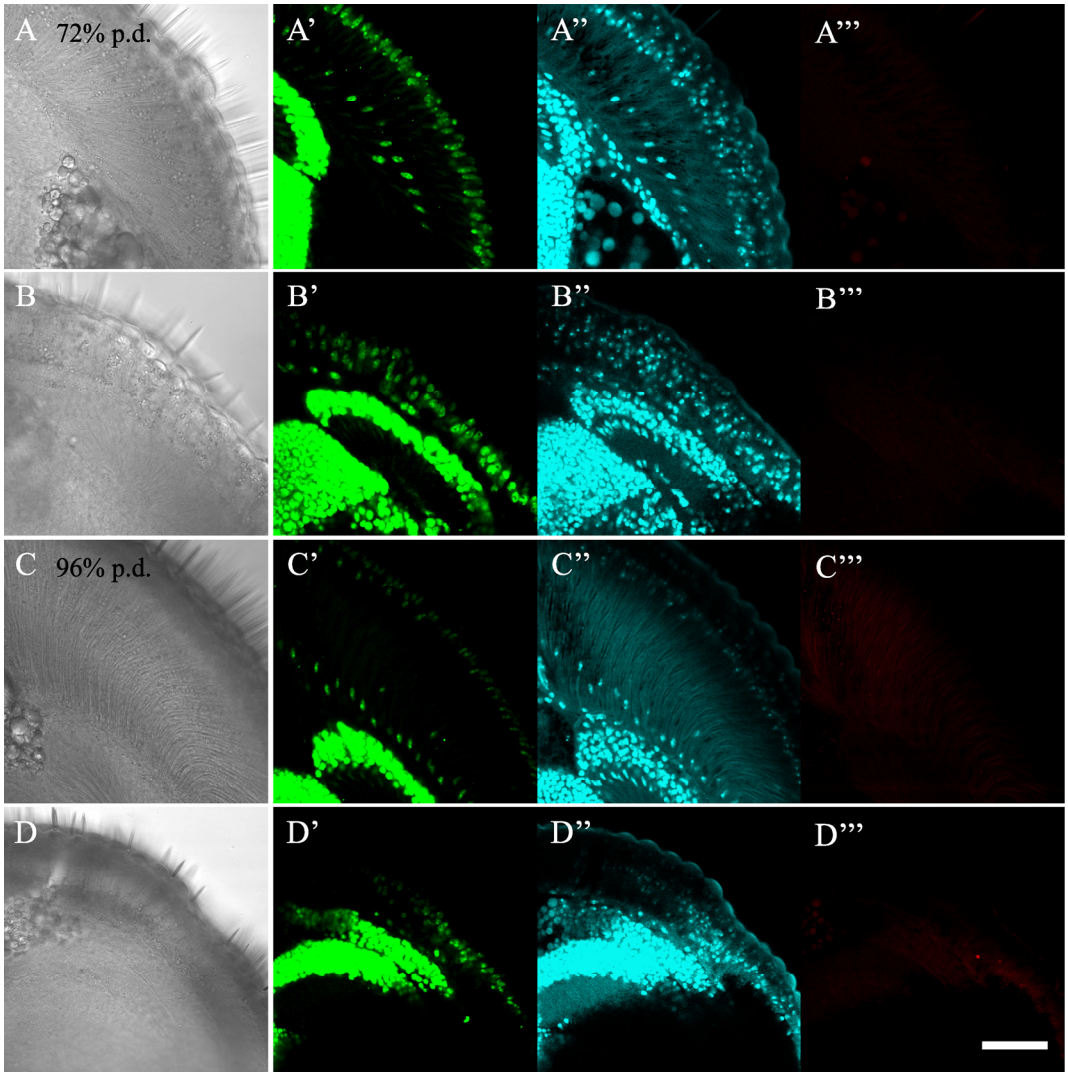
A 72% p.d.
A'
A''
A'''
B
B'
B''
B'''
C 96% p.d.
C'
C''
C'''
D
D'
D''
D'''

Figure 3. No increase in cell death in *Dg*^{248} large patch mosaic retina during late pupal development.

Late pupal retinal sections 75% p.d. (DIC, A, B) and 95% p.d. (DIC, C and D) were assayed for cell death using Tunel (A''' – D'''). Wt large patch mosaics (A and C) showed no cell death. *Dg*^{248} large patch mosaics (B and D) also showed no cell death. Sections were counterstained for the neuronal marker elav (A' to D') and for Hoechst (A'' to D''). Scale bar is 37 microns.

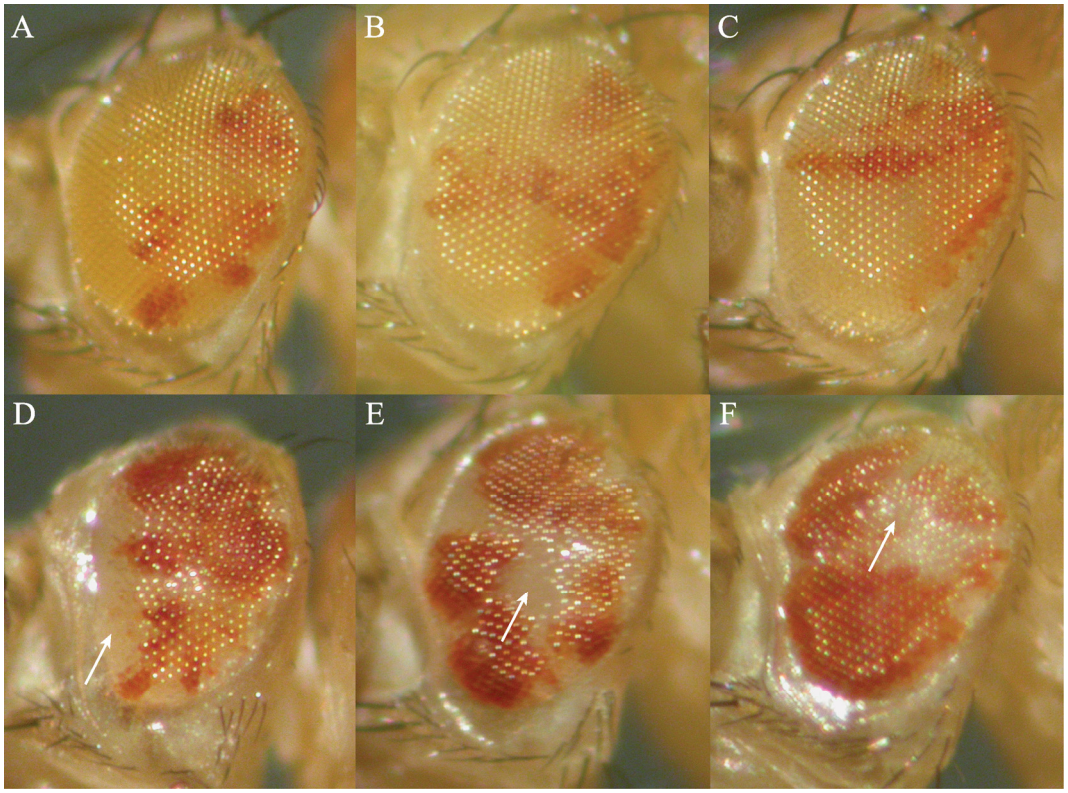
A
B
C
D
E
F

Figure 4. Expression of the anti-apoptotic protein p35 in specified R cells during development does not inhibit the adult eye morphology of *Dg*^{248} large patch mosaics.

Wt large patch eye mosaics (A-C) and *Dg*^{248} large patch eye mosaics (D-F) had *UAS-p35* driven only in the developing R cells using the R cell specific driver *elav-gal4*. The presence of the driver alone (A and D) and the *UAS-p35* alone (B and E) had no effect on the outer eye morphology of either mosaic (arrow D-F). Mosaic patches have pale eye pigment. The expression of p35 in R cells did not affect the wt large patch mosaic eye (C). The expression of p35 in R cells did not change the development of an abnormal *Dg*^{248} large patch mosaic eye (F). [n=25 adults per genotype]. Scale bar is 100μm.

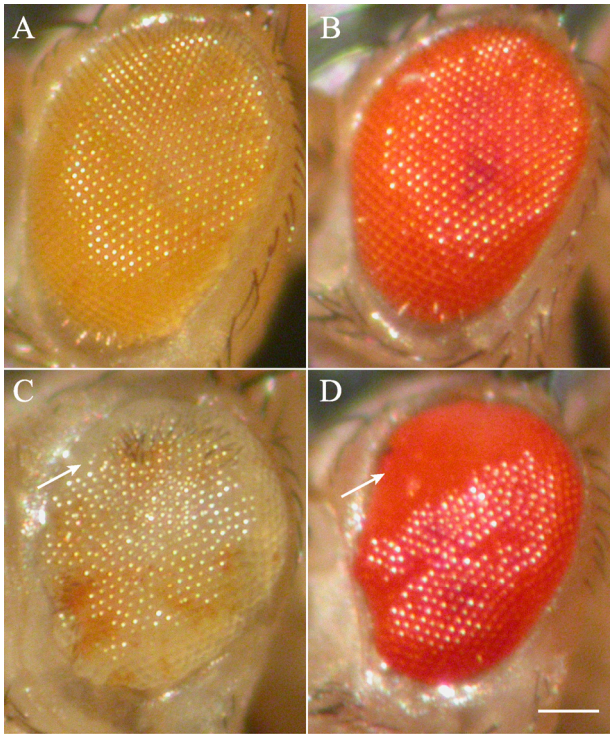
A
B
C
D

Figure 5. Expression of the anti-apoptotic protein p35 in all specified cell types during eye development does not inhibit the adult eye morphology of *Dg*^{248} mosaics.

The mosaic system which generates an eye of a single genotype was used to express the apoptotic inhibitor p35 in the developing eye disc. In wt mosaics (A) and *Dg*^{248} mosaics (C), p35 was expressed in all eye disc cell types beginning at the MF by introducing the transgene *GMR-p35*. Presence of *GMR-p35* had no significant effect on the outer eye morphology (arrow C and D) of either the wt mosaic (B) or the *Dg*^{248} mosaic (D). Scale bar is 100μm.

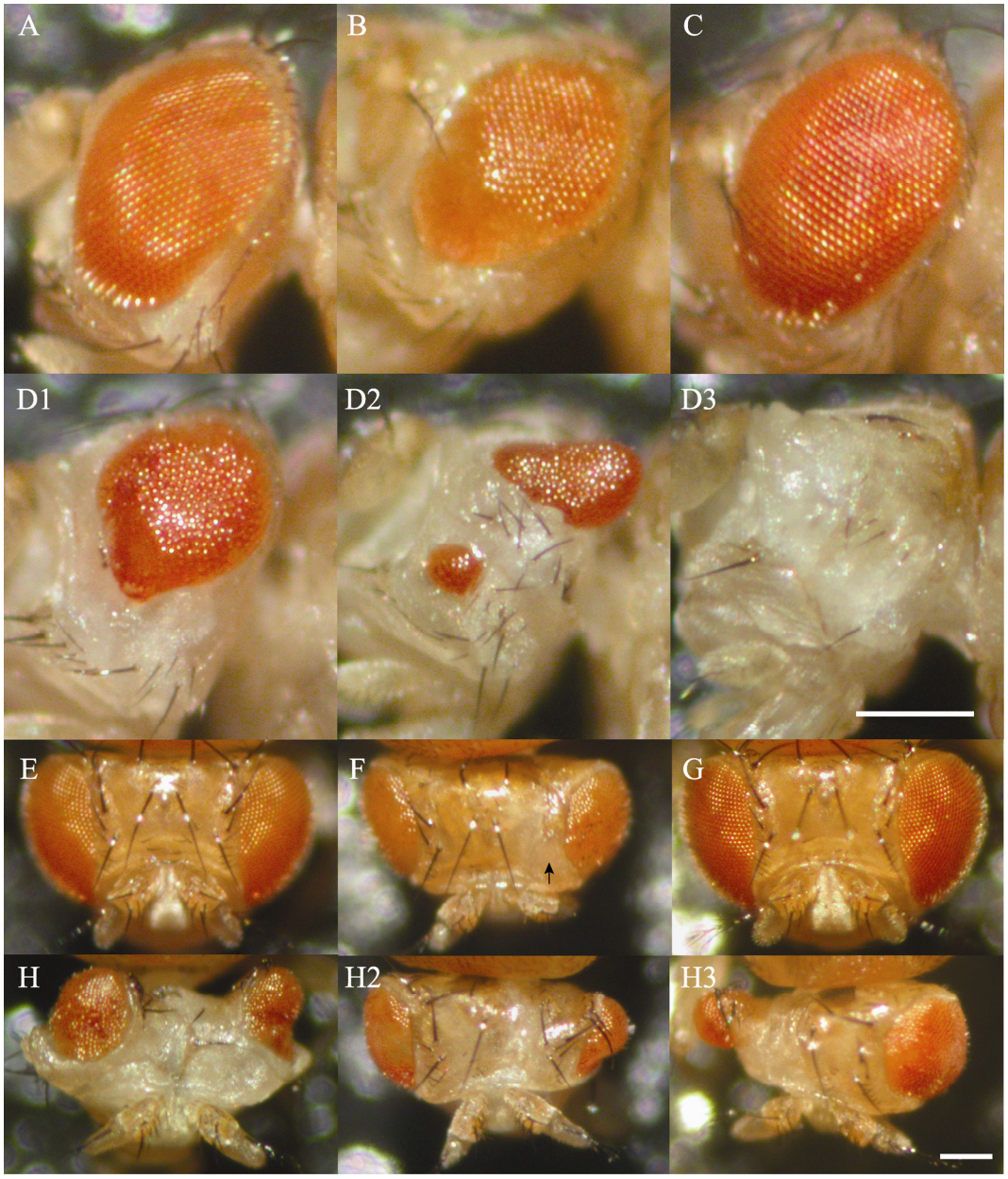
A
B
C
D1
D2
D3
E
F
G
H
H2
H3

Figure 6. Expression of p35 early during eye development prior to the third instar stage worsens the development of the *Dg*^{248} adult eye.

Using the mosaic system which generates an eye of a single genotype, the apoptotic inhibitor p35 was expressed starting early in eye development. Adult male *Dg*^{248} mosaics expressing p35, driven by the promoter eyeless which expresses in all cell types during early development, mainly developed eyes of reduced size (60%, D1-3). A sub-population of males (12%) developed eyes that were smaller and fragmented (D2) or no at all (D3). Wt mosaic driver alone control (A) developed normally as does the wt mosaic expressing p35 during early eye development (C). The *Dg*^{248} mosaic driver alone develops as previously noted (B). Adult female *Dg*^{248} mosaics expressing p35, during early eye development, developed eyes of reduced size (H, 50%). A sub-population of females (23%) developed eyes of extremely reduced size either bilaterally (H) or unilaterally (H2-3). Wt mosaic driver alone control (E) develop normally as do the wt mosaics expressing p35 (G). The *Dg*^{248} mosaic driver alone develops as previously noted (B), note the absence of bristles around the left eye (F arrow). The scale bars are 100μm.

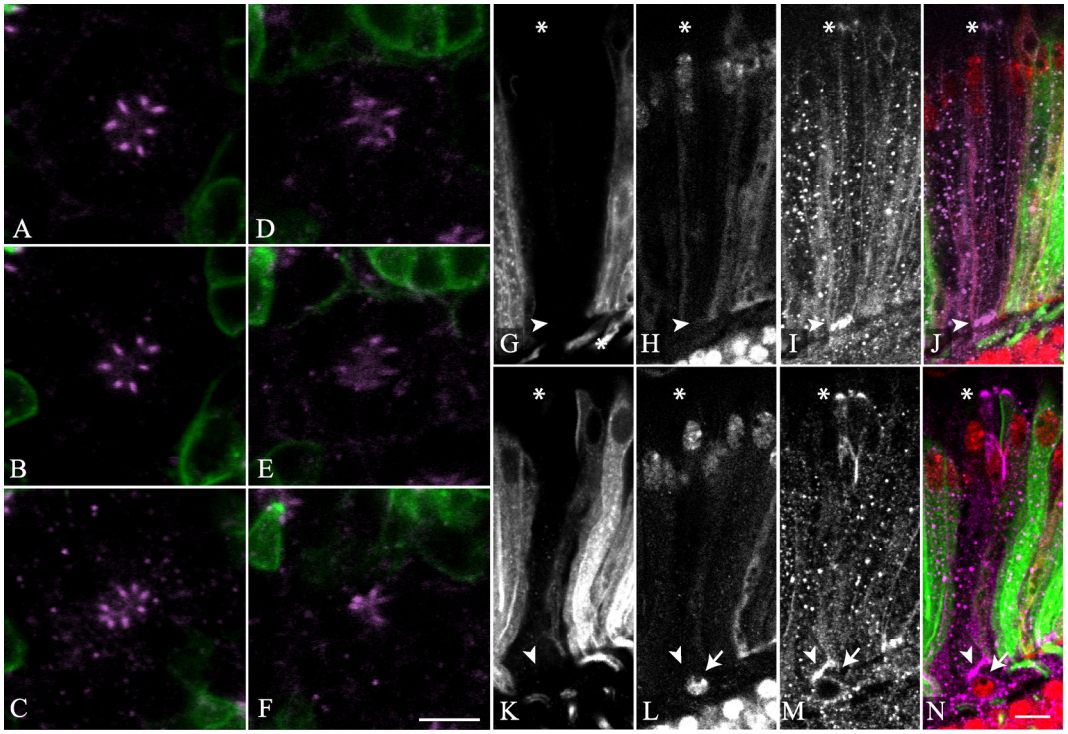
A
D
B
E
C
F
G
H
I
J
K
L
M
N

Figure 7. As in wild type, the zonula adherens marker β-catenin localises apically in *Dg*^{248} ommatidia.

Small patch mosaic 50% p.d. ommatidia (A-F) and 75% p.d. ommatidia (G-N) were examined. A wt 50% p.d. ommatidium (A-C) localises β-catenin, magenta, at photoreceptor: R cell contact points spanning the length of the ommatidium, A, distal, B, midpoint and C proximal. Lack of GFP (green) identifies the mosaic patch. A *Dg*^{248} 50% p.d. ommatidium (D-F), localises β-catenin, magenta, to the apical membrane. The concentration of β-catenin is slightly more diffused, but still present at R cell: R cell contact points. β-catenin also spans the length of the *Dg*^{248} ommatidium, D, distal, E, midpoint, F, proximal. A wt 75% p.d. ommatidium localises β-catenin at the apical membrane of the entire length of the ommatidium with higher concentrations at the proximal and distal adherens junctions (I). A lack of GFP (G and K) identifies the patch. Elav (H and L) identifies neuronal nuclei. β-catenin (I and M) identifies the zonula adherens. A *Dg*^{248} 75% p.d. ommatidium localises β-catenin to the apical membrane with higher concentrations distally and proximally (M). Proximally the pattern of β-catenin suggests deformed zonula adherens junction and the presence of a photoreceptor nuclei below the retinal floor (arrow) suggests it has descended from its cell body. (G-N) asterisk identifies the distal AJ, the arrowhead identifies the proximal AJ. Scale bar = 6 microns

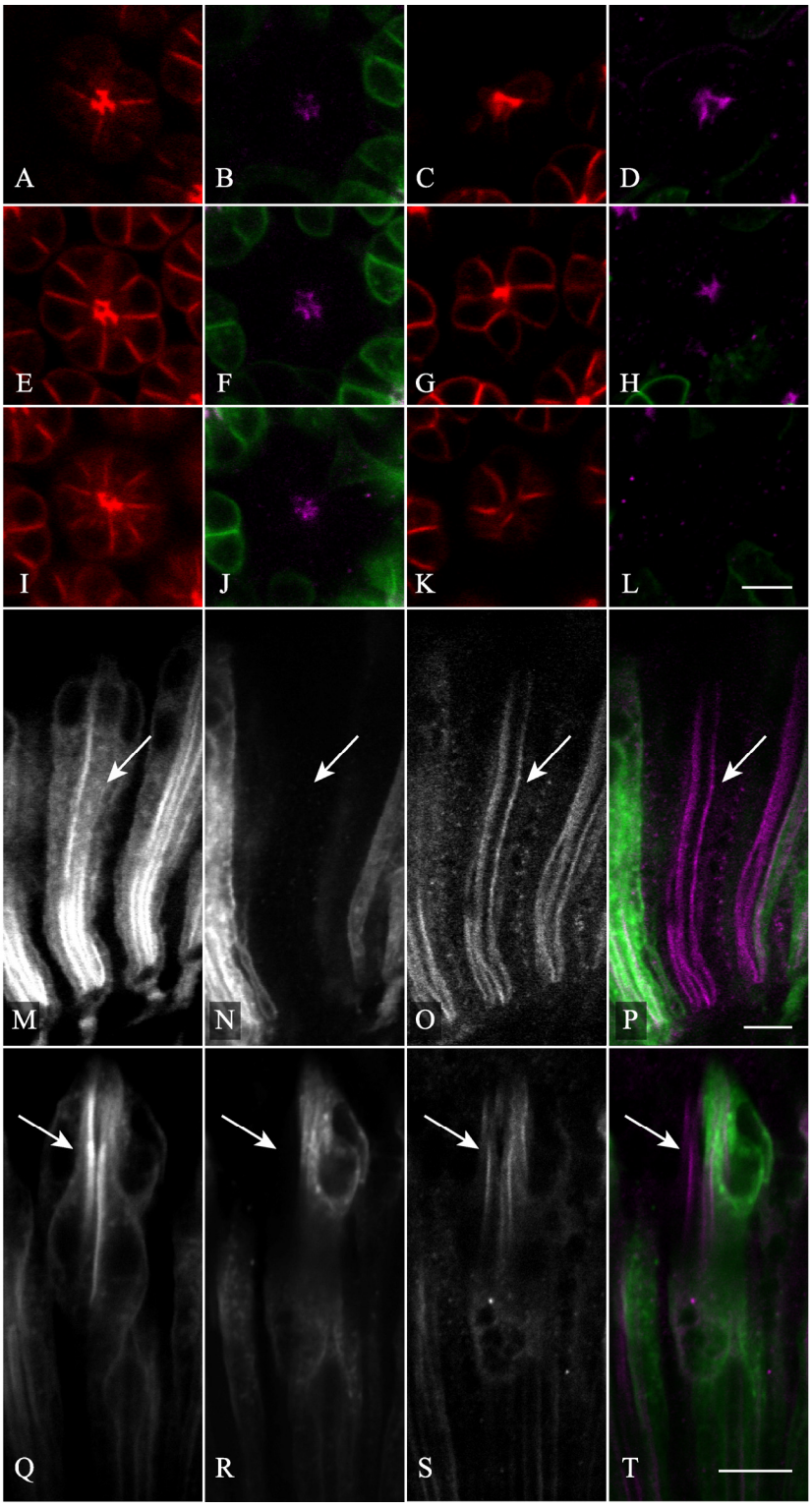
A
B
C
D
E
F
G
H
I
J
K
L
M
N
O
P
Q
R
S
T

Figure 8. Apical localisation of the apical determinant crumbs occurs in *Dg*^{248} R cells.

Crumbs was localised in 50% p.d. pupae (A-L) and 75% p.d. pupae (M-T) of wt and *Dg*^{248} small patch mosaics, where a lack of GFP identifies the mutant patch. A wt 50% pupae ommatidium (A, B, E, F, I and J) localises crumbs to its apical membrane which spans the length of the ommatidium. Crumbs in magenta and GFP in green (B, F and J). A lack of GFP identifies the patch. Chaoptin in red (A, E and I) identifies the R cells. A *Dg*^{248} 50% ommatidium (C, D, G, H, K and L) localises crumbs to the apical membrane of the R cells in the distal regions of the ommatidium. Chaoptin in red (C, G and K) identifies the R cells. Crumbs in magenta and GFP in green (D, H, L). An ommatidium is studied by examining planar sections through the distal end of ommatidia (wt A; *Dg*^{248} D); the midpoint of ommatidia (wt E; *Dg*^{248} H) and the proximal end of ommatidia (wt I; *Dg*^{248} -L). Scale bar is 6 microns. A 75% wt ommatidium (M, N, O and P). Chaoptin (M) identifies the R cells. GFP (N) identifies the genotype. Crumbs (O), localises to the apical membrane. P is a merge of N and O, crumbs in magenta, GFP in green. Scale bar is 6 microns. A 75% *Dg*^{248} ommatidium (Q, R, S and T) is stained for chaoptin (Q) which identifies the R cells, arrow points to a set of nuclei which are positioned lower than their surrounding wild type photoreceptors. GFP (R) identifies the genotype. Crumbs (S) localises to the

apical membrane. T is a merge of R and S, crumbs in magenta, GFP in green. Arrow points to a GFP negative *Dg*^{248} cell (M-T). Scale bar is 5 microns.

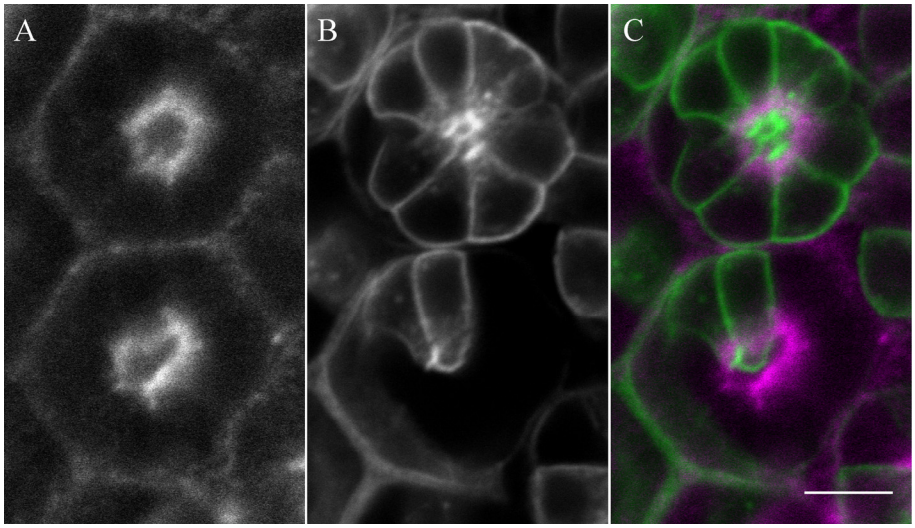
A
B
C

Figure 9. The microtubule cytoskeleton is not disrupted in *Dg*^{248} ommatidia.

The microtubule cytoskeleton localises to the apical region of *Dg*^{248} R cells. β-tubulin (A and C magenta) and GFP (B and C green) were localised in a planar confocal section through a whole mount 50% p.d. *Dg*^{248}small patch mosaic retina. Lack of GFP identifies *Dg*^{248} R cells. Scale bar is 13 microns.

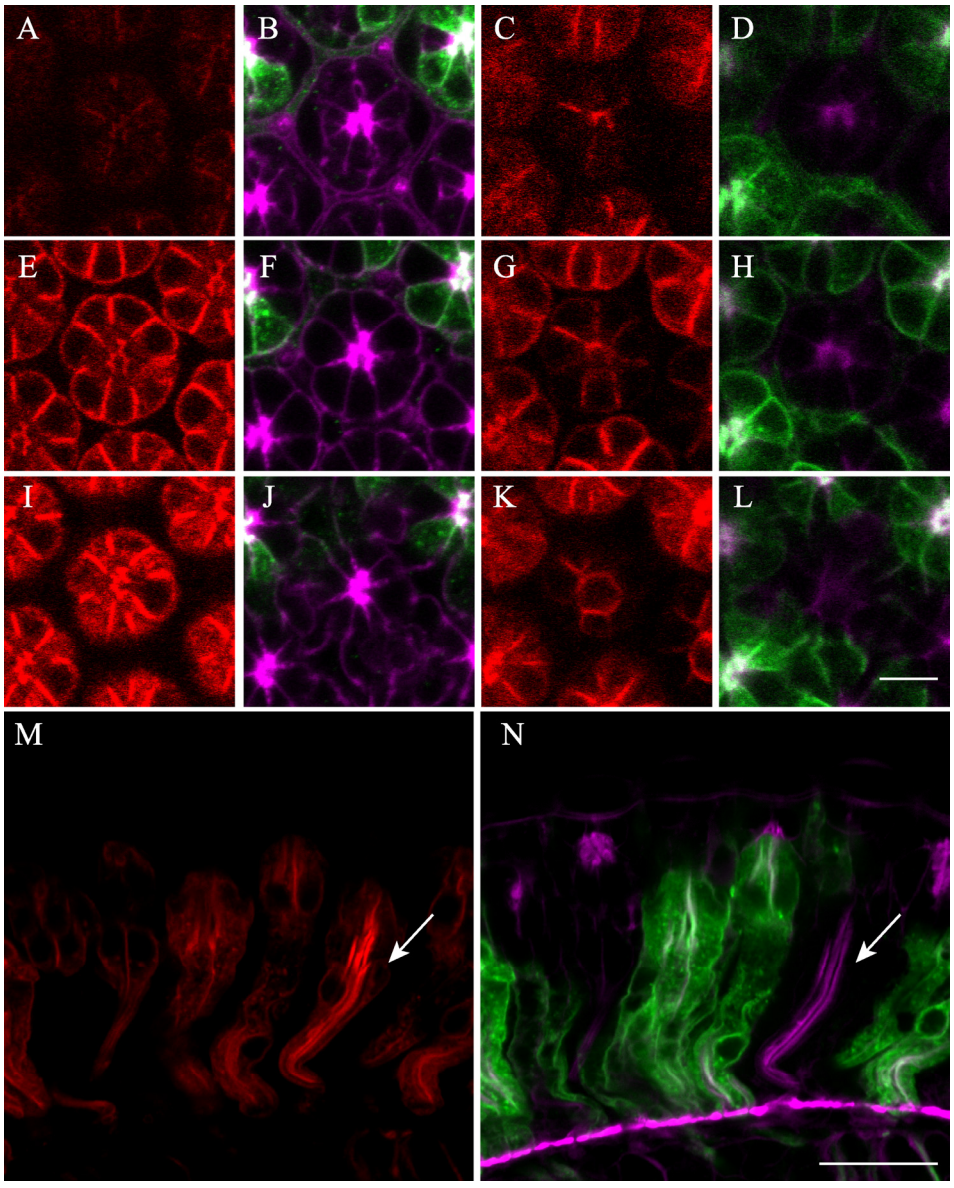
A
B
C
D
E
F
G
H
I
J
K
L
M
N

Figure 10. The actin cytoskeleton is undisrupted in *Dg*^{248} ommatidia but does reveal morphological abnormality during *Dg*^{248} R cell development.

Wt 50% pd ommatidium (A, B, E, F, I and J) has a concentration of f-actin, as revealed by phalloidin staining (magenta B, F, J), at the apical rhabdomere which extends the entire length of the photoreceptor outlined by chaoptin (A, E and I). The distal plane is shown by A, B, midpoint by E and F and the proximal planar plane by I and J. *Dg*^{248} 50% p.d. ommatidium localises f-actin (phalloidin in magenta D, H and L) at its apical surface, but at a lower concentration and only in the distal half of the ommatidium, revealing a developmental delay in rhabdomere formation. The chaoptin staining (C, G and K), demonstrates that *Dg*^{248} R cells fail to orient themselves normally (G and K). *Dg*^{248} 75% p.d. ommatidium as revealed by a lack of GFP expression (N), has a rhabdomere labelled by phalloidin (N magenta) spanning the length of ommatidium. R cell are identified by chaoptin expression (M). Arrow points to a GFP negative *Dg*^{248} cell. Note the retinal tissue is compressed causing the R cells not to appear straight (M and N). A-L scale bar is 6 microns. M and N scale bar is 16 microns.

Discussion

The deletion of *mRpL34* (Mirouse et al 2009) in the *Dg* deletion series of alleles offered the opportunity to study the role of DG during metabolic stress through an inhibitory effect on mitochondrial function (Miller et al 2004, O'Brien et al 2005). Recent findings suggest that deletion of DG's first non-coding exon is associated with an increase in metabolic rate (Takeuchi et al 2009). The Dg^{248} deletion may therefore have serendipitously generated cells under great metabolic stress since the reduced energetic output, due to the deletion of *mRpL34,* may not meet the energetic demand generated by the partial deletion of *Dg*.

Cells unable to adapt to a source of stress may respond by initiating cell death (Bursch et al 2008). Apoptotic cell death was found during early but not late Dg^{248} eye disc development. The increase in apoptotic cell death observed occurs during third instar at a time when retinal cells become specified. An absence of apoptotic cell death during late pupa Dg^{248} eye development may be a consequence of metabolic stress. Apoptotic programmed cell death is a highly regulated energy demanding process. During a deficiency in energy levels alternative cell death pathways, such as autophagy, must be used (Edinger & Thompson 2004). Autophagy programmed cell death machinery is expressed in *Drosophila* and is induced in response to a variety of stress conditions (Bursch et

al 2008). Autophagy is a tightly regulated programmed self-digestion process, which can actually promote cell survival (Fung et al 2008), by producing crucial nutrients to promote cell survival. Autophagy may be contributing to the survival of the *Dg*^{248} tissue.

Inhibition of apoptotic cell death, using the baculovirus p35 caspase inhibitor, in cells posterior to the MF, did not have a significant impact on the development of the aberrant *Dg*^{248} mosaic eye. This suggests that the timing of inhibition may be too late to prevent the cell death observed during third instar *Dg*^{248} eye disc. Inhibition of apoptosis prior to the detected high levels of cell death causes a sex-dependent, detrimental effect on *Dg*^{248} eye development. This result suggests that the early survival of *Dg*^{248} cells, with decreased DG expression and under metabolic stress, is detrimental to the development of the eye. Previous *Drosophila* studies found that when cells which would normally die, but were inhibited to do so, induced over proliferation of neighbouring cells a phenomena called compensatory proliferation, resulting in an overgrown adult tissue (Kondo et al 2006). Our findings in the developing *Dg*^{248} eye where p35 inhibits early apoptotic cell death results in the opposite effect, a reduced size of the adult tissue. The fact that p35 had a detrimental effect during early eye development and not after the eye tissue had become specified may be explained by the different compensatory proliferation mechanisms used between

proliferating and differentiating tissue (Wells et al 2006). These data may suggest that compensatory proliferation mechanisms are disrupted in the proliferative tissue of the developing *Dg*^{248} eye disc.

The development of R cell polarity is not prevented during *Dg*^{248} R cell development, nor is the cytoskeleton grossly perturbed. The difference seen between wt and *Dg*^{248} at 50% p.d., and its recovery by 75% p.d. suggests that there may be a developmental delay in the extension of the ZA and the rhabdomere from the distal to proximal end of R cells. This result does not support a role, as in follicular epithelial cells, for DG in polarity maintenance (Mirouse et al 2009). It does however support the finding that AMPK, an important regulator of the metabolic adaptation pathways, is not required for R-cell polarity maintenance during metabolic stress (Spasic et al 2008). Though the cytoskeleton network is present in the developing *Dg*^{248} R cells, the migration of their nuclei from the cell soma into their axons suggests a deregulation of the cytoskeleton. It would be interesting to determine where the nuclei terminate, if the cell soma ever follows and if they undergo degeneration.

Together the data suggest that DG plays a role in R cell morphogenesis during metabolic stress. This will need to be confirmed in mutants deficient only in *Dg,* by placing them under metabolic stress through glucose reduction. Apoptotic cell death occurs prior to the MF critical to the development of the

Dg^{248} eye, suggesting that DG's role in cell death is more complex than previously predicted (Li et al 2002) and may be involved in compensatory proliferation.

Bridging Text

The work presented in chapter 2 focused on the role of DG during eye development where it was found to have a role in mouse and *Drosophila* eye development. In *Drosophila*, DG-C was found to be localised at the apical membrane of the developing R cells, where one of its functions may be to regulate the elongation of R cells. The RNAi knockdown of DG led to a disrupted retina which was phenocopied by the RNAi knockdown of DYS. This suggested that DG may be interacting with the known binding partner DYS (Yatsenko et al 2009) to mediate its functions. In chapter 3, the *Dg* deletion allele series was used as a model for the role of DG in eye development under metabolic stress, due to the lack of mRpL34. The findings suggested that DG may have roles in nuclear migration as well as in apoptotic compensatory proliferation during metabolic stress. Together these data suggest that DG may be regulating multiple molecular pathways.

Further knowledge of how DG regulates molecular pathways may be gained by determining novel binding partners. I participated in a project to identify novel mammalian DG intracellular binding proteins in the brain, more specifically at synapses(Zhan et al 2005). My role was to confirm whether a candidate novel DG binding protein could co-localise with DG in the retinal inner plexiform layer (Montanaro et al 1995). This would provide supporting evidence

that DG's interaction with the candidate binding protein may have physiological significance.

Chapter 4 - Evidence That Dystroglycan Is Associated with Dynamin and Regulates Endocytosis

By:

Yougen Zhan, Mathieu R. Tremblay, Nadia Melian, and Salvatore Carobonetto

This Research was originally published in the Journal of Biological Chemistry. Yougen Zhan, Mathieu R. Tremblay, Nadia Melian, and Salvatore Carobonetto. Evidence that dystroglycan is associated with dynamin and regulates endocytosis. *The Journal of Biological Chemistry*. 2005, Vol.: 280, pages 18015 – 18024.

Summary

Disruption of the dystroglycan gene in humans and mice leads to muscular dystrophies and nervous system defects including malformation of the brain and defective synaptic transmission. To identify proteins that interact with dystroglycan in the brain we have used immunoaffinity purification followed by mass spectrometry (LC/MS-MS) and found that the GTPase dynamin1 is a novel dystroglycan-associated protein. The β-dystroglycan-dynamin 1 complex also included α-dystroglycan and Grb2. Overlay assays indicated that dynamin interacts directly with dystroglycan, and immunodepletion showed that only a pool of dynamin is associated with dystroglycan. Dystroglycan was associated and colocalized immunohistochemically with dynamin 1 in the central nervous system in the outer plexiform layer of retina where photoreceptor terminals are found. Endocytosis in neurons is both constitutive, as in non-neural cells, and regulated by neural activity. To assess the function of dystroglycan in the former, we have assayed transferrin uptake in fibroblastic cells differentiated from embryonic stem cells null for both dystroglycan alleles. In wild-type cells, dystroglycan formed a complex with dynamin and codistributed with cortactin at membrane ruffles, which are organelles implicated in endocytosis. Dystroglycan-null cells had a significantly greater transferrin uptake, a process well known to require dynamin. Expression of dystroglycan in null cells by infection with an

adenovirus containing dystroglycan reduced transferrin uptake to levels seen in wild type embryonic stem cells. These data suggest that dystroglycan regulates endocytosis possibly as a result of its interaction with dynamin.

Introduction

Dystroglycan (DG) is encoded by a single gene (*dag1*), and is synthesized as a precursor protein that is cleaved into α and β subunits. α-DG is a peripheral membrane protein that binds, via its carbohydrate side chains (1, 2), to globular motifs in the α chain of several laminins (3-5), agrin (6-9), perlecan (10, 11) and α-neurexin (12). β-DG is a transmembrane protein bound non-covalently to α-DG that interacts intracellularly with dystrophin, utrophin, rapsyn, caveolin-3 and growth factor receptor-bound protein 2 (Grb2)(13). In skeletal muscle α- and β-DG form the functional core of a larger complex that links the extracellular matrix to the cytoskeleton and serves to maintain the integrity of myofibers faced with the stress of repeated contractions (14). Hence, mice with skeletal muscle deficient in DG develop a severe muscular dystrophy (15-16).

DG is expressed in the nervous system and in many tissues other than skeletal muscle (17) and mice null for *dag1* die at E6.5-7.0, long before muscle differentiation (18). DG has been implicated in the formation of several (2, 11, 19), but not all basement membranes (15-16, 20-21) and in *Drosophila* DG is necessary for epithelial polarization (22). In the nervous system DG is localized at glial end feet in contact with basement membranes around blood vessels (23) and beneath the meninges of the brain (2). DG is also concentrated at peripheral

(24-26) and central synapses (27-30). Recent work has shown that myodystrophy (*myd*) mice, which have a mutation in *LARGE*, a gene that encodes an enzyme involved in O-glycosylation of α-DG (31), have decreased affinity for laminin and disrupted meningeal basement membranes (2). As well, these mice have defects in neuronal migration in the cerebral cortex and cerebellum (2). In humans similar defects, called lissencephalies, are associated with profound mental retardation and are manifested in Walker Warburg Syndrome, Muscle Eye Brain Disease and Fukuyama Muscular Dystrophy. All of these are congenital muscular dystrophies that result from mutations in genes known or suspected to regulate glycosylation of α-DG (32). Interestingly, mice with a targeted deletion of *dag1* in the brain have a similar phenotype (19) suggesting that many functions of DG are mediated by carbohydrate side chains which are responsible for most ligand binding (1, 2, 33). In addition, mice lacking DG in the brain have defects in long-term potentiation in the hippocampus (19) and *myd* mice have anabnormal electroretinogram with no signs of disrupted neuronal migration in the retina (20). DG is also necessary for stabilization of the postsynaptic density of acetylcholine receptors on skeletal myotubes in culture (11, 34) and at nerve-muscle synapses in vivo (11,15)

Emerging evidence indicates that the proteins that interact with DG in non-muscle tissues differ from those in muscle. For example, α-neurexin is complexed with α-DG in the central nervous system (CNS) (12) while periaxin is associated with DG in Schwanncells (35). To identify novel DG interactors we have used immunoaffinity chromatographyto purify DG and its associated proteins from rat brains. We report that β-DG forms a complex with dynamin 1, a GTPase essential for several modes of endocytosis including regulated endocytosis during synaptic vesicle release and constitutive endocytosis which occurs in neuronal and non-neuronal cells alike (36-38).The β-DG-dynamin complex in the CNS also contains α-DG and the SH2 (src homology 2)/SH3 (src homology 3) adapter protein Grb2 and has the potential to anchor dynamin at discrete sites within the cell. In an overlay assay, β-DG interacts directly with brain dynamin. In the retina DG is associated and immunohistochemically colocalized with dynamin at the outer plexiform layer where previous ultrastructural studies (27, 39) have found DG to be distributed presynaptically in synapses formed by photoreceptors onto bipolar and horizontal cells. Finally, in fibroblasts differentiated from embryonic stem (ES) cells DG associates with dynamin and codistributes with cortactin at membrane ruffles, which are organelles implicated in endocytosis. Cells null for DG have an increased uptake

of transferrin, and re-introduction of DG into these null cells reduces this increase to normal levels.

Experimental Procedures

Antibodies

Antisera to α–DG and monoclonal antibody (mAb 1B7) to α-DG were characterizedpreviously (11, 40). MAbs to the following proteins were used for western blotting: β-DG (1:250) (*Novocastra Laboratories Ltd.*); α-DG (IIH6) (1:1000) (*Upstate Biotechnology*); Grb2 (1:500); GST (1:1000) (*Santa Cruz Biotechnology*). MAb Hudy-1 (*Upstate Biotechnology*) that recognizes dynamin 1 found in the brain as well as the more ubiquitous dynamin 2 (41) was used at 1:40,000 for western blotting and 1:200 for immunocytochemistry. MAbs to cortactin (*Upstate Biotechnology*) were used at 1:250. Antisera to amphiphysin 1874) was a gift from Peter McPherson (McGill). Horseradish peroxidase–conjugated goat anti-mouse (1:2000) and goat anti-rabbit antisera (1:4000) (*Jackson ImmunoResearch Laboratories*) were used as secondary antibodies in westernblots. Rhodamine (TRITC) conjugated donkey anti-rabbit (1:200) and fluorescein (FITC) conjugated donkey anti-mouse antisera (1:200) (*Jackson ImmunoResearch Laboratories*) were used for immunofluorescence staining.

Tissue extraction

Rat brains and hippocampi were dissected from adult rats euthanized according to the Guidelines of McGill University Health Center Animal Facility.

Tissues were homogenized on ice four times (10 sec each) with a Polytron tissue homogenizer in phosphate-buffered saline (PBS; pH 9.0) containing 1% sodium deoxycholate, 0.5mM $CaCl_2$, and a protease inhibitor cocktail (*Boehringer Mannheim*). The homogenates were incubated at 37° for 30 min followed by addition of Triton X-100 (TX-100) to a final concentration of 0.5% in a total volume of 6 ml. After 2 hrs of incubation at 4°C with occasional vortexing, the homogenates were centrifuged at 37,000x g for 30 min. The supernatants were collected and protein concentrations were determined (DC Protein Assay Kit; *Bio-Rad*).

Synaptosomes were prepared from rat brains as described by Sugita et al. (12) with minor modification. Briefly, rat brains were removed and homogenized with a Teflon glass homogenizer in a buffer containing 20mM Tris-HCL (pH7.2), 0.32M sucrose, 1mM $CaCl_2$, and protease inhibitor cocktail. The homogenates were centrifuged for 10 min at 700x g to remove nuclei. The post-nuclear supernatants were collected and centrifuged for 30 min at 9,800x g, and the resulting pellets were collected as crude synaptosomes.

Immunoaffinity chromatography

Antisera to β-DG (11), bovine serum albumin (control) or rabbit immunoglobulin (control) were covalently coupled to Affigel 10 following the manufacturer's instructions (*Bio-Rad*). Five mgs of hippocampal extract (2-3ml) were incubated overnight with 1 ml of each Affigel-protein conjugate. The slurry was packed into a column, washed first with 10 ml of PBS (pH 9.0) containing 1% sodium deoxycholate, 0.5% TX-100 and 0.15M sodium chloride (buffer A), followed by a wash with 10 ml of 0.5M NaCl in buffer A, and finally 10ml of 5mM EDTA in buffer A. Proteins still bound to the column were eluted at low pHwith 0.1M glycine (pH2.5) and neutralized with 0.3ml of 1M Tris-HCl (pH8.0). The columns then were equilibrated each with 10 ml of PBS and any remaining proteins were eluted with 3ml of 0.1M triethylamine (pH11.5) and neutralized with 0.3ml of 1MTris-HCl (pH8.0). The glycine and triethylamine eluates were pooled, dialyzed against PBS overnight and then concentrated to equal volumes (*Millipore Centricon* filters), and equal aliquots of the eluates were subjected to SDS-PAGE. The SDS-PAGE and western blotting were carried out as described previously (3).

Immunoprecipitation

Crude synaptosomes or retinas were solubilized in PBS (pH 9.0) containing 1% sodium deoxycholate, 0.5% TX-100, 1mM $CaCl_2$ and protease

inhibitor cocktail (buffer B) and centrifuged for 37,000x g for 30 min. 60-100 μl of supernatant was pre-cleared with 20 μl of protein G agarose (*GibcoBRL*) for 1 hr. After preclearing 20 ⌠l of protein G beads conjugated to relevant antibodies or pre-immune sera were added to the pre-cleared supernatants, and incubated overnight at 4° with constant shaking. The agarose beads were then pelleted by centrifugation at 4,000x g for 2 min. The supernatants were collected and the beads were washed twice with 1 ml of buffer C, followed by 0.5 ml of 0.5M NaCl in buffer B, and finally with 0.5 ml of buffer B containing 5mM EDTA. The washed beads were then boiled in sample buffer for 5 min and subjected to SDS-PAGE and western blotting.

Overlay Assay

The cytoplasmic tail of β-DG was amplified by PCR from a plasmid containing the full-length DG cDNA sequence using sense 5'AAGATCTTCTATCGCAAGAAGAGG-3', and anti-sense primers 5'-GCTCTAGATTAAGGGGGAACATACGG-3'. Theamplified β-DG_{cyto} was digested with Bgl II and gel purified. Plasmid pGEX-3x (*Amersham Biosciences*) was digested with EcoR I, blunt-ended, digested with Bam HI and gel-purified. The purified pGEX-3X vector and β-DG_{cyto} fragment were ligated to produce pGST-®DG_{cyto} plasmid. The DH5α *E. coli* strain was transformed with plasmids pGST-

3X and pGSTβDG$_{cyto}$, and proteins induced with 1mM IPTG for 2-3 hrs were purified according to the procedures described by Frangioni and Neel (42) using glutathione Sepharose (*Amersham Biosicence*).

To assay the interaction of dynamin with β-DG, dynamin was immunoprecipitated from 0.4 mg of synaptosomal extracts with 6⌠g of mAb Hudy-1 (43). The immunoprecipitated dynamin was electrophoresed in a 4-15% acrylamide gel and electroblotted onto a PVDF membrane (*Bio-Rad*). The membrane was blocked for 1 hour with 5% powdered skim in TBST (10mM Tris-HCL, 150mM NaCL, 0.1%Tween-20) and incubated overnight with GST (20 ⌠g/ml) or GST-βDG$_{cyto}$ (20 ⌠g/ml) in TBST containing 5% skim milk. The membranes were washed three times with TBST (10 min each) and incubated with HRP-conjugated mouse anti-GST antibody (*Bio-Rad*) for 1 hr. After three washes with TBST (15 min each), the signals were visualized by chemiluminescence (*PerkinElmer Life Sciences*).

Cell culture, immunocytochemistry and transferrin uptake assay

Wild type and DG null embryonic stem cells were engineered as previously described (15). Cells were differentiated into embryoid bodies that were grown on 0.1% gelatin-coated tissue culture dishes (11). After 3 d in

culture, cells from the embryoid bodies spread and fibroblast-like flat cells appear at the periphery. At this point, cultures were treated with 200 μg/ml transferrin (*SIGMA*) at 4° for 15 min, after which cells were washed extensively with PBS and incubated with 20 μg/ml of rhodamine-conjugated transferrin in fresh growth medium at 37° for 15 or 120 mins. After washing in PBS, cells were fixed in 4% paraformaldehyde in PBS, and permeablized in 0.5% TX-100 in PBS for 10 min. Nuclei were stained with DAPI (*Sigma*) for 10 min at room temperature. Immunocytochemistry followed previously described methods (11). Briefly, cells were washed with PBS, fixed in 4% paraformaldehyde, permeablized in 0.5% TX-100, incubated with primary antibodies for 1 hr, then washed with PBS 3 times and incubated with fluorescently-labeled secondary antibodies for 1 hour. Cells were washed prior to mounting on slides in Immunofloure mounting medium (*ICN Biomedicals, Inc.*) and observed under a 63X objective using a Zeiss Axioskop fluorescent microscope. Images were captured with a Retiga 1300 Monochrome 10 bit digital camera (*Qimaging Corp.*) and analyzed with Northern Eclipse software (*Empix*). Quantifications were done on 8-bit images using threshold values of 86-255 pixels (11). The sum of the areas that were fluorescent were obtained for each field and normalized to the number of cells per field. Measurements were tabulated with Microsoft Excel and analyzed statistically using StatView (*Abacus Concepts, Inc.*).

To isolate and expand fibroblastic cells, wild type and DG null embryoid bodies were grown for 3 weeks. At this point embryoid bodies were surrounded by a halo of fibroblastic cells. The central cell mass was aspirated and the remaining adherent cells on the periphery were grown for 2d after which cells that did not appear fibroblastic were carefully aspired. The fibroblastic cells were then harvested and grown on 175 cm_2 dishes for 4d. Some cells were passaged onto dishes for transferrin uptake assays with same procedures as before except that cells are incubated with transferrin at 37° for 15 min. Others were harvested, solubilized in 1% TX-100 containing 20mM Tris-HCl, 150mM NaCl, 1mM $CaCl_2$ and protease inhibitor cocktail, centrifuged at 16,000x g for 20 min and supernatants were used for immunochemical studies.

Adenoviral Constructs and Infection

To express full-length DG in DG-null fibroblastic cells, we generated a replication-defective adenovirus using the AdEasy system (*Qbiogene*) as described by the manufacturer. In brief, DG cDNA was subcloned into the multiple cloning site of pAdTrack-CMV(GFP) (GFP and DG are under separate CMV promoters producing two separate proteins), linearized using PmeI, and cotransfected with pAdEasy-1 into BJ5183, an electrocompetent E.coli strain.

Recombinants (AdDG/GFP) were screened by colony size and confirmed by restriction digests. They were then linearized using PacI, purified, and transfected into HEK293 cells using Lipofectamine reagent (*Invitrogen*). Adenovirus production was observed by plaque formation and by GFP fluorescence. Viral particles were isolated from cellular lysates and amplified through several rounds of infections in HEK293 cells. Titers were determined by $TCID_{50}$ infection test as described by the manufacturer (*Qbiogene*). For DG expression, ES cells were grown at low confluence, infected with 10_3 plaque forming units/mL (MOI 5) of control AdGFP or of AdDG/GFP for 18 hrs in growth medium. Infection efficiency was monitored by GFP reporter gene expression and was maximal 2 days post-infection. At this point, transferrin uptake was assayed

Immunohistochemistry

Three-month-old male mice (strain C57BL/6) were anaesthetized using xylazine (2mg/ml, *Bayer Inc.*) and ketamine hydrochloride (15 mg/ml, *Ayerst veterinary Lab.*). After anesthesia mice were perfused intraventricularly with PBS followed by 4% paraformaldehyde. Whole eyes were dissected from the animals and post-fixed overnight in 4% paraformaldehyde followed by cryopreservation in 30% sucrose. Eyes were then frozen in Tissue-Tek O.C.T. compound (*Sakura*

Finetek U.S.A.) on crushed dried ice and stored at -80°. Eight μm horizontal sections were cut using a Leica CM3050S cryostat and stored at -20°. Sections were thawed to room temperature, washed with PBS and blocked with 10% horse serum and 0.3% TX-100 in PBS for 1 hr prior to immunostaining. The retinal sections were incubated 1.5 hrs in blocking buffer containing both Hudy-1 and β-DG antiserum. Incubation with secondary antibodies was done in blocking buffer containing both RITC-conjugated donkey anti-rabbit antiserum and FITC-conjugated donkey anti-mouse immunoglobulins. Sections were washed 3 times with PBS after both primary and secondary antibody incubations, mounted in immunofloure mounting medium (*ICN*) and visualized using a Leica TCSNTSP confocal microscope.

Results

Identification of dynamin 1 as a β-DG associated protein in brain

Hippocampal homogenates were extracted directly with 1% sodium deoxycholate (pH9.0) and 0.5% TX-100. This effectively solubilizes DG as well as most pre- and post-synaptic proteins (44). Immunoaffinity columns conjugated with antisera to β-DG, non-immune rabbit IgGs (control), or BSA (control) were equilibrated with the extracts, washed extensively and eluted first at low and then at high pH (Methods). Following SDS-PAGE analysis of the eluates and Coomassie blue staining, several protein bands were evident at 43 kDa and ~100 kDa (Fig, 1A) that bound specifically to β-DG antibody columns. The 43 kDa band was confirmed to contain β-DG in western blots (Fig. 1B). The ~100 kDa band was cut out, digested with trypsin and subjected to LC/MS-MS analysis (Montreal Proteomics Network). This yielded 21 tryptic peptides whose sequences matched that of rat dynamin 1 (gi: 118966; 97 kDa) with the peptides covering 25% of the sequence of dynamin 1. The 55 kDa band yielded peptides matching to the IgG heavy chain. Peptides from the ~66 kDa band matched to Hsc70 (not shown). Consistent with the MS results, western blotting indicated that dynamin 1 was enriched along, with α-DG, in brain extracts subjected to immunoaffinity chromatography (Fig. 1B). Since dynamin is a relatively abundant cytosolic protein and β-DG is a transmembrane protein, we sought to determine

the amount of dynamin 1 bound to β-DG. β-DG could be immunodepleted from brain extracts, although a significant amount of dynamin 1 remained in the supernatant (Fig. 2A, B). No immunoprecipitation of either protein with control IgG (Fig. 2B) was observed. These results suggest that there is a pool of dynamin 1 tightly associated with β-DG, and a pool of unbound dynamin 1.

Detection of other DG-associated proteins in brain

To further characterize the β–DG-dynamin complex in the CNS we used antibodies to several DG-associated proteins in muscle. Immunoaffinity-purified fractions of β-DG from brain were western blotted with two monoclonal antibodies (mAb IIH6 and 1B7), that detect differentially glycosylated forms of α-DG (25, 40). MAb IIH6, that recognizes larger and more heavily glycosylated forms, detected a band of α-DG enriched in the affinity-purified fraction (lane 2 of Fig. 3A), consistent with our previous data (28). MAb 1B7 that recognizes smaller and, hence, hypoglycosylated forms of α-DG (25) also detected an enriched band with lower molecular weight (lane 3 of Fig. 3A). Thus the brain contains complexes of β-DG and α-DG with different levels of glycosylation that may affect ligand binding of the α subunit (2, 25).

Grb2 is an SH2-SH3 containing adapter protein that is associated with dynamin in brain through its SH3 domains (45, 46). In muscle Grb2 has also been shown to associate with β-DG through its SH3 domain (47, 48). We therefore asked whether Grb2 could be part of a complex with DG and dynamin 1 in brain. All three proteins (DG, dynamin and Grb2) were immunoprecipitated from the synaptosomes using antibodies against β-DG (Fig. 3B), and in the immunoaffinity-purified fractions from brain (data not shown). Taken together these data indicate that the brain contains a complex of α-/β-DG with dynamin 1 and Grb2.

Although Grb2 has the potential to mediate binding to dynamin, other data indicate that SH2-SH3 domain-containing proteins such as amphiphysin (49, 50) and endophilin (51, 52) preferentially bind to proline-rich domains of dynamin (53). This suggested that dynamin might bind directly to β-DG. To test this, brain dynamin was immunoprecipitated with Mab Hudy-1, fractionated electrophoretically and transferred to PVDF membranes. The PVDF membranes were overlaid with a recombinant protein encompassing the entire cytoplasmic domain of β-DG fused to GST (GST-β-DGcyto). We found that GST-βDGcyto but not GST alone bound to bands containing dynamin (Fig. 4A). Thus there appears to be a direct interaction of dynamin with the intracellular region of DG.

Interestingly, β-DG immunoaffinity purification (Fig. 3, lanes 6, 7) revealed no detectable association of DG with amphiphysin suggesting that binding of Grb2 directly or via its SH3 domain occludes binding of amphiphysin in dynamin associated with DG.

Association and colocalization of DG and dynamin in the outer plexiform layer of the retina

DG has been localized to synaptic regions in the brain (40, 54, 55) as well as at GABAergic synapses in culture by immunofluorescence microscopy (29, 30). It is challenging to localize antigens within most regions of the CNS so as to ascertain whether they are synaptically localized without resorting to EM. In the retina, however, rod and cone photoreceptors synapse on bipolar and horizontal cells and form so-called “ribbon” synapses where the presynaptic ribbon is readily detectable by light microscopy as plaques (cones) or large puncta (rods) running through the outer plexiform layer (54). Both α- and β-DG have been shown to be expressed in the outer plexiform layer of retina (27, 56, 57), where they are thought to form a complex with dystrophin and β-dystrobrevin (58). To extend these studies we determined whether β-DG is associated with dynamin in the retina. As in the brain, both dynamin and β-DG were co-precipitated (Fig. 5A) with antisera to β-DG. Conversely immunoprecipitation with an antibody to

dynamin (Fig. 5B) precipitated β-DG and Grb2 together with dynamin. The amount of β-DG precipitated was less than that in Fig. 5A, consistent with previous data (Fig. 2A) that there is a pool of dynamin unbound to β-DG. Immunohistochemically β-DG immunoreactivity (Fig. 5C, arrowheads) was found in puncta and bands in the outer plexiform layer of retina characteristic of rod and cone photoreceptor terminals (27, 39). Dynamin immunoreactivity (Fig.5C, arrowhead) was also restricted largely to the outer plexiform layer of the retina and, as expected; its distribution is more diffuse than that of β-DG. Double labeling immunofluorescence showed, however, that essentially all photoreceptor synapses labeled with antisera to β-DG were also positive for dynamin (Fig. 5C, merge). Grb2 was expressed diffusely in virtually all cells of the retina, and, while it overlaped with the distribution of β-DG and dynamin, it is not obvious that this is meaningful (data not shown). Taken together, these data suggest that in the retina β-DG, dynamin and possibly Grb2 form a complex in the outer plexiform layer and this complex is presynaptically localized.

DG in endocytosis

Previously, we have studied DG function in differentiated ES cells wherein both *dag1* alleles had been disrupted by homologous recombination (11, 15, 21). Here we first generated mixed cultures of differentiated cells to monitor by

immunofluorescence the effect of deletion of *dag1* on dynamin-mediated endocytosis. Differentiated ES cells yield a variety of cell types, including fibroblastic cells that quickly migrate out of the embryoid body and are easily visualized as well-spread cells on the periphery of the cell mass. In addition, we have established lines of these fibroblastic cells that permit biochemical analysis. Unfortunately, we have not been able to isolate neural stem cells for similar studies nor do we have mice null for *dag1* in the CNS from which we could make primary neuronal cultures (19). Nevertheless, constitutive endocytosis of transferrin is essentially the same in neuronal and non-neuronal cells and shares many features with regulated vesicular endocytosis in nerve terminals, including a requirement for dynamin (37).

Fibroblastic cells differentiated from wild-type ES cells express both ⟨-DG (data not shown) and β-DG (Fig. 6C and G) on the surface of the plasma membrane, preferentially in regions called membrane ruffles (Fig. 6A). Ruffles also contain dynamin, β-DG and cortactin (Fig.6). Thus DG in these cells might be involved in endocytosis, which frequently occurs at membrane ruffles, and/or could regulate the actin cytoskeleton, a function also attributed to dynamin (59). To assess this further, wild-type or DG-null cells were differentiated from embryoid bodies, and incubated with RITC-labeled transferrin. In mixed cultures

both wild-type and DG-null fibroblastic cells take up transferrin, as demonstrated by the presence of many small, fluorescent puncta visible throughout the thickness of the cells (Fig. 7). Wild-type cells showed both submembranous and cytoplasmic localization of labeled transferrin, indicative of uptake into early and late endosomes (Fig. 7A and C). Few cells had perinuclear staining. In contrast, in DG-null cells transferrin labeling was less frequently concentrated in the region of plasma membrane and most, if not all cells had intense labeling in the cytoplasm especially around the nucleus (Fig. 7D). We quantified the area occupied by transferrin labeling in wild-type and DG-null cells (methods). DG-null cells show a significant, 2.25-fold increase ($P<0.05$), in transferrin uptake (Fig. 7E) when compared with wild-type cells. To confirm that DG is associated with dynamin we isolated and expanded fibroblastic cells that appeared essentially identical to those which migrate from embryoid bodies (Fig. 6 and 7). Transferrin uptake by these cell lines was the same as that of fibroblastic cells in mixed cultures (Fig. 8A and B). Furthermore, immunoprecipitation from wild type cells showed that a portion of dynamin is associated with β-DG (Fig. 8C, lane wt of upper panel under IP). There was no DG detectable in DG-null cells (Fig. 8C, Pre-IP) and no dynamin was precipitated from these cells (Fig. 8C, IP). Taken together, these observations indicate that β-DG interacts with dynamin at

membrane ruffles, and suggests a role for DG in regulating endocytosis of transferrin.

To confirm that the difference in endocytosis between wild-type and DG-null cells was due to DG, we re-introduced DG into the DG-null fibroblastic cells by infection with an adenovirus containing DG/GFP. In these experiments, GFP expression driven by a separate CMV promoter served as a reporter of successful infection. In DG-null cells infected with the DG/GFP virus DG is expressed in the plasma membrane and in ruffles (arrowhead, Fig. 9A, c') similar to the pattern in wild-type cells (Fig. 6). There was no DG expression seen in cells infected with the control adenovirus (GFP) (Fig. 9A, b'). To determine whether transferrin uptake was restored to wild-type levels in infected cells, we incubated wild-type and DG-null cells with rhodamine conjugated transferrin for 15 min 24 hrs after adenovirus infection (Fig. 9B). In uninfected cells transferrin uptake was significantly greater in DG null cells than in wild-type cells, as noted previously (Figs. 7and 8). In DG null cells infected with DG/GFP there was a decrease in transferrin uptake when compared with DG null cells infected with GFP alone. The decrease was equivalent to that seen in wild-type cells uninfected or infected with GFP. DG-null cells infected with virus containing DG/GFP (DG-null:DG/GFP) had about a 2-fold reduction in transferring uptake

compared to DG-null cells or null cells infected with GFP ($P<0.05$), but no difference compared to wild-type cells or wild-type cells infected with GFP ($P>0.05$). Wild-type cells infected with GFP alone have the same transferrin uptake as non-infected wild-type cells ($P>0.05$).

Figures

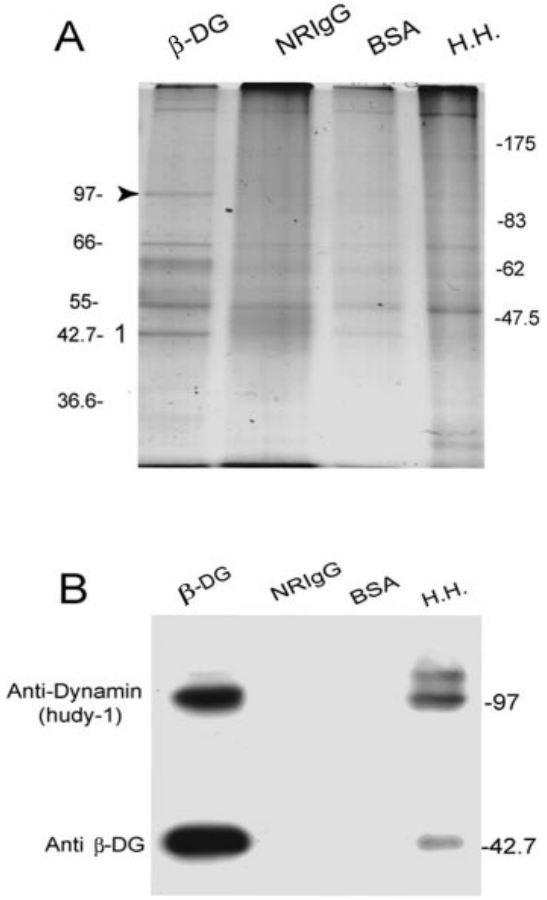
A
β-DG
NRIgG
BSA
H.H.
-175
97-
-83
66-
-62
55-
-47.5
42.7-
1
36.6-
B
β-DG
NRIgG
BSA
H.H.
Anti-Dynamin
(hudy-1)
-97
Anti β-DG
-42.7

Figure 1: Immunoaffinity purification of dystroglycan-associated proteins from brain.

A: Equivalent volumes of eluate (Methods) from anti β-DG antibody affinity column (β-DG), non-immune rabbit IgG column (NRIgG), BSA column (BSA), and hippocampal homogenates (H.H., 2⌈g.) were loaded, and subjected to SDS-PAGE and stained with Coomassie blue. Two sets of molecular weight markers (36.6-175 kDa) are shown. The arrowhead points to a ~100 kDa band seen only in eluates from the β-DG antibody affinity column. Band 1 is β-DG (43 kDa). The band at 55 kDa is the IgG heavy chain and the band at ~70 kDa is Hsc70 (data not shown). The band at ~100 kDa was identified as dynamin 1 (97 kDa) by LC/MS-MS. B: Column eluates (5%) from 5 mg of hippocampal homogenates were collected, electrophoresed and western blotted with antibodies to dynamin and β-DG to confirm the data in A. Equivalent amounts of eluate from the NRIgG and BSA columns served as controls. The antibodies used as probes are noted on the left and molecular weight markers (kDa) are on the right. Image A or B is from a single gel.

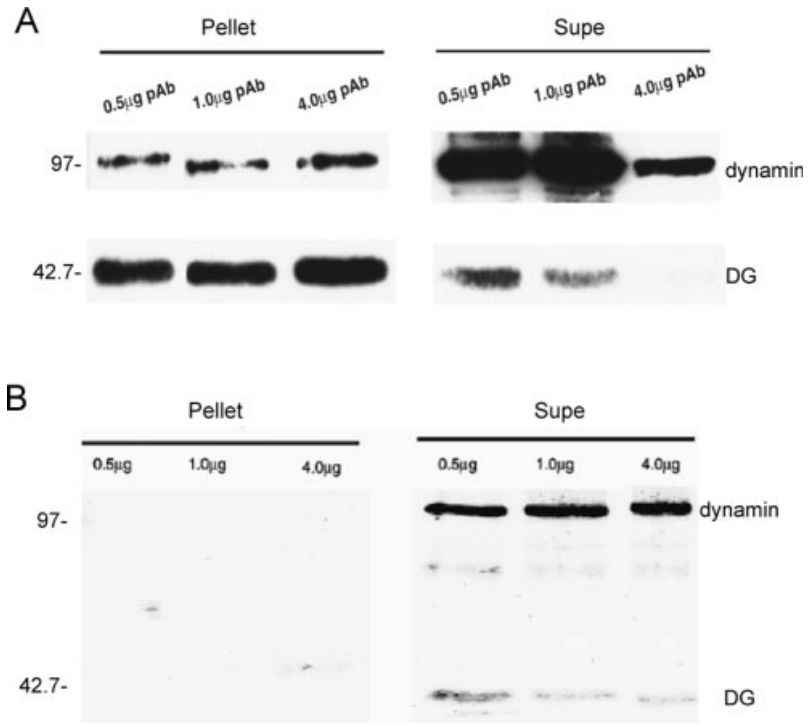
A
Pellet
Supe
0.5μg pAb
1.0μg pAb
4.0μg pAb
0.5μg pAb
1.0μg pAb
4.0μg pAb
97-
dynamin
42.7-
DG
B
Pellet
Supe
0.5μg
1.0μg
4.0μg
0.5μg
1.0μg
4.0μg
97-
dynamin
42.7-
DG

Figure 2: Immunodepletion of β-DG from rat brain extracts.

60 μg of rat brain homogenate was immunoprecipitated with 0.5 μg, 1.0 μg or 4.0 μg of anti β-DG antiserum (pAb) coupled to agarose beads (A) or with non-immune rabbit IgG coupled to agarose beads (B). The beads were washed extensively (Methods) with solubilization buffer containing 5 mM EDTA and 0.5M NaCl, and the precipitated proteins (Pellet) as well as the supernatants (Supe) were analyzed by western blotting with antibodies to dynamin and β-DG. With increasing amounts of β-DG antiserum (A) there is an increase in the amount of both β-DG and dynamin in the pellet and corresponding reduction in the Supe. At 4.0 μg of antiserum β-DG is entirely depleted from the Supe but a prominent band of dynamin remains. (B) Immunoprecipitations with agarose beads coupled to non-immune rabbit IgG produced no precipitation of β-DG or dynamin (Pellet) which remained in the Supe. The lanes in B contain 30% of the supernatants. Lanes in A or B are grouped from a single western blot that was scanned and computer reconstructed under the same conditions.

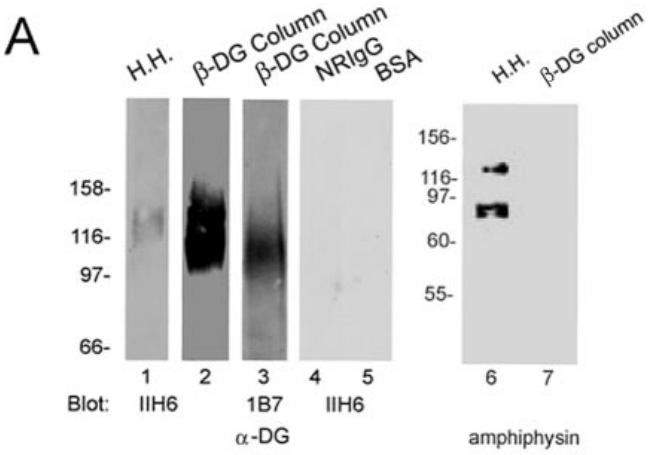
A
H.H.
β-DG Column
β-DG Column
NRIgG
BSA
H.H.
β-DG column
158-
116-
97-
66-
156-
116-
97-
60-
55-
1
2
3
4
5
6
7
Blot:
IIH6
1B7
IIH6
α-DG
amphiphysin

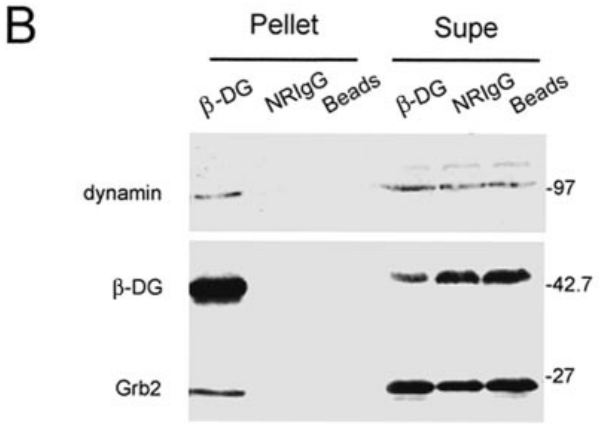
B
Pellet
Supe
β-DG
NRIgG
Beads
β-DG
NRIgG
Beads
dynamin
-97
β-DG
-42.7
Grb2
-27

Figure 3: α-DG, Grb2 and β-DG co-purification from brain.

A: Five mgs of hippocampal homogenate were subjected to immunoaffinity purification and 10% of the eluate volume was electrophoresed and blotted with α-DG antibodies IIH6 (lane 2) and 1B7 (lane 3). An equivalent volume of eluate from columns with normal rabbit IgG (lane 4) or BSA (lane 5) served as controls. 35 μg of hippocampal homogenate (H.H.) (lane 1) was loaded as positive control. Note that 〈-DG is recognized by both mAbs IIH6 and 1B7, moreover, the forms recognized by mAb 1B7 are smaller reflecting hypoglycosylation (Leschziner et al., 2000). Antiserum (1874) detected amphiphysin I and II (Ramjaun et al., 1997) in the homogenates (lane 6), but no amphiphysin in the β-DG column eluates (lane 7). B: β-DG, Grb2 and dynamin are associated in synaptosomes. Solubilized synaptosomes (Method) were immunoprecipitated with an antibody to β-DG, and the precipitated proteins (Pellet) and the supernatant (Supe) were subjected to SDS-PAGE and probed with antibodies to β-DG, Grb2 and dynamin. Both Grb2 and dynamin are co-immunoprecipitated with β-DG (lane β-DG, Pellet). The non-immune rabbit IgG (NRIgG) and agarose beads alone were used as controls. Antibodies used for western blots are indicated (left) and the position of molecular markers are shown (right). Lanes 1-5, lanes 6-7 and lanes in B are grouped from a single western blot that was scanned and computer reconstructed under the same conditions.

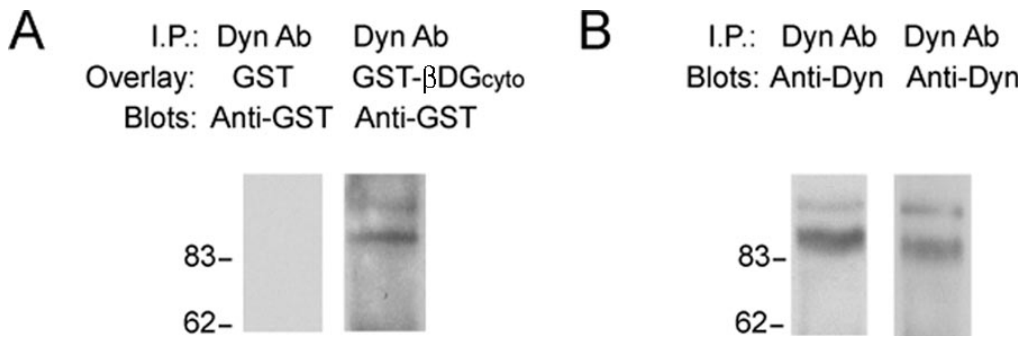
A
I.P.: Dyn Ab Dyn Ab
Overlay: GST GST-βDGcyto
Blots: Anti-GST Anti-GST
83–
62–
B
I.P.: Dyn Ab Dyn Ab
Blots: Anti-Dyn Anti-Dyn
83–
62–

Figure 4: The intracellular portion of β-DG interacts with dynamin.

A: Dynamin was immunoprecipitated (I.P.) from 300 μg of brain synaptosomes with 6 μg of dynamin antibodies, subjected to SDS-PAGE in 4-20% acrylamide gradient gel (*Bio-Rad*) and transferred to a PVDF membrane. The membranes were incubated with 20 ⌈μg/ml of recombinant GST-β-DG_{cyto} (right lane) or GST alone (left lane) overnight, washed and blotted with a HRP-conjugated anti-GST antibody. GST-β-DG binds to two bands that react with antibodies to dynamin (right lane, B). The two bands either represent a dynamin doublet (86, 87) or possibly a proteolytic product of dynamin. Neither of these bands reacted with antibodies to GST (left lane, A). B: Membranes were subsequently stripped and re-probed with anti-dynamin antibodies (Hudy-1). Lanes in A or B are from one single gel and membrane.

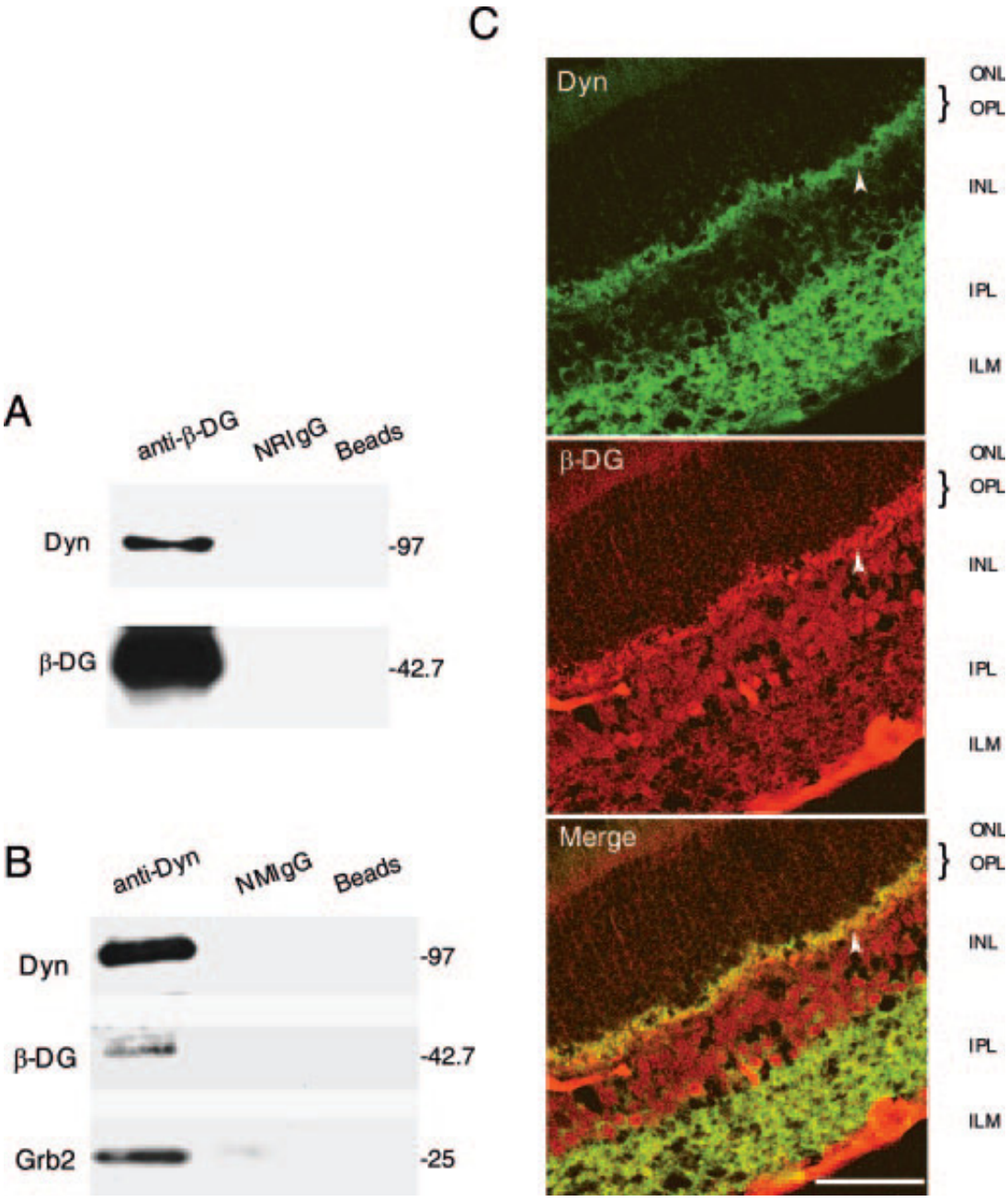
A
anti-β-DG
NRIgG
Beads
Dyn
-97
β-DG
-42.7
B
anti-Dyn
NMIgG
Beads
Dyn
-97
β-DG
-42.7
Grb2
-25
C
Dyn
β-DG
Merge
ONL
OPL
INL
IPL
ILM

Figure 5: β-DG, dynamin 1 and Grb2 are associated in the retina.

β-DG was immunoprecipitated from rat retinal homogenates with antisera to β-DG (anti-β-DG) (A), or antibody to dynamin (Hudy-1, anti-Dyn) (B). In A the controls included normal rabbit IgG (NRIgG), and agarose beads alone (Beads), and in B, normal mouse IgG (NMIgG) and agarose beads alone (Beads). The precipitated proteins were subjected to SDS-PAGE and probed with antibodies (panel A and B, left) to dynamin (Dyn), β-DG (β-DG) or Grb2. The positions of molecular weight markers are shown on the right. C: Immunohistochemistry in the mouse retina shows that dynamin 1 (Top) is localized in the outer plexiform layer (OPL) and inner plexiform layer (IPL). β-DG (C, middle) is localized in outer plexiform layer (OPL), inner limiting membrane (ILM) and blood vessels. In the outer plexiform layer (OPL) puncta of β-DG and dynamin 1 are often colocalized as shown by the merged image (C, yellow). Arrowheads point to one example of puncta or ribbon synapse. ONL: Outer nuclear layer. OPL: Outer plexiform layer. INL: Inner nuclear layer. IPL: Inner plexiform layer. ILM: Inner limiting membrane. Lanes in A or B were grouped from single gel and under same exposure. Bar, 50 microns.

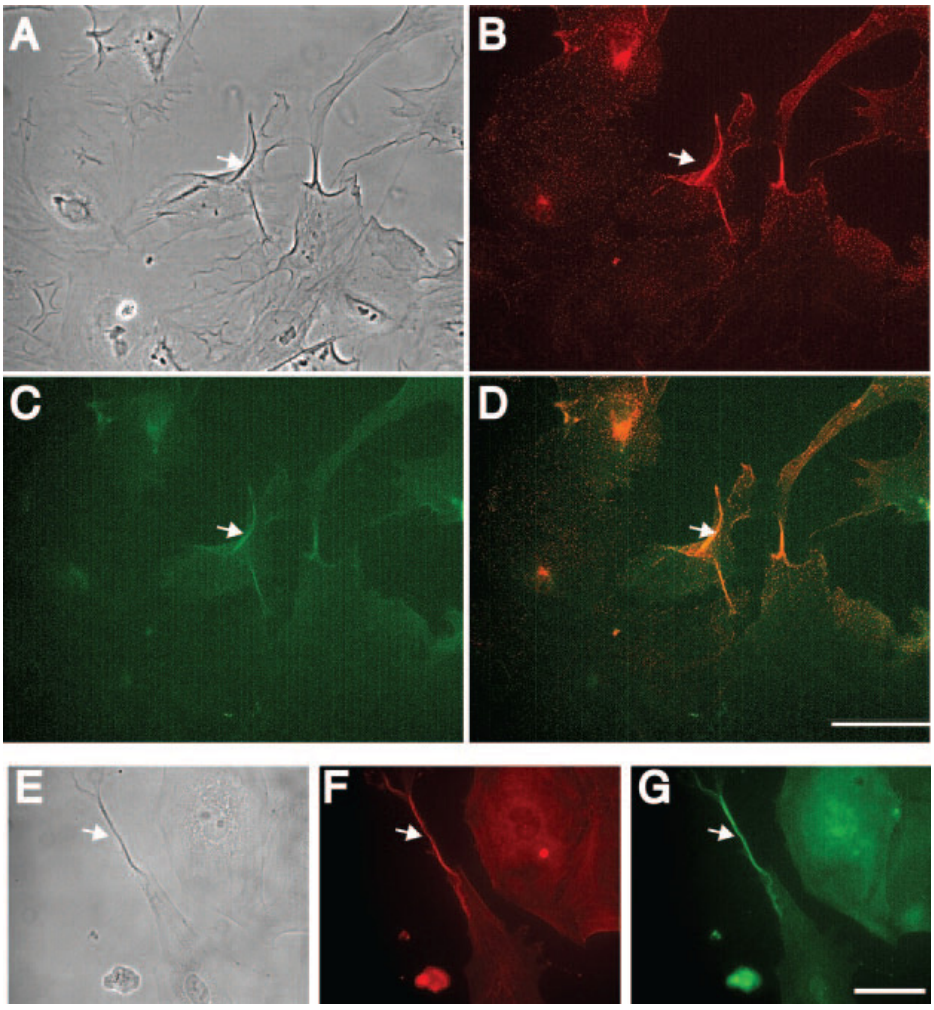
A
B
C
D
E
F
G

Figure 6: DG, dynamin and cortactin are co-localized at membrane ruffles of fibroblastic cells.

A and E: Phase images of fibroblastic cells derived from wild type ES cells. The arrow shows a typical membrane ruffle. B, C, F and G: Immunolocalization of dynamin (B, Hudy-1), β-DG (C, G) and cortactin (F) show that all three proteins are concentrated in ruffles. D: The merged image of B and C shows DG and dynamin in ruffles. Bars, 50 microns.

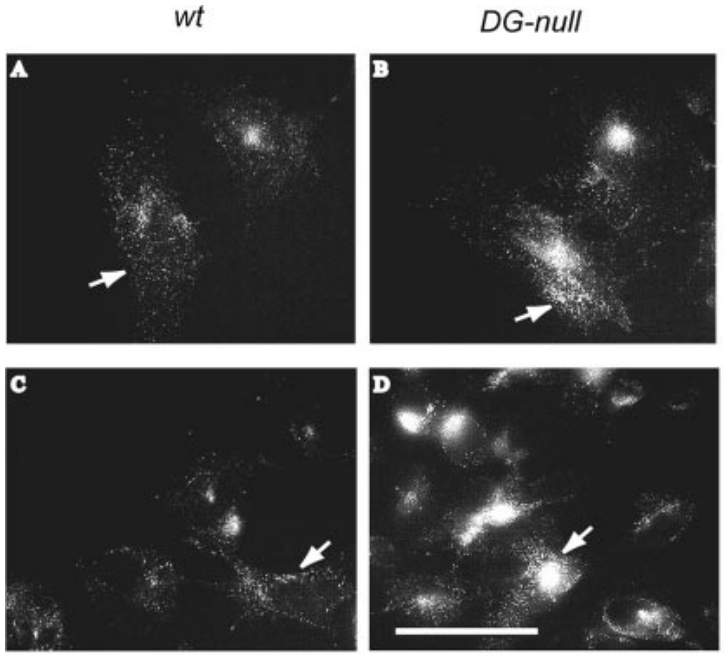
wt
DG-null
A
B
C
D

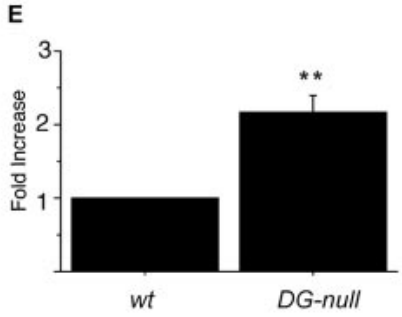
E
3
2
1
Fold Increase
**
wt
DG-null

Figure 7: DG regulates endocytosis in differentiated ES cells in culture.

Uptake of rhodamine-labeled transferrin was studied in fibroblastic cells on the periphery of adherent embryoid bodies derived from wild-type (wt) (A and C) and DG-null (B and D) ES cells. Arrowheads point to typical labeled cells. Fluorescent puncta were observed in the cytoplasm and around the nuclei of DG-null cells (B, D), but this was substantially sparser and less intense than in the wild type cells (A, C). E shows quantification of the area occupied by transferrin labeling (Methods) in (A, C and B, D). Error bars show the S.E.M. Bar, 50 microns.

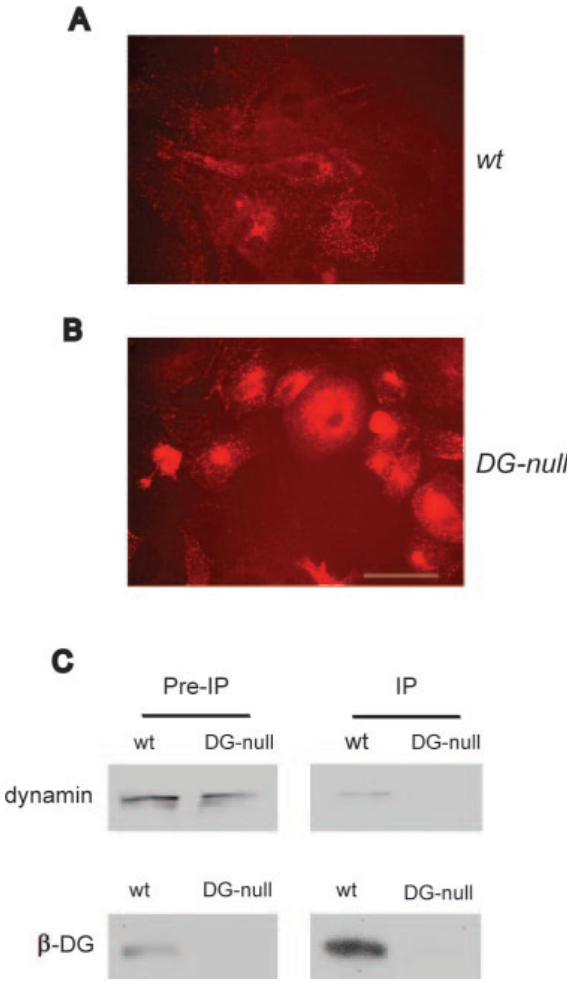
A
wt
B
DG-null
C
Pre-IP
IP
wt
DG-null
wt
DG-null
dynamin
wt
DG-null
wt
DG-null
β-DG

Figure 8: β-DG is associated with dynamin in fibroblastic cells isolated from differentiated ES cells.

A and B show a prominent increase in transferrin uptake (as in Fig.7) in DG-null fibroblasts (DG-null, B) compared with wild-type (wt) fibroblastic cells (wt, A) when cells are incubated with transferrin at 37° for 15 min before fixation. C: Immunoprecipitation (IP) of β–DG-dynamin complex from fibroblastic cells. Fibroblastic cell lysates from both wt and DG-null were electrophoresed, and blotted with antibody to dynamin (upper panel, Pre-IP) and β-DG (lower panel, Pre-IP). Antiserum to β-DG was used for immunoprecipitation from both fibroblastic cell lysates. The immunoprecipitated proteins were subjected to SDS-PAGE and probed with antibodies to dynamin (upper panel, IP) and β-DG (lower panel, IP). Note dynamin was co-immunoprecipitated from wt cell lysates (lane wt, upper panel, IP) but not DG-null cell lysates (lane DG-null, upper panel, IP). All images in C were grouped from a single gel and composed into a figure under uniform conditions of exposure. Bar, 50 microns.

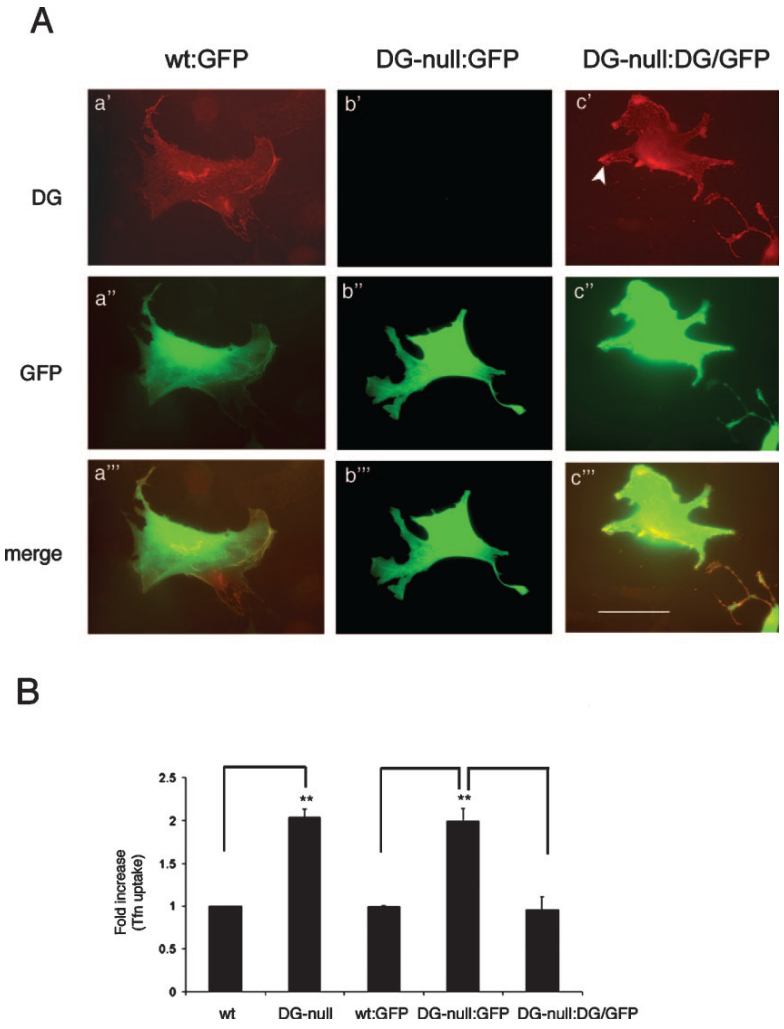
A
wt:GFP
DG-null:GFP
DG-null:DG/GFP
DG
GFP
merge
a'
b'
c'
a''
b''
c''
a'''
b'''
c'''
B
Fold increase (Tfn uptake)
2.5
2
1.5
1
0.5
0
**
**
wt
DG-null
wt:GFP
DG-null:GFP
DG-null:DG/GFP

Figure 9: Expression of DG in DG-null cells restores normal levels of transferrin uptake.

A: Fibroblasts derived from both wild-type (wt) (a'-a''') and DG-null (b'-b''' and c'-c''') ES cells were infected with an adenovirus containing GFP (a'-a''', b'-b''') or DG/GFP (c'-c'''), and stained with antiserum to DG followed by RITC-labeled secondary antibody(a', b', c'). DG was observed at the cell surface and ruffles in DG-null cells infected with DG/GFP (arrowhead, c'), similar to labeling in wt cells (Fig. 6) or wt cells infected with GFP (a'). B: Rhodamine-conjugated transferrin (Tfn) was incubated with fibroblastic cells for 15 min 24hr after infection with an adenovirus containing GFP or DG/GFP. DG-null cells infected with virus containing DG/GFP (DG-null:DG/GFP) had decreased Tfn uptake compared with non-infected (DG-null) cells or cells infected with GFP alone (DG-null:GFP). The level of uptake was essentially the same as in wt cells infected with GFP (wt:GFP) or wt cells without viral infection (wt). Fluorescence was quantified (Methods) in cells 25-35 um in diameter to control for variation in cell size. Transferrin fluorescence is often concentrated in a portion of the cell so the full size of the cell was determined from GFP fluorescence in infected cells (A) or by phase imaging of uninfected cells. More than 20 cells were quantified for each treatment and fluorescence intensity was normalized to that in wild-type cells. Bar in A is 50 um.

Discussion

Our results reveal that a complex of β-DG, α-DG, dynamin 1, and Grb2, is found in presynaptic terminals of CNS neurons. This complex is also present in non-neuronal cells where it appears to regulate endocytosis. Several lines of evidence support this claim. First, immunopurification of β-DG-associated proteins followed by SDS-PAGE yielded a 97 kDa band, whose sequence by LC/MS-MS resulted in 21 peptides that covered 25% of the sequence of rat dynamin 1. Sixteen of these peptides were unique for dynamin 1 and five were shared with dynamin 2 but not dynamin 3, both of which are also expressed in the CNS (60). This suggests that dynamin 1 is the major dynamin isoform associated with DG. Second, the association of dynamin was confirmed by immunoprecipitation and extended to show interaction of β-DG with α-DG and Grb2. Other immunoprecipitation data indicate that only a subset of dynamin is associated with β-DG in brain and retina. In an overlay assay, dynamin purified from brain bound directly to the intracellular portion of recombinant β-DG. Third, β-DG is associated and immunohistochemically colocalized with dynamin at ribbon synapses within the outer plexiform layer of the retina. Fourth, in fibroblast-like cells in culture DG is associated with dynamin at cortactin-rich membrane ruffles that are sites of endocytosis (61, 62). Finally, ES cells null for DG had a greater uptake of transferrin, a dynamin mediated process, than that of

wild type cells. Expression of full length DG in DG-null ES cells restored transferrin endocytosis to levels seen in wild-type cells.

Dystroglycan is found in nerve terminals in the CNS

DG is concentrated at some central (28, 29) and peripheral synapses (8, 25, 26). At neuromuscular junctions DG binds to perlecan (10, 11) and contributes to the assembly of acetylcholinesterase (11) in the synaptic basement membrane. In addition, DG participates in the aggregation of acetylcholine receptors (11, 34) into stable plaques within the myotube membrane. In the hippocampus DG is involved in LTP (19) where it has also been reported to function postsynaptically. In our studies immunoaffinity chromatography identified dynamin 1, a neuron-specific form of dynamin (60), as the dominant dynamin isoform associated with DG. Dynamin 2 is also expressed in the CNS and is recognized by mAb Hudy-1 (41). As a result immunoprecipitations with this mAb from brain homogenates may contain DG that is associated with dynamin 2. However, in synaptosomes DG is likely bound to dynamin 1, the dominant isoform in neurons. Kroger and colleagues (27,39) have localized DG in the vicinity of synaptic ribbons in the nerve terminals of photoreceptors in the outer plexiform layer of the retina (27, 39) and we have found that DG and dynamin colocalize in ribbon synapses in the outer plexiform

layer of the retina (Fig. 5) that are readily detectable by light microscopy (27, 56). We conclude that DG is localized presynaptically where it is associated with dynamin 1.

Interactions of DG-dynamin in the CNS

Blank et al (58) have suggested that α-dystrobrevin and dystrophin are bound to β-DG based on their localization in the retina. Our biochemical and other data indicate that Grb2 and dynamin also interact with the cytoplasmic tail of β-DG. Thus in the CNS β and α-DG appear to be complexed with conventional components found in muscle, such as dystrobrevin, as well as a novel one, dynamin. Grb2 is an SH2-SH3 domain protein that binds to β-DG via either of its SH3 domains (47, 63) but with different affinities (48). Grb2 also binds to dynamin 1 in brain, again via SH3 domain binding to proline-rich motifs (45,46). The N-terminal SH3 domain of Grb2 is essential for binding to dynamin (64). So it is reasonable to think that Grb2 may bind to dynamin with its N-terminal SH3 domain and to DG with C-terminal SH3 domain, to form DG-Grb2-dynamin complex. Other studies indicated that amphiphysin and endophillin rather than Grb2 are the major SH3-domain containing protein that interacts with dynamin at nerve terminals (49, 65). We have not, however, detected amphiphysin in immunoprecipitates of DG that contain dynamin (Fig. 3A). Moreover, our overlay

data (Fig. 4) indicated that DG can interact directly with dynamin and may not require the intercession of Grb2 in-situ. Taken together it appears that DG, Grb2 and dynamin form a complex distinct from dynamin and amphiphysin.

In addition to its intracellular interactions, β-DG also binds to ⟨-DG conferring on the complex the ability to interact with its ligands in the extracellular matrix (32) as well as on other cells (12). For many of its ligands of α-DG binds via its carbohydrate side chain(s) (1) to laminin-like globular motifs (3, 66). Recent data show that aberrant glycosylation of DG in several muscular dystrophies and in the *myd* mouse leads to greatly reduced ligand binding and electroretinograms with altered b-waves indicative of defective synaptic transmission in the outer plexiform layer (20, 31). Agrin, which contains several G domains and binds to DG (6-9), is found within the synaptic cleft in the outer plexiform layer of the retina (67). Moreover, the ability of α-DG to bind ligand appears necessary for normal synaptic function (2, 31). Thus linkage of dynamin to a transmembrane receptorcomplex and possibly to the matrix or cell adhesion molecules (3, 8, 10, 12, 68) may be important in vesicle recycling during synaptic transmission where spatially regulated subdomains of endocytosis and exocytosis are thought to be critical for evoked release of neurotransmitter (69, 70).

Dystroglycan in endocytosis

To assess the biochemical interactions of DG in cells we have resorted to cultured cells that/are null for DG. Unfortunately, we do not have lines of neuronal precursors null for DG, but we do have fibroblastic and epitheliod cells. As a result, we have assayed in fibroblasts dynamin-mediated uptake of transferrin, a constitutive mode of endocytosis which employs many of the same molecules, including dynamin and clathrin, as the tightly regulated release during synaptic transmission (37). We have found that transferrin uptake is significantly greater in cell lines null for DG when compared with wild-type cells (Fig. 7-9). This holds for cells in mixed cultures differentiated from embryoid bodies as well as fibroblastic cell lines established from differentiated ES cells. In the latter instance, dynamin, most likely dynamin 2, is associated with DG (Fig. 8). This complex appears to be concentrated at membrane ruffles which have a high density of transferrin receptors (71) and are also prominent sites of endocytosis (61, 62). Furthermore, Grb 2, that is associated with DG, has been implicated in endocytosis, most notably of the EGF receptor (72-75), but also in the internalization of β-adrenergic receptors in response to insulin (76).

In principle the inhibition of endocytosis by DG could be achieved by a number of mechanisms. Most obviously, DG may decrease the GTPase activity of dynamin, which is essential for its function in endocytosis. This seems unlikely to occur via Grb2 bound to DG since SH3-domain containing proteins are reported to increase the enzymatic activity of dynamin and endocytosis (77-79). It is possible, however, that direct binding of DG to dynamin is inhibitory or that indirect binding via its SH3 domain displaces amphiphysin from a subset of dynamin (Fig. 3A) associated with DG at the cell surface. The SH3 domain protein amphiphysin 1 appears to function in the assembly of dynamin 1 into the ring-like structures around coated pits (53, 80, 81). Conceivably Grb2 localized to the cell surface through DG could compete with amphiphysin or other SH3 domain proteins to inhibit their function in endocytosis and regulate the activity of membrane-associated dynamin (79). Second, anchorage of a pool of dynamin at the membrane via DG may restrict it from movement into active sites of vesicles turnover. This may be the case in photoreceptors where DG is distant from the synaptic ribbon (27). Third, in addition to its mechanochemical role in pinching off vesicles during endocytosis, dynamin can reorganize the cytoskeleton (59, 82) by interacting with several actin-binding proteins including cortactin (59) at membrane ruffles (82). DG itself may then contribute to actin organization. In fact β-DG has been reported to bind directly to actin (83) and to reorganize the actin

cytoskeleton (83, 84). This may be related to observations that the cortical actin cytoskeleton inhibits endocytosis (85). Thus, it is conceivable that the differences seen in endocytosis of wild-type and DG null cells are an indirect manifestation of altered cytoskeletal organization. We have not, however, detected any obvious abnormalities in cell attachment, actin or tubulin distribution in these cell types. Future experiments will be aimed at determining the mechanism of inhibition of endocytosis and whether DG directly inhibits dynamin function. At this point, however, our findings indicate that DG is associated with the GTPase dynamin, and provide evidence that this complex regulates endocytosis. In view of recent work implicating DG in synapse formation/function and in neural development, these observations may contribute to our understanding of the mental retardation associated with Duchenne and several other muscular dystrophies (32).

Acknowledgments

We thank Dr. Peter McPherson for his advice and comments on the manuscript. We also thank our coworkers Waris Shah, Huashan Peng and Mingying Hu for their valuable assistance in this study. Finally, we are grateful to Dr. Alex Bell of the Montreal Proteomics Facility for his invaluable advice.

References

1. Ervasti, J.M., and Campbell, K. P. (1993). *J. Cell Biol.* 122:809-23.

2. Michele, D.E., Barresi, R., Kanagawa, M., Saito, F., Cohn, R.D., Satz, J.S., Dollar, J.,Nishino, I., Kelley, R.I., Somer, H., Straub, V., Mathews, K.D., Moore, S.A., andCampbell, K.P. (2002). *Nature.* 418:417-22.

3. Gee, S.H., Blacher, R.W., Douville, P.J., Provost, P.R., Yurchenco, P.D., andCarbonetto, S. 1993. *J. Biol. Chem.* 268:14972-80.

4. Talts, J.F., Sasaki, T., Miosge, N., Gohring, W., Mann, K., Mayne, R., Timpl, R. (2000).*J. Biol. Chem.* 275:35192-9.

5. Ido, H., Harada, K., Futaki, S., Hayashi, Y., Nishiuchi, R., Natsuka, Y., Li, S., Wada, Y.,Combs, A.C., Ervasti, J.M., Sekiguchi, K. (2004). *J. Biol. Chem.* 279:10946-54.

6. Bowe, M.A., Deyst, K.A., Leszyk, J.D., Fallon, J.R. (1994). *Neuron.* 12:1173-80.

7. Campanelli, J.T., Roberds, S.L., Campbell, K.P., Scheller, S.H. (1994). *Cell.* 77:663-74.

8. Gee, S.H., Montanaro, F., Lindenbaum, M.H., Carbonetto, S. (1994). *Cell.* 77:675-86.

9. Sugiyama, J., Bowen, D.C., Hall, Z.W. (1994). *Neuron.* 13:103-15.

10. Peng, H.B., Ali, A.A., Daggett, D.F., Rauvala, H., Hassell, J.R., Smalheiser, N.R.(1998). *Cell Adhes. Commun.* 5:475-89.

11. Jacobson, C., Cote, P.D., Rossi, S.G., Rotundo, R.L., and Carbonetto, S. (2001). *J. Cell Biol.* 152:435-450.

12. Sugita, S., Saito, F., Tang, J., Satz, J., Campbell, K.P., Sudhof, T.C. (2001). *J. Cell Biol.* 154:435-445.

13. Winder, S.J. (2001). *Trends Biochem. Sci.* 26:118-24.

14. Durbeej, M., and Campbell, K.P. (2002). *Curr. Opin. Genet. Dev.* 12:349-61.

15. Côté, P.D., Moukhles, H., Lindenbaum, M., Carbonetto, S. (1999). *Nat. Genet* 23:338-342.

16. Cohn, R.D., Henry, M.D., Michele, D.E., Barresi, R., Saito, F., Moore, S.A., Flanagan, J.D., Skwarchuk, M.W., Robbins, M.E., Mendell, J.R., Williamson, R.A., Campbell, K.P. (2002). *Cell.* 110:639-48.

17. Durbeej, M., Henry, M.D., Campbell, K.P. (1998). *Curr. Opin. Cell Biol.* 10:594-601.

18. Williamson, R.A., Henry, M.D., Daniels, K.J., Hrstka, R.F., Lee, J.C., Sunada, Y.,Ibraghimov-Beskrovnaya, O., Campbell, K.P. (1997). *Hum. Mol. Genet.* 6: 831-841.

19. Moore, S., Saito, F., Chen, J., Michele, D.E. Henry, M.D., Messing, A., Cohn, R.D.,Ross-Barta, S.E., Westra, S., Williamson, R.A., Hoshi, T., Campbell, K.P. (2002). *Nature.*418:422-425.

20. Holzfeind, P.J., Grewal, P.K., Reitsamer, H.A., Kechvar, J., Lassmann, H., Hoeger, H.,Hewitt, J.E., Bittner, R.E. (2002). *Hum. Mol. Genet.* 11:2673-2687.

21. Li, S., Harrison, D., Carbonetto, S., Fassler, R., Smyth, N., Edgar, D., Yurchenco, P.D.(2002). *J. Cell Biol.*157:1279-1290.

22. Deng, W.M., Schneider, M., Frock, R., Castillejo-Lopez, C., Gaman, E.A.,Baumgartner, S., Ruohola-Baker, H. (2003). *Development*. 130:173-84.

23. Tian, M., Jacobson, C., Gee, S.H., Campbell, K.P., Carbonetto, S., Jucker, M. (1996).*Eur. J. Neurosci.* 8:2739-2747.

24. Cohen, M.W., Jacobson, C., Godfrey, E.W., Campbell, K.P., Carbonetto, S. (1995). *J.Cell Biol.* 129:1093-101.

25. Leschziner, A., Moukhles, H., Lindenbaum, M., Gee, S.H., Butterworth, J., Campbell,K.P., Carbonetto, S. (2000). *J. Neurochem.* 74:70-80.

26. Gingras, J., and Ferns, M. (2001). *J. Neurobiol.* 48:228-42.

27. Koulen, P., Blank, M., and Kroger, S. (1998). *J. Neurosci. Res.* 51:735-747.

28. Moukhles, H., and Carbonetto, S. (2001). *J. Neurochem.* 78:824-34.

29. Levi, S., Grady, R.M., Henry, M.D., Campbell, K.P., Sanes, J.R., and Craig, A.M.(2002). *J. Neurosci.* 22:4274-4285.

30. Brunig, I., Suter, A., Knuesel, I., Luscher, B., and Fritschy, J.M. (2002). *J. Neurosci.* 22:4805-13.

31. Grewal, P.K., Holzfeind, P.J., Bittner, R.E., and Hewitt, J.E. (2001). *Nat. Genet.*28:151-4.

32. Montanaro, F., and Carbonetto, S. (2003). *Neuron.* 37:193-6.

33. Kanagawa, M., Saito, F. , Kunz, S., Yoshida-Moriguchi, T., Barresi, R., Kobayashi,Y.M., Muschler, J., Dumanski, J.P., Michele, D.E., Oldstone, M.B., and Campbell, K.P.(2004). *Cell.* 117:953-64.

34. Grady, R.M., Zhou, H., Cunningham, J.M., Henry, M.D., Campbell, K.P., and Sanes,J.R. (2000). *Neuron.* 25:279-293.

35. Sherman, D.L., Fabrizi, C., Gillespie, C.S., and Brophy, P.J. (2001). *Neuron.*30:677-87.

36. D'Hondt, K., Heese-Peck, A., and Riezman, H. (2000). *Annu. Rev. Genet.* 34:255-295.

37. Jarousse, N., and Kelly, R.B. (2001). *Curr. Opin. Cell Biol.* 13:461-9.

38. Praefcke, G.J., and McMahon, H.T. (2004).*Nat. Rev. Mol. Cell Biol.* 5:133-47.

39. Blank, M., Koulen, P., Blake, D.J., and Kroger, S. (1999). *Eur. J. Neurosci.*11:2121-2133.

40. Moukhles, H., Roque, R., and Carbonetto, S. (2000). *J. Comp. Neurol.* 420:182-94.

41. Damke, H., Baba, T., Warnock, D.E., and Schmid, S.L. (1994). *J. Cell Biol.*127:915-34.

42. Frangioni, J.V., and Neel, B.G. (1993). *Anal. Biochem.* 210:179-87.

43. Warnock, D.E., Terlecky, L.J., and Schmid, S.L. (1995). *EMBO J.* 14:1322-8.

44. Huang, Y.Z., Won, S., Ali, D.W., Wang, Q., Tanowitz, M., Du, Q.S., Pelkey, K.A.,Yang, D.J., Xiong, W.C, Salter, M.W., and Mei, L. (2000). *Neuron.* 26:443-55.

45. Gout, I., Dhand, R., Hiles, I.D., Fry, M.J., Panayotou, G., Das, P., Truong, O., Totty, N.F., Hsuan, J., and Booker, G.W. (1993). *Cell.* 75:25-36.

46. McPherson, P.S., Czernik, A.J., Chilcote, T.J., Onofri, F., Benfenati, F., Greengard, P., Schlessinger, J., and De Camilli, P. (1994). *Proc. Natl. Acad. Sci. USA.* 91:6486-90.

47. Yang, B., Jung, D., Motto, D., Meyer, J., Koretzky, G., and Campbell, K.P. (1995). *J.Biol. Chem.* 270:11711-4

48. Russo, K., Di Stasio, E., Macchia, G., Rosa, G., Brancaccio, A., and Petrucci, T.C.(2000). *Biochem. Biophys. Res. Commun*. 274:93-98.

49. David, C., McPherson, P.S., Mundigl, O., de Camilli, P. (1996). *Proc. Natl. Acad. Sci. U S A.* 93:331-5.

50. Ramjaun, A.R., Micheva, K.D., Bouchelet, I., and McPherson, P.S. (1997). *J. Biol.Chem.* 272:16700-6.

51. de Heuvel, E., Bell, A.W., Ramjaun, A.R., Wong, K., Sossin, W.S., and McPherson,P.S. (1997). *J. Biol. Chem.* 272:8710-6.

52. Ringstad, N., Nemoto, Y., and DeCamilli, P. (1997). *Proc. Natl. Acad. Sci. U.S.A.*94:8569-74.

53. McPherson, P.S. (1999). *Cell Signal.* 11:229-238.

54. Blake, D.J., and Kroger, S. (2000). *Trends Neurosci.* 23:92-9.

55. Zaccaria, M.L., Di Tommaso, F., Brancaccio, A., Paggi, P., and Petrucci, T.C. (2001). *Neuroscience.* 104:311-24.

56. Montanaro, F., Carbonetto, S., Campbell, K.P. and Lindenbaum, M. (1995). *J.Neurosci. Res.* 42:528-38.

57. Dalloz, C., Claudepierre, T., Rodius, F., Mornet, D., Sahel, J., and Rendon, A. (2001).*Mol. Cell Neurosci.* 17:908-20.

58. Blank, M., Blake, D.J. and Kroger, S. (2002). *Neuroscience*. 111:259-273.

59. McNiven, M.A., Kim, L., Krueger, E.W. Orth, J.D. Cao, H. and Wong, T.W. (2000). *J.Cell Biol.* 151:187-98.

60. Urrutia, R., Henley, J.R., Cook, T., and McNiven, M.A. (1997). *Proc. Natl. Acad. Sci. U S A.* 94:377-84.

61. Cao, H., Orth, J.D., Chen, J., Weller, S.G., Heuser, J.E. and McNiven, M.A. (2003). *Mol. Cell Biol.* 23:2162-70.

62. Lynch, D.K., Winata, S.C., Lyons, R.J., Hughes, W.E., Lehrbach, G.M., Wasinger, V., Corthals, G., Cordwell, S., Daly, R.J. (2003). *J. Biol. Chem.* 278:21805-13.

63. Oak, S.A., Russo, K., Petrucci, T.C., Jarrett, H.W. (2001). *Biochemistry*. 40:11270-8.

64. Vidal, M., Goudreau, N., Cornille, F., Cussac, D., Gincel, E., and Garbay, C. (1999). *J. Mol. Biol.* 290:717-30.

65. Micheva, K.D., Kay, B.K., and McPherson, P.S. (1997). *J. Biol. Chem.* 272:27239-45.

66. Michele, D.E., and Campbell K.P. (2003). *J. Biol. Chem.* 278:15457-60.

67. Koulen, P., Honig, L.S., Fletcher, E.L., and Kroger, S. (1999). *Eur. J. Neurosci.*11:4188-96.

68. Smalheiser, N.R., and Kim, E. (1995). *J. Biol. Chem.* 270:15425-33.

69. Estes, P.S., Roos, J., van der Bliek, A., Kelly, R.B., Krishnan, K.S. and Ramaswami, M. (1996). *J. Neurosci.* 16:5443-56.

70. Roos, J., and Kelly, R.B. (1999). *Curr. Biol.* 9:1411-4.

71. Bretscher, M.S., and Aguado-Velasco, C. (1998). *Curr. Biol.* 8:721-4.

72. Wang, Z., and Moran, M.F. (1996). *Science*. 272:1935-9.

73. Vieira, A.V., Lamaze, C., and Schmid, S.L. (1996). *Science.* 274:2086-9.

74. Yamazaki, T., Zaal, K., Hailey, D., Presley, J., Lippincott-Schwartz, J., and Samelson L.E. (2002). *J. Cell Sci.* 115:1791-802.

75. Huang, F., Khvorova, A., Marshall, W., and Sorkin, A. (2004). *J. Biol. Chem.* 279:16657-61.

76. Karoor, V., Wang, L., Wang, H.Y. and Malbon, C.C. (1998). *J. Biol. Chem.* 273:33035-41.

77. Wigge, P., Vallis, Y., and McMahon, H.T. (1997). *Curr. Biol.* 7:554-60.

78. Shupliakov, O., Low, P., Grabs, D., Gad, H., Chen, H., David, C., Takei, K., De Camilli, P., and Brodin, L. (1997). *Science.* 276:259-63.

79. Simpson, F., Hussain, N.K., Qualmann, B., Kelly, R.B., Kay, B.K., McPherson, P.S., and Schmid, S.L. (1999). *Nat. Cell Biol.* 1:119-124.

80. Schmid, S.L., McNiven, M.A., De Camilli, P. (1998). *Curr. Opin. Cell Biol.* 10:504-12.

81. Takei, K., Slepnev, V.I., Haucke, V., De Camilli, P. (1999). *Nat. Cell Biol.* 1:33-9.

82. Orth, J.D., and McNiven, M.A. (2003). *Curr. Opin. Cell Biol.* 15:31-9.

83. Chen, Y.J., Spence, H.J., Cameron, J.M., Jess, T., Ilsley, J.L., and Winder, S.J. (2003). *Biochem. J.* 375:329-37.

84. Spence, H.J., Chen, Y.J., Batchelor, C.L., Higginson, J.R., Suila, H., Carpen, O., and Winder, S.J. (2004). *Hum. Mol. Genet.* 13:1657-1668.

85. Qualmann, B., Kessels, M.M., and Kelly, R.B. (2000). *J. Cell Biol.* 150:F111-6.

86. Cook, T.A., Urrutia, R., and McNiven, M.A. (1994). *Proc. Natl. Acad. Sci. U S A.* 91:644-8.

87. Robinson, P.J., Sontag, J.M., Liu, J.P., Fykse, E.M., Slaughter, C., McMahon, H., and Sudhof, T.C. (1993). *Nature*. 365:163-6.

Final Discussion

Dystroglycan is a cell surface receptor expressed in a wide number of cell types and involved in multiple cellular processes. The aim of my research was to gain further information about DG's role in eye development. I initially became interested in DG's function in eye development when working with *Dag1* chimeric mice, this lead to my participation in the project of finding novel binding partners for DG in the vertebrate brain. Finally, I furthered my studies using the versatile CNS model, the *Drosophila* developing eye.

My initial work with *Dag1* chimeric mice indicated an important role for DG during eye development. Chimeric mice with a high contribution of *Dag1* cells developed significant levels of eye anomalies, including anophthalmia, microphthalmia and corneal clouding. The retina of these chimeras showed normal but thinner retinal layering. The anomalies observed in the *Dag1* chimeric mice are found in patients with Dystroglycanopathy MDs, demonstrating DG's role in disease progression in tissues other than muscle. DG may contribute to signalling pathways specifically in the CNS. The colocalisation of DG with dynamin in the outer plexiform layer of murine retina contributed to evidence that DG may be regulating endocytosis in the CNS.

My interests in DG's role in eye development lead me to *Drosophila* genetics. The precise structure of the *Drosophila* eye coupled to the multiple

genetics tools available made this a powerful model to gain insight to DG's role in eye development. In *Drosophila*, unlike vertebrates, DG is present in multiple isoforms as a consequence of alternative splicing of DG's mRNA. The putatively glycosylated isoform DG-C, was found to be expressed during eye development. DG-C was found in the proliferating area of the *Drosophila* eye disc prior to cellular specification. DG-C was also found at the initiation site of specification of the eye disc. Once cells were specified DG-C was found specifically in R cells with a high concentration at their apical surfaces. This location was maintained throughout early pupal development. These different locations would allow DG to function both in the proliferation of cells and their specification within the eye tissue. Once specified DG-C is restricted to the developing R cells where DG could regulate its differentiation.

The strategy of reducing DG protein during eye development was used to determine which cellular processed DG regulated; two methods were used to achieve this. The first was the interference RNA mediated reduction of endogenous DG in a wt genetic background. The second was the use of genetic *Dg* alleles either hypomorph or believed to be null.

Interference RNA was used to mediate down regulation of endogenous DG starting at the time of R cell specification, which led to the disruption of the adult eye suggesting that DG has a role in the differentiation of R cells. The

phenocopy of this disruption by interference RNA of *Dys* suggests it is in the same pathway as DG. The RNAi work suggested that DG has a role during R cell development but its localisation suggested it may have an earlier role. To answer this question *Dg* alleles were studied. The initial series of alleles available were a deletion series, which included Dg^{248}. The Dg^{248} mosaic adult eye was highly disrupted with a lack of retinal patterning, flattened facets, with ommatidia lacking the full compliment of R cells and the R cells present had disrupted morphologies.

The deletions series was recently found to contain a deletion of a neighbouring gene the mitochondrial ribosomal protein L34, *mRpL34*. The dysfunction of *mRpL34* introduced metabolic stress to the *Dg* hypomorph. DG has recently been implicated in maintaining oocyte epithelial polarity during metabolic stress. Analysis of the developing Dg^{248} mosaic eye, demonstrated that DG is not required for polarity maintenance during metabolic stress. Dg^{248} R cells do have a disruption of the maintenance of the nuclei in the cell soma. A response to stress may be cell death. Dg^{248} mosaic eye cell death levels were higher in the early eye development and inhibition of this cell death was detrimental to the development of the Dg^{248} mosaic eye. This may reflect an inability of compensatory proliferation of cells with reduced levels of DG and placed under metabolic stress.

The apparent degeneration of the *Dg*^{248} mosaic eye was shown to be rescued by the transgenic expression of *mRpL34*. The *Dg*^{248} mosaic eyes + *mRpL34* had normal retinal patterning. A second series of EMS *Dg*^{0*} alleles, that affect only *Dg,* are believed to be null for DG but some do have residual levels of DG-C expression, suggesting they may actually be severe hypomorphic alleles. The EMS *Dg*^{0*} allele series develop normally patterned retina; however they were shown to be thinner suggesting a signalling role for *Dg* in activating the elongation of R cells.

The discrepancy in the consequence of reduced levels of DG on eye development found between the vertebrate and the invertebrate; as well as the discrepancy between the *Dg* interference RNA disrupted eye and the EMS *Dg*^{0*} mutants and *Dg*^{248} mosaic + mRpL34, requires further analysis. Resolution may occur by generating a *Dg* deficiency where the entire coding region of *Dg* is excised. Such a deficiency would perturb only *Dg* and prevent the production of any isoforms which may have a compensatory effect. The development of the eye in the complete absence of DG may demonstrate a greater role for DG during eye development. The resulting phenotype may be closer to the *DgRNAi* disrupted eye than to the EMS *Dg*^{0*} mutant allele eyes. Alternatively, if there is no significant developmental effect on eye development. It may suggest that *Dg's* role in the *Drosophila* is one of neuroprotection from metabolic stress. Exposing

these *Dg* deficient animals to decreased glucose intake may reveal DG function in protecting R cells from neurodegeneration.

Any anomalies found in these complete *Dg* deficiencies will require rescue by transgenic expression of *Dg* to confirm the function of DG in preventing the anomaly. To date only the DG isoforms expressed in the oocyte have been determined. The isoforms, other than DG-C shown in this study, expressed during eye development will need to be determined. This may reveal novel DG isoforms specific to the eye. If multiple isoforms are expressed, their differential spatiotemporal expression patterns will need to be established and their function confirmed through rescue experiments in the *Dg* deficiency. The complexity of DG's function in the *Drosophila* eye may yet to be determined.

This present study suggests that DG may have early developmental role in eye specification and retinal cell survival. Together the discrepancies that exist between the different *Dg* alleles suggest that the complexity of DG's function in the *Drosophila* eye may yet to be determined. Dissecting this complexity may lead to a better understanding of the complexity in the aetiologies muscular dystrophy.

Appendices

Guidelines for completing the form are available at www.mcgill.ca/research/compliance/animal/forms

McGill University
Animal Use Protocol – Research

For Office Use Only:
Protocol #:
Approval End Date:
Facility Committee:

Title: Dystrophin associated protein in synapse structure and function
(must match the title of the funding source application)

☐ New Application ☒ Renewal of Protocol # 4528 ☒ Pilot Category *(see section 11)*: _____

1. Investigator Data:

Principal Investigator: Salvatore Carbonetto **Phone #:** 514-934-1934 x4237
Unit/Department: Neurology **Fax#:** 514-934-8265
Address: Montreal General Hospital, 1650 Cedar Avenue, Montreal, Quebec, H3G 1A4 **Email:** sal.carbonetto@mcgill.ca

2. Emergency Contacts: Two people must be designated to handle emergencies.

Name: Salvatore Carbonetto **Work #:** 934-1934 x4237 **Emergency #:** (514) 932-7016
Name: Waris Ali Shah **Work #:** 934-1934 x4575 **Emergency #:** (450) 678-1486

3. Funding Source:

External ☒	**Internal** ☐
Source (s): MDA4136, CIHR6477	**Source (s):** _____
Peer Reviewed for the project proposed in this Animal Use Protocol: ☒YES ☐ NO**	**Peer Reviewed:** ☐ YES ☐ NO**
Status : ☒ Awarded ☐ Pending	**Status:** ☐ Awarded ☐ Pending
Funding period: 2006-2009	**Funding period:**_____

For Office Use Only:

** All projects that have not been peer reviewed for scientific merit by the funding source require 2 Peer Review Forms to be completed e.g. Projects funded from industrial sources. Peer Review Form available at www.mcgill.ca/research/compliance/animal/forms

Proposed Start Date of Animal Use (d/m/y): _____ **or ongoing** ☒

Expected Date of Completion of Animal Use (d/m/y): _____ **or ongoing** ☒

Investigator's Statement: The information in this application is exact and complete. I assure that all care and use of animals in this proposal will be in accordance with the guidelines and policies of the Canadian Council on Animal Care and those of McGill University. I shall request the Animal Care Committee's approval prior to any deviations from this protocol as approved. I understand that this approval is valid for one year and must be approved on an annual basis.

Principal Investigator's signature: [signature] **Date:** 12 Dec 2007

Approved by:

Chair, Facility Animal Care Committee:		**Date:**
University Veterinarian:		**Date:**
Chair, Ethics Subcommittee (as per UACC policy):		**Date:**
Approved Animal Use	**Beginning:**	**Ending:**

☐ This protocol has been approved with the modifications noted in Section 13.

☐ **Renewal requires submission of full Animal Use Protocol form**

May 2006

Bibliography

Adams JM, Cory S. 2002. Apoptosomes: engines for caspase activation. *Curr Opin Cell Biol* 14: 715-20

Beltran-Valero De Bernabe D, Currier S, Steinbrecher A, Celli J, Van Beusekom E, et al. 2002. Mutations in the O-Mannosyltransferase Gene POMT1 Give Rise to the Severe Neuronal Migration Disorder Walker-Warburg Syndrome. *Am J Hum Genet* 71: 1033-43.

Blank M, Koulen P, Kroger S. 1997. Subcellular concentration of beta-dystroglycan in photoreceptors and glial cells of the chick retina. *J Comp Neurol* 389: 668-78.

Bonini NM, Leiserson WM, Benzer S. 1993. The eyes absent gene: genetic control of cell survival and differentiation in the developing Drosophila eye. *Cell* 72: 379-95

Bursch W. 2004. Multiple cell death programs: Charon's lifts to Hades. *FEMS Yeast Res* 5: 101-10.

Bursch W, Karwan A, Mayer M, Dornetshuber J, Frohwein U, et al. 2008. Cell death and autophagy: cytokines, drugs, and nutritional factors. *Toxicology* 254: 147-57

Cagan RL, Ready DF. 1989. The emergence of order in the Drosophila pupal retina. *Dev Biol* 136: 346-62

Campos AR, Fischbach KF, Steller H. 1992. Survival of photoreceptor neurons in the compound eye of Drosophila depends on connections with the optic ganglia. *Development* 114: 355-66

Campos AR, Lee KJ, Steller H. 1995. Establishment of neuronal connectivity during development of the Drosophila larval visual system. *J Neurobiol* 28: 313-29

Charles DJ, Lee CY. 1980. Biochemical and immunological characterization of genetic variants of phosphoglucose isomerase from mouse. *Biochem Genet* 18: 153-69

Chen B, Cepko CL. 2009. HDAC4 regulates neuronal survival in normal and diseased retinas. *Science* 323: 256-9

Chintapalli VR, Wang J, Dow JA. 2007. Using FlyAtlas to identify better Drosophila melanogaster models of human disease. *Nat Genet* 39: 715-20

Cho KO, Chern J, Izaddoost S, Choi KW. 2000. Novel signaling from the peripodial membrane is essential for eye disc patterning in Drosophila. *Cell* 103: 331-42

Cho KO, Choi KW. 1998. Fringe is essential for mirror symmetry and morphogenesis in the Drosophila eye. *Nature* 396: 272-6

Chow RL, Lang RA. 2001. Early eye development in vertebrates. *Annu Rev Cell Dev Biol* 17: 255-96

Christoforou CP, Greer CE, Challoner BR, Charizanos D, Ray RP. 2008. The detached locus encodes Drosophila Dystrophin, which acts with other components of the Dystrophin Associated Protein Complex to influence intercellular signalling in developing wing veins. *Dev Biol* 313: 519-32

Cohn RD. 2005. Dystroglycan: important player in skeletal muscle and beyond. *Neuromuscul Disord* 15: 207-17

Côté PD, Moukhles H, Lindenbaum M, Carbonetto S. 1999. Chimaeric mice deficient in dystroglycans develop muscular dystrophy and have disrupted myoneural synapses. *Nat Genet* 23: 338-42.

Deng WM, Schneider M, Frock R, Castillejo-Lopez C, Gaman EA, et al. 2003. Dystroglycan is required for polarizing the epithelial cells and the oocyte in Drosophila. *Development* 130: 173-84.

Dietzl G, Chen D, Schnorrer F, Su KC, Barinova Y, et al. 2007. A genome-wide transgenic RNAi library for conditional gene inactivation in Drosophila. *Nature* 448: 151-6

Dincer P, Balci B, Yuva Y, Talim B, Brockington M, et al. 2003. A novel form of recessive limb girdle muscular dystrophy with mental retardation and abnormal expression of alpha-dystroglycan. . *Neuromuscul Disord* 13: 771-8.

Dorstyn L, Colussi PA, Quinn LM, Richardson H, Kumar S. 1999. DRONC, an ecdysone-inducible Drosophila caspase. *Proc Natl Acad Sci U S A* 96: 4307-12

Durbeej M, Campbell KP. 1999. Biochemical characterization of the epithelial dystroglycan complex. *J Biol Chem* 274: 26609-16.

Durbeej M, Henry MD, Ferletta M, Campbell KP, Ekblom P. 1998. Distribution of dystroglycan in normal adult mouse tissues. *J Histochem Cytochem* 46: 449-57.

Durbeej M, Larsson E, Ibraghimov-Beskrovnaya O, Roberds SL, Campbell KP, Ekblom P. 1995. Non-muscle alpha-dystroglycan is involved in epithelial development. *J Cell Biol* 130: 79-91.

Edinger AL, Thompson CB. 2004. Death by design: apoptosis, necrosis and autophagy. *Curr Opin Cell Biol* 16: 663-9

Edwards KA, Kiehart DP. 1996. Drosophila nonmuscle myosin II has multiple essential roles in imaginal disc and egg chamber morphogenesis. *Development* 122: 1499-511

Erickson AC, Couchman JR. 2000. Still more complexity in mammalian basement membranes. *J Histochem Cytochem* 48: 1291-306.

Ervasti JM, Campbell KP. 1993. A role for the dystrophin-glycoprotein complex as a transmembrane linker between laminin and actin. *J Cell Biol* 122: 809-23

Fan Y, Bergmann A. 2008a. Apoptosis-induced compensatory proliferation. The Cell is dead. Long live the Cell! *Trends Cell Biol* 18: 467-73

Fan Y, Bergmann A. 2008b. Distinct mechanisms of apoptosis-induced compensatory proliferation in proliferating and differentiating tissues in the Drosophila eye. *Dev Cell* 14: 399-410

Fischer-Vize JA, Mosley KL. 1994. Marbles mutants: uncoupling cell determination and nuclear migration in the developing Drosophila eye. *Development* 120: 2609-18

Franc NC. 2002. Phagocytosis of apoptotic cells in mammals, caenorhabditis elegans and Drosophila melanogaster: molecular mechanisms and physiological consequences. *Front Biosci* 7: d1298-313.

Fung C, Lock R, Gao S, Salas E, Debnath J. 2008. Induction of autophagy during extracellular matrix detachment promotes cell survival. *Mol Biol Cell* 19: 797-806

Gaengel K, Mlodzik M. 2008. Microscopic analysis of the adult Drosophila retina using semithin plastic sections. *Methods Mol Biol* 420: 277-87

Gee SH, Blacher RW, Douville PJ, Provost PR, Yurchenco PD, Carbonetto S. 1993. Laminin-binding protein 120 from brain is closely related to the dystrophin-associated glycoprotein, dystroglycan, and binds with high affinity to the major heparin binding domain of laminin. *J Biol Chem* 268: 14972-80.

Gee SH, Montanaro F, Lindenbaum MH, Carbonetto S. 1994. Dystroglycan-alpha, a dystrophin-associated glycoprotein, is a functional agrin receptor. *Cell* 77: 675-86.

Gibson MC, Schubiger G. 2000. Peripodial cells regulate proliferation and patterning of Drosophila imaginal discs. *Cell* 103: 343-50

Gibson MC, Schubiger G. 2001. Drosophila peripodial cells, more than meets the eye? *Bioessays* 23: 691-7

Greener MJ, Roberts RG. 2000. Conservation of components of the dystrophin complex in Drosophila. *FEBS Lett* 482: 13-8

Grether ME, Abrams JM, Agapite J, White K, Steller H. 1995. The head involution defective gene of Drosophila melanogaster functions in programmed cell death. *Genes Dev* 9: 1694-708

Grewal PK, Hewitt JE. 2003. Glycosylation defects: a new mechanism for muscular dystrophy? *Hum Mol Genet* 12 Spec No 2: R259-64

Haines N, Seabrooke S, Stewart BA. 2007. Dystroglycan and Protein O-Mannosyltransferases 1 and 2 Are Required to Maintain Integrity of Drosophila Larval Muscles. *Mol Biol Cell*

Hanson I, Van Heyningen V. 1995. Pax6: more than meets the eye. *Trends Genet* 11: 268-72

Hay BA, Wolff T, Rubin GM. 1994. Expression of baculovirus P35 prevents cell death in Drosophila. *Development* 120: 2121-9

Haynie JLaB, P.J. 1977. The effects of X-rays on the proliferation dynamics of cells in the imaginal disc of *Drosophila melanogaster. Roux's Arch Dev Biol* 183: 85-100

Higginson JR, Thompson O, Winder SJ. 2008. Targeting of dystroglycan to the cleavage furrow and midbody in cytokinesis. *Int J Biochem Cell Biol* 40: 892-900

Hsiung F, Moses K. 2002. Retinal development in Drosophila: specifying the first neuron. *Hum Mol Genet* 11: 1207-14

Huet F, Lu JT, Myrick KV, Baugh LR, Crosby MA, Gelbart WM. 2002. A deletion-generator compound element allows deletion saturation analysis for genomewide phenotypic annotation. *Proc Natl Acad Sci U S A* 99: 9948-53

Huizing M, Rakocevic G, Sparks SE, Mamali I, Shatunov A, et al. 2004. Hypoglycosylation of alpha-dystroglycan in patients with hereditary IBM due to GNE mutations. *Mol Genet Metab* 81: 196-202

Ibraghimov-Beskrovnaya O, Ervasti JM, Leveille CJ, Slaughter CA, Sernett SW, Campbell KP. 1992. Primary structure of dystrophin-associated glycoproteins linking dystrophin to the extracellular matrix. *Nature* 355: 696-702.

Ichimiya T, Manya H, Ohmae Y, Yoshida H, Takahashi K, et al. 2004. The twisted abdomen phenotype of Drosophila POMT1 and POMT2 mutants coincides with their heterophilic protein O-mannosyltransferase activity. *J Biol Chem* 279: 42638-47

Jabbour AM, and Hawkins, C.J. 2004. The p35 Family of Apoptosis Inhibitors. *Curr Genomics* 5: 215-29

Jacobson C, Cote PD, Rossi SG, Rotundo RL, Carbonetto S. 2001. The dystroglycan complex is necessary for stabilization of acetylcholine receptor clusters at neuromuscular junctions and formation of the synaptic basement membrane. *J Cell Biol* 152: 435-50.

James M, Nguyen TM, Wise CJ, Jones GE, Morris GE. 1996. Utrophin-dystroglycan complex in membranes of adherent cultured cells. *Cell Motil Cytoskeleton* 33: 163-74

Jastrow H, Koulen P, Altrock WD, Kroger S. 2006. Identification of a {beta}-Dystroglycan Immunoreactive Subcompartment in Photoreceptor Terminals. *Invest Ophthalmol Vis Sci* 47: 17-24

Joo NE, Watanabe T, Chen C, Chekenya M, Stallcup WB, Kapila YL. 2008. NG2, a novel proapoptotic receptor, opposes integrin alpha4 to mediate anoikis through PKCalpha-dependent suppression of FAK phosphorylation. *Cell Death Differ* 15: 899-907

Jung D, Yang B, Meyer J, Chamberlain JS, Campbell KP. 1995. Identification and characterization of the dystrophin anchoring site on beta-dystroglycan. *J Biol Chem* 270: 27305-10.

Kaplow ME, Mannava LJ, Pimentel AC, Fermin HA, Hyatt VJ, et al. 2007. A genetic modifier screen identifies multiple genes that interact with Drosophila Rap/Fzr and suggests novel cellular roles. *J Neurogenet* 21: 105-51

Kim JH, Youn HD. 2009. C-terminal binding protein maintains mitochondrial activities. *Cell Death Differ* 16: 584-92

Koc EC, Burkhart W, Blackburn K, Moyer MB, Schlatzer DM, et al. 2001. The large subunit of the mammalian mitochondrial ribosome. Analysis of the complement of ribosomal proteins present. *J Biol Chem* 276: 43958-69

Kondo S, Senoo-Matsuda N, Hiromi Y, Miura M. 2006. DRONC coordinates cell death and compensatory proliferation. *Mol Cell Biol* 26: 7258-68

Koulen P, Blank M, Kroger S. 1998. Differential distribution of beta-dystroglycan in rabbit and rat retina. *J Neurosci Res* 51: 735-47.

Kronhamn J, Frei E, Daube M, Jiao R, Shi Y, et al. 2002. Headless flies produced by mutations in the paralogous Pax6 genes eyeless and twin of eyeless. *Development* 129: 1015-26

Kucherenko MM, Pantoja M, Yatsenko AS, Shcherbata HR, Fischer KA, et al. 2008. Genetic modifier screens reveal new components that interact with the Drosophila dystroglycan-dystrophin complex. *PLoS ONE* 3: e2418

Langenbach KJ, Rando TA. 2002a. Inhibition of dystroglycan binding to laminin disrupts the PI3K/AKT pathway and survival signaling in muscle cells. *Muscle Nerve* 26: 644-53.

Langenbach KJ, Rando TA. 2002b. Inhibition of dystroglycan binding to laminin disrupts the PI3K/AKT pathway and survival signaling in muscle cells. *Muscle Nerve 2002 Nov;26(5):644-53.*

Leist M, Jaattela M. 2001. Four deaths and a funeral: from caspases to alternative mechanisms. *Nat Rev Mol Cell Biol* 2: 589-98.

Li S, Harrison D, Carbonetto S, Fassler R, Smyth N, et al. 2002. Matrix assembly, regulation, and survival functions of laminin and its receptors in embryonic stem cell differentiation. *J Cell Biol* 157: 1279-90.

Liu C, Nathans J. 2008. An essential role for frizzled 5 in mammalian ocular development. *Development* 135: 3567-76

Lockshin RA, Zakeri Z. 2002. Caspase-independent cell deaths. *Curr Opin Cell Biol* 14: 727-33.

Longley RL, Jr., Ready DF. 1995. Integrins and the development of three-dimensional structure in the Drosophila compound eye. *Dev Biol* 171: 415-33

Lunardi A, Cremisi F, Dente L. 2006. Dystroglycan is required for proper retinal layering. *Dev Biol*

Mani R, St Onge RP, Hartman JLt, Giaever G, Roth FP. 2008. Defining genetic interaction. *Proc Natl Acad Sci U S A* 105: 3461-6

Martin D, Zusman S, Li X, Williams EL, Khare N, et al. 1999. wing blister, a new Drosophila laminin alpha chain required for cell adhesion and migration during embryonic and imaginal development. *J Cell Biol* 145: 191-201

Martin PT. 2005. The dystroglycanopathies: the new disorders of O-linked glycosylation. *Semin Pediatr Neurol* 12: 152-8

Martin PT. 2006. Mechanisms of disease: congenital muscular dystrophies-glycosylation takes center stage. *Nat Clin Pract Neurol* 2: 222-30

Marygold SJ, Coelho CM, Leevers SJ. 2005. Genetic analysis of RpL38 and RpL5, two minute genes located in the centric heterochromatin of chromosome 2 of Drosophila melanogaster. *Genetics* 169: 683-95

Medioni C, Astier M, Zmojdzian M, Jagla K, Semeriva M. 2008. Genetic control of cell morphogenesis during Drosophila melanogaster cardiac tube formation. *J Cell Biol* 182: 249-61

Meier P, Silke J, Leevers SJ, Evan GI. 2000. The Drosophila caspase DRONC is regulated by DIAP1. *Embo J* 19: 598-611

Miller C, Saada A, Shaul N, Shabtai N, Ben-Shalom E, et al. 2004. Defective mitochondrial translation caused by a ribosomal protein (MRPS16) mutation. *Ann Neurol* 56: 734-8

Milner MJ, Bleasby, A.J., Pyott, A. 1983. The Role of the Peripodial Membrane in the Morphogenesis of the Eye-Antennal Disc of *Drosophila melanogaster*. *Roux's Arch Dev Biol* 192: 164-70

Miner JH, Yurchenco PD. 2004. Laminin functions in tissue morphogenesis. *Annu Rev Cell Dev Biol* 20: 255-84

Minke B, Agam K. 2003. TRP gating is linked to the metabolic state and maintenance of the Drosophila photoreceptor cells. *Cell Calcium* 33: 395-408

Mirouse V, Christoforou CP, Fritsch C, St Johnston D, Ray RP. 2009. Dystroglycan and perlecan provide a basal cue required for epithelial polarity during energetic stress. *Dev Cell* 16: 83-92

Mongiat M, Ligresti G, Marastoni S, Lorenzon E, Doliana R, Colombatti A. 2007. Regulation of the extrinsic apoptotic pathway by the extracellular matrix glycoprotein EMILIN2. *Mol Cell Biol* 27: 7176-87

Monserrate JP, Baker Brachmann C. 2006. Identification of the death zone: a spatially restricted region for programmed cell death that sculpts the fly eye. *Cell Death Differ*

Montanaro F, Carbonetto S, Campbell KP, Lindenbaum M. 1995. Dystroglycan expression in the wild type and mdx mouse neural retina: synaptic colocalization with dystrophin, dystrophin-related protein but not laminin. *J Neurosci Res* 42: 528-38.

Montanaro F, Lindenbaum M, Carbonetto S. 1999. alpha-Dystroglycan is a laminin receptor involved in extracellular matrix assembly on myotubes and muscle cell viability. *J Cell Biol* 145: 1325-40.

Moore SA, Saito F, Chen J, Michele DE, Henry MD, et al. 2002. Deletion of brain dystroglycan recapitulates aspects of congenital muscular dystrophy. *Nature* 418: 422-5.

Moses K, Rubin GM. 1991. Glass encodes a site-specific DNA-binding protein that is regulated in response to positional signals in the developing Drosophila eye. *Genes Dev* 5: 583-93

Moukhles H, Roque R, Carbonetto S. 2000. alpha-dystroglycan isoforms are differentially distributed in adult rat retina. *J Comp Neurol* 420: 182-94.

Nagy A, Rossant J, Nagy R, Abramow-Newerly W, Roder JC. 1993. Derivation of completely cell culture-derived mice from early-passage embryonic stem cells. *Proc Natl Acad Sci U S A* 90: 8424-8.

Neumann CJ, Nuesslein-Volhard C. 2000. Patterning of the zebrafish retina by a wave of sonic hedgehog activity. *Science* 289: 2137-9

O'Brien TW, O'Brien BJ, Norman RA. 2005. Nuclear MRP genes and mitochondrial disease. *Gene* 354: 147-51

Ohtsuka-Tsurumi E, Saito Y, Yamamoto T, Voit T, Kobayashi M, Osawa M. 2004. Co-localization of fukutin and alpha-dystroglycan in the mouse central nervous system. *Brain Res Dev Brain Res* 152: 121-7

Pacquelet A, Rorth P. 2005. Regulatory mechanisms required for DE-cadherin function in cell migration and other types of adhesion. *J Cell Biol* 170: 803-12

Pall EA, Bolton KM, Ervasti JM. 1996. Differential heparin inhibition of skeletal muscle alpha-dystroglycan binding to laminins. *J Biol Chem* 271: 3817-21.

Papayannopoulos V, Tomlinson A, Panin VM, Rauskolb C, Irvine KD. 1998. Dorsal-ventral signaling in the Drosophila eye. *Science* 281: 2031-4

Pappu KS, Mardon G. 2004. Genetic control of retinal specification and determination in Drosophila. *Int J Dev Biol* 48: 913-24

Parks AL, Cook KR, Belvin M, Dompe NA, Fawcett R, et al. 2004. Systematic generation of high-resolution deletion coverage of the Drosophila melanogaster genome. *Nat Genet* 36: 288-92

Peng HB, Xie H, Rossi SG, Rotundo RL. 1999. Acetylcholinesterase clustering at the neuromuscular junction involves perlecan and dystroglycan. *J Cell Biol* 145: 911-21.

Peterson AC, Frair PM, Wong GG. 1978. A technique for detection and relative quantitative analysis of glucosephosphate isomerase isozymes from nanogram tissue samples. *Biochem Genet* 16: 681-90.

Pham H, Yu H, Laski FA. 2008. Cofilin/ADF is required for retinal elongation and morphogenesis of the Drosophila rhabdomere. *Dev Biol* 318: 82-91

Puthalakath H, Villunger A, O'Reilly LA, Beaumont JG, Coultas L, et al. 2001. Bmf: a proapoptotic BH3-only protein regulated by interaction with the myosin V actin motor complex, activated by anoikis. *Science* 293: 1829-32

Ready DF, Hanson TE, Benzer S. 1976. Development of the Drosophila retina, a neurocrystalline lattice. *Dev Biol* 53: 217-40

Reddien PW, Cameron S, Horvitz HR. 2001. Phagocytosis promotes programmed cell death in C. elegans. *Nature* 412: 198-202

Reginato MJ, Mills KR, Paulus JK, Lynch DK, Sgroi DC, et al. 2003. Integrins and EGFR coordinately regulate the pro-apoptotic protein Bim to prevent anoikis. *Nat Cell Biol* 5: 733-40

Reiter LT, Potocki L, Chien S, Gribskov M, Bier E. 2001. A systematic analysis of human disease-associated gene sequences in Drosophila melanogaster. *Genome Res* 11: 1114-25

Rezaval C, Werbajh S, Ceriani MF. 2007. Neuronal death in Drosophila triggered by GAL4 accumulation. *Eur J Neurosci* 25: 683-94

Richard M, Roepman R, Aartsen WM, van Rossum AG, den Hollander AI, et al. 2006. Towards understanding CRUMBS function in retinal dystrophies. *Hum Mol Genet* 15 Spec No 2: R235-43

Richardson H, Kumar S. 2002. Death to flies: Drosophila as a model system to study programmed cell death. *J Immunol Methods* 265: 21-38.

Romani P, Bernardi F, Hackney J, Dobens L, Gargiulo G, Cavaliere V. 2009. Cell survival and polarity of Drosophila follicle cells require the activity of ecdysone receptor B1 isoform. *Genetics* 181: 165-75

Ryoo HD, Bergmann A, Gonen H, Ciechanover A, Steller H. 2002. Regulation of Drosophila IAP1 degradation and apoptosis by reaper and ubcD1. *Nat Cell Biol* 4: 432-8

Ryoo HD, Gorenc T, Steller H. 2004. Apoptotic cells can induce compensatory cell proliferation through the JNK and the Wingless signaling pathways. *Dev Cell* 7: 491-501

Sato S, Omori Y, Katoh K, Kondo M, Kanagawa M, et al. 2008. Pikachurin, a dystroglycan ligand, is essential for photoreceptor ribbon synapse formation. *Nat Neurosci* 11: 923-31

Satz JS, Barresi R, Durbeej M, Willer T, Turner A, et al. 2008. Brain and eye malformations resembling Walker-Warburg syndrome are recapitulated in mice by dystroglycan deletion in the epiblast. *J Neurosci* 28: 10567-75

Schmidt KG, Bergert H, Funk RH. 2008. Neurodegenerative diseases of the retina and potential for protection and recovery. *Curr Neuropharmacol* 6: 164-78

Schneider M, Baumgartner S. 2008. Differential expression of Dystroglycan-spliceforms with and without the mucin-like domain during Drosophila embryogenesis. *Fly (Austin)* 2

Schroder JE, Tegeler MR, Grosshans U, Porten E, Blank M, et al. 2007. Dystroglycan regulates structure, proliferation and differentiation of neuroepithelial cells in the developing vertebrate CNS. *Dev Biol* 307: 62-78

Schwarzbauer J. 1999. Basement membranes: Putting up the barriers. *Curr Biol* 9: R242-4.

Sciandra F, Bozzi M, Bianchi M, Pavoni E, Giardina B, Brancaccio A. 2003. Dystroglycan and muscular dystrophies related to the dystrophin-glycoprotein complex. *Ann Ist Super Sanita* 39: 173-81

Shcherbata HR, Yatsenko AS, Patterson L, Sood VD, Nudel U, et al. 2007. Dissecting muscle and neuronal disorders in a Drosophila model of muscular dystrophy. *Embo J* 26: 481-93

Smith RS, Roderick TH, Sundberg JP. 1994. Microphthalmia and associated abnormalities in inbred black mice. *Lab Anim Sci* 44: 551-60

Spasic MR, Callaerts P, Norga KK. 2008. Drosophila alicorn is a neuronal maintenance factor protecting against activity-induced retinal degeneration. *J Neurosci* 28: 6419-29

Srivastava M, Scherr H, Lackey M, Xu D, Chen Z, et al. 2007. ARK, the Apaf-1 related killer in Drosophila, requires diverse domains for its apoptotic activity. *Cell Death Differ* 14: 92-102

Stowers RS, Schwarz TL. 1999. A genetic method for generating Drosophila eyes composed exclusively of mitotic clones of a single genotype. *Genetics* 152: 1631-9

Strasser A, O'Connor L, Dixit VM. 2000. Apoptosis signaling. *Annu Rev Biochem* 69: 217-45.

Syntichaki P, Tavernarakis N. 2002. Death by necrosis. Uncontrollable catastrophe, or is there order behind the chaos? *EMBO Rep* 3: 604-9.

Takeuchi K-i, Nakano Y, Kato U, Kaneda M, Aizu M, et al. 2009. Changes in Temperature Preferences and Energy Homeostasis in Dystroglycan Mutants. *Science* 323: 1740-3

Talts JF, Andac Z, Gohring W, Brancaccio A, Timpl R. 1999. Binding of the G domains of laminin alpha1 and alpha2 chains and perlecan to heparin, sulfatides, alpha-dystroglycan and several extracellular matrix proteins. *Embo J* 18: 863-70.

Tepass U, Harris KP. 2007. Adherens junctions in Drosophila retinal morphogenesis. *Trends Cell Biol* 17: 26-35

Thaker HM, Kankel DR. 1992. Mosaic analysis gives an estimate of the extent of genomic involvement in the development of the visual system in Drosophila melanogaster. *Genetics* 131: 883-94

Theodosiou NA, Xu T. 1998. Use of FLP/FRT system to study Drosophila development. *Methods* 14: 355-65

Thomas BJ, Wassarman DA. 1999. A fly's eye view of biology. *Trends Genet* 15: 184-90

Tremblay MR, Carbonetto S. 2006. An extracellular pathway for dystroglycan function in acetylcholine receptor aggregation and laminin deposition in skeletal myotubes. *J Biol Chem* 281: 13365-73

Valentin-Vega YA, Okano H, Lozano G. 2008. The intestinal epithelium compensates for p53-mediated cell death and guarantees organismal survival. *Cell Death Differ* 15: 1772-81

van de Pavert SA, Kantardzhieva A, Malysheva A, Meuleman J, Versteeg I, et al. 2004. Crumbs homologue 1 is required for maintenance of photoreceptor cell polarization and adhesion during light exposure. *J Cell Sci* 117: 4169-77

van der Plas MC, Pilgram GS, de Jong AW, Bansraj MR, Fradkin LG, Noordermeer JN. 2007. Drosophila Dystrophin is required for integrity of the musculature. *Mech Dev* 124: 617-30

Venken KJ, Bellen HJ. 2007. Transgenesis upgrades for Drosophila melanogaster. *Development* 134: 3571-84

Verma AS, Fitzpatrick DR. 2007. Anophthalmia and microphthalmia. *Orphanet J Rare Dis* 2: 47

Walther RF, Pichaud F. 2006. Immunofluorescent staining and imaging of the pupal and adult Drosophila visual system. *Nat Protoc* 1: 2635-42

Wech I, Nagel AC. 2005. Mutations in rugose promote cell type-specific apoptosis in the Drosophila eye. *Cell Death Differ* 12: 145-52

Wells BS, Yoshida E, Johnston LA. 2006. Compensatory proliferation in Drosophila imaginal discs requires Dronc-dependent p53 activity. *Curr Biol* 16: 1606-15

Williamson RA, Henry MD, Daniels KJ, Hrstka RF, Lee JC, et al. 1997. Dystroglycan is essential for early embryonic development: disruption of Reichert's membrane in Dag1-null mice. *Hum Mol Genet* 6: 831-41.

Wolff T, Ready DF. 1991a. The beginning of pattern formation in the Drosophila compound eye: the morphogenetic furrow and the second mitotic wave. *Development* 113: 841-50

Wolff T, Ready DF. 1991b. Cell death in normal and rough eye mutants of Drosophila. *Development* 113: 825-39

Xu D, Wang Y, Willecke R, Chen Z, Ding T, Bergmann A. 2006. The effector caspases drICE and dcp-1 have partially overlapping functions in the apoptotic pathway in Drosophila. *Cell Death Differ* 13: 1697-706

Xu T, Rubin GM. 1993. Analysis of genetic mosaics in developing and adult Drosophila tissues. *Development* 117: 1223-37

Yang B, Jung D, Motto D, Meyer J, Koretzky G, Campbell KP. 1995. SH3 domain-mediated interaction of dystroglycan and Grb2. *J Biol Chem* 270: 11711-4.

Yatsenko AS, Gray EE, Shcherbata HR, Patterson LB, Sood VD, et al. 2007. A putative Src homology 3 domain binding motif but not the C-terminal dystrophin WW domain binding motif is required for dystroglycan function in cellular polarity in Drosophila. *J Biol Chem* 282: 15159-69

Yatsenko AS, Kucherenko MM, Pantoja M, Fischer KA, Madeoy J, et al. 2009. The conserved WW-domain binding sites in Dystroglycan C-terminus are essential but partially redundant for Dystroglycan function. *BMC Dev Biol* 9: 18

Zaccaria ML, Di Tommaso F, Brancaccio A, Paggi P, Petrucci TC. 2001. Dystroglycan distribution in adult mouse brain: a light and electron microscopy study. *Neuroscience* 104: 311-24.

Zajac AL, Discher DE. 2008. Cell differentiation through tissue elasticity-coupled, myosin-driven remodeling. *Curr Opin Cell Biol* 20: 609-15

Zhan Y, Tremblay MR, Melian N, Carbonetto S. 2005. Evidence that dystroglycan is associated with dynamin and regulates endocytosis. *J Biol Chem* 280: 18015-24